


# **MECHANICAL PROPERTIES OF POLYMERS AND COMPOSITES**



**SECOND EDITION, REVISED AND EXPANDED**

**LAWRENCE E. NIELSEN  
ROBERT F. LANDEL**

Library of Congress Cataloging-in-Publication Data

Nielsen, Lawrence E.

Mechanical properties of polymers and composites / Lawrence E.

Nielsen, Robert F. Landel. — 2nd ed., rev. and expanded.

p. cm. — (Mechanical engineering ; 90)

Includes bibliographical references and index.

ISBN 0-8247-8964-4

1. Polymers—Mechanical properties. 2. Polymeric composites—  
Mechanical properties. I. Landel, Robert F. II. Title.

III. Series: Mechanical engineering (Marcel Dekker) ; 90.

TA455.P58N48 1994

620.1 '9204292—d:20

93-38364

CIP

The publisher offers discounts on this book when ordered in bulk quantities. For more information, write to Special Sales/Professional Marketing at the address below.

This book is printed on acid-free paper.

Copyright © 1994 by Marcel Dekker, Inc. All Rights Reserved.

Neither this book nor any part may be reproduced or transmitted in any form or by any means, electronic or mechanical, including photocopying, microfilming, and recording, or by any information storage and retrieval system, without permission in writing from the publisher.

**Marcel Dekker, Inc.**  
270 Madison Avenue, New York, New York 10016

Current printing (last digit):  
10 9 8

PRINTED IN THE UNITED STATES OF AMERICA



# MECHANICAL PROPERTIES OF POLYMERS AND COMPOSITES



SECOND EDITION, REVISED AND EXPANDED

**LAWRENCE E. NIELSEN**

*Monsanto Company  
St. Louis, Missouri*

**ROBERT F. LANDEL**

*Jet Propulsion Laboratory  
California Institute of Technology  
Pasadena, California*

|           |  |             |
|-----------|--|-------------|
| III.      | Stress or Strain Amplitude Effects                         | 184         |
| IV.       | Thermal History  | 137         |
| V.        | Effect of Molecular Weight                                 | 1 &         |
| VI.       | Effect of Cross-linking                                    | 1*7         |
| VII.      | Effects of Crystallinity and Morphology                    | H5          |
| VIII.     | Effects of Plasticizers and Copolymerization               | 181         |
| IX.       | Effect of Molecular Orientation                            | 188         |
| X.        | Effect of Strength of Intermolecular Forces                | 194         |
| XI.       | Polyblends, Block, and Graft Polymers                      | m           |
| XII.      | Secondary Damping Peaks                                    | 282         |
|           | Summary  | 212         |
|           | Problems   | 3 §         |
|           | Reference  | ^           |
| <b>5.</b> | <b>Stress-Strain Behavior and Strength</b>                 | <b>3353</b> |
| I.        | Stress-Strain Tests  | \$3\$       |
| A.        | Introduction   | ^ §         |
| B.        | Models   | Hg\$        |
| C.        | Form of the stress—strain curve; Multiaxial response       | 36          |
| D.        | Compression and shear versus tensile tests: Rigid polymers | 249         |
| E.        | Effect of temperature                                      | 253         |
| F.        | Role of testing and the failure envelope                   | 256         |
| G.        | Effect of hydrostatic pressure                             | 273         |
| H.        | Effect of molecular weight and branching                   | 265         |
| I.        | Effect of cross-linking                                    | 268         |
| J.        | Relationships and inclusions                               | 277         |
| K.        | Effect of crystallinity                                    | 280         |
| L.        | Effects of plasticization and copolymerization             | 283         |
| M.        | Molecular orientation                                      | 285         |
| N.        | Polyblends, block, and graft polymers                      | 292         |
| II.       | Brittle Fracture and Stress Concentrators                  | 295         |
| A.        | Stress concentrators                                       | 295         |
| B.        | Fracture theory  | 297         |
| III.      | Theories of Yielding and Cold-Drawing                      | 299         |
| IV.       | Impact Strength and Tearing                                | 307         |
| A.        | Nature of impact tests                                     | 307         |
| B.        | Effect of notched  | 308         |
| C.        | Effects of temperature                                     | 310         |
| D.        | Effects of orientation                                     | 313:        |
| E.        | Other factors effecting impact strength                    | HI          |

|              |  |            |
|--------------|--|------------|
| F.           | Impact strength of polyblends                    | 315        |
| G.           | Tearing  | 317        |
|              | Summary  | 318        |
|              | Problems   | 319        |
|              | References                                       | 322        |
| <b>6.</b>    | <b>Other Mechanical Properties</b>               | <b>337</b> |
| <b>I.</b>    | Heat Distortion Temperature                      | 337        |
| <b>II.</b>   | Fatigue           **                             | 342        |
| <b>III.</b>  | Friction   | 352        |
| <b>IV.</b>   | Abrasion, Wear, and Scratch Resistance-          | 358        |
| <b>V.</b>    | Hardness and Indentation Tests                   | 362        |
| <b>VI.</b>   | Stress Cracking and Cracking in Fluids           | 366        |
|              | Summary  | 368        |
|              | Problems   | 368        |
|              | References                                       | 369        |
| <b>%</b>     | <b>Particulate-Filled Polymers</b>               | <b>377</b> |
| <b>I.</b>    | Introduction to Composite Systems                | 377        |
| <b>II.</b>   | Rheology of Suspensions                          | 378        |
| <b>III.</b>  | Relation between Viscosity and Shear Modulus     | 384        |
| <b>IV.</b>   | Modulii of Filled Polymers                       | 384        |
|              | A- Regular systems                               | 384        |
|              | B. Inverted systems and phase inversion          | 392        |
|              | C. Errors in composite moduli                    | 398        |
|              | D. Experimental examples                         | 401        |
| <b>V.</b>    | Strength and Stress <sup>^</sup> Strain Behavior | 401        |
|              | A. Rigid fillers                                 | 401        |
|              | B. Polyblends, block polymers, and foams         | 411        |
| <b>VI.</b>   | Creep and Stress Relaxation                      | 422        |
| <b>VII.</b>  | Dynamic Mechanical Properties                    | 425        |
| <b>VIII.</b> | Other Mechanical Properties                      | 435        |
|              | A. Impact strength                               | 435        |
|              | 8. Heat distortion temperature                   | 436        |
|              | C. Hardness, wear, and fatigue life              | 437        |
|              | D. Coefficients of thermal expansion             | 440        |
| <b>IX.</b>   | Composites with Thick Interlayers                | 443        |
| <b>X-</b>    | Syntactic Foums                                  | 444        |
| <b>XI.</b>   | Structural Foams                                 | 445        |
|              | Summary  | 446        |

|   |             |
|---|-------------|
| <b>Contents</b>   | <b>XIII</b> |
| Problems  | 447         |
| References  | 450         |
| <b>8. Fiber-Filled Composites and Other Composites</b>  | <b>461</b>  |
| I. Introduction   | 461         |
| II. Moduli of Fiber-Filled Composites   | 463         |
| III. Strength of Fiber-Filled Composites  | 471         |
| A. Uniaxially oriented fibers   | 472         |
| B. Strength of randomly oriented fiber<br>composites and laminates  | 479         |
| IV. Other Properties  | 483         |
| A. Creep  | 483         |
| B. Fatigue  | 485         |
| C. Heat distortion temperature  | 486         |
| D. Impact strength  | 488         |
| E. Acoustic emission  | 491         |
| F. Dynamic mechanical properties  | 491         |
| G. Coefficients of thermal expansion  | 492         |
| V. Ribbon-Filled Composites   | 495         |
| VI. Other Types of Composites   | 500         |
| A. Flake-filled polymers  | 500         |
| B. Composites with thick interlayers  | 502         |
| C. Interpenetrating network composites  | 502         |
| Summary   | 503         |
| Problems  | 504         |
| References  | 505         |
| <b>Appendixes</b>   | <b>515</b>  |
| I. Chemical Structure of Common Polymers  | 516         |
| II. Conversion Factors for Moduli, Stress, and Viscosity  | 519         |
| III. Glass Transition Temperatures and Melting Points<br>of Polymers  | 520         |
| IV. Relations Between Engineering Moduli and<br>Tensor Moduli and Tensor Compliances for<br>Anisotropic Methods | 524         |
| V. On Rubberlike Elasticity   | 528         |
| VI. List of Symbols   | 533         |
| <b>Index</b>  | <b>545</b>  |

# Contents

|  |           |
|--|-----------|
| <b>Preface to the Second Edition</b>               | <b>it</b> |
| <b>Preface to the First Edition</b>                | <b>fg</b> |
| <b>1. Mechanical Tests and Polymer Transitions</b> | <b>I</b>  |
| <b>I.</b> Introduction                             |           |
| <b>II.</b> Mechanical Tests                        |           |
| A. Creep tests                                     | jp        |
| B. Stress-relaxation tests                         | P         |
| C. Stress-strain tests                             | \$j       |
| D. Dynamic mechanical test?                        | <b>if</b> |
| E. Other tests                                     | l§        |
| <b>III.</b> Glass Transitions                      | <b>M</b>  |
| A. Chemical structure and $T_g$                    | <i>iJ</i> |
| B. Structural factors affecting $T_g$              | 19        |
| <b>IV.</b> Crystallinity                           | 23        |
| A. Melting points                                  | 24        |
| Problems   | 27        |
| References   | 28        |

|  |            |
|--|------------|
| <b>2. Elastic Moduli</b>                               | <b>33</b>  |
| 1. Isotropic and Anisotropic Materials                 | 33         |
| A- Isotropic materials                                 | 33         |
| if.. Anisotropic materials                             | 34         |
| 17. Methods of Measuring Moduli                        | 36         |
| A. Young's modulus                                     | 36         |
| B. Young's and shear moduli from vibration frequencies | 40         |
| JJI. Relations of Moduli to Molecular Structure        | 43         |
| A. Effects of molecular weight                         | 44         |
| B_ Effect of cross-linking                             | 49         |
| C. Effect of crystallinity                             | 50         |
| 13. Copolymerization and plasticization                | 53         |
| E- Block and graft polymers and polyh. (n4)»:          | 54         |
| Problems   | 56         |
| References   | 58         |
| <b>3. Creep and Stress Relaxation</b>                  | <b>63</b>  |
| 1. Introduction  | 63         |
| II. Models   | 64         |
| III. Distribution of Relaxation and Retardation Times  | 69         |
| IV. Superposition Principles                           | 73         |
| 'Ui Nonlinear Response                                 | 82         |
| A. Strain dependence of stress relaxation              | 82         |
| B. Stress dependence of creep                          | 84         |
| VI. Effect of Pressure                                 | 87         |
| YLJ. Thermal Treatments                                | 87         |
| VII). Effect of Molecular Weight: Molecular Theory     | 89         |
| IX. Effect of Plasticizers on Melt Viscosity           | 100        |
| X. Cross-linking                                       | 102        |
| XI. Crystallinity                                      | 109        |
| XII. Copolymers and Plasticization                     | 113        |
| XHf. Effect of Orientation                             | 115        |
| XIV. Block Polymers and Polyblends:-                   | 117        |
| Summary  | 118        |
| Problems   | 120        |
| References   | 123        |
| <b>4. Dynamical Mechanical Properties</b>              | <b>131</b> |
| I- Introduction and Instruments                        | 131        |
| H. Temperature and Frequency Effects                   | 135        |



# Mechanical Tests and Polymer Transitions

## 1. INTRODUCTION

Most plastic materials are used because they have desirable mechanical properties at an economical cost. For this reason, the mechanical properties may be considered the most important of all the physical and chemical properties of high polymers for most applications. Thus everyone working with such materials needs at least an elementary knowledge of their mechanical behavior and how this behavior can be modified by the numerous structural factors that can be varied in polymers. High polymers, a few of which have their chemical structure shown in Appendix I, have the widest variety and range of mechanical properties of all known materials. Polymers vary from liquids and soft rubbers to very hard and rigid solids.

Unfortunately, this virtuosity is sometimes viewed instead as a baffling complexity. One of the purposes of this book, therefore, is to show that there is an underlying order and organization that can serve as a logical framework and guide to this variety and to the interplay between properties and these structural features. The interplay is important because of the need to understand how structural modifications made to achieve some desired property can affect other properties at the same time. There are a great many structural factors that determine the nature of the mechanical behavior of such materials. One of the primary aims of this book is to

show how the following structural factors, in addition to the chemical composition, affect all of the major mechanical properties of polymers:

1. Molecular weight
2. Cross-linking and branching
3. Crystallinity and crystal morphology
4. Copolymerization (random, block, and graft)
5. Plasticization
6. Molecular orientation
7. Fillers
8. Blending
9. Phase separation and orientation in blocks, grafts, and blends

In addition to the structural and molecular factors listed above, the following environmental or external variables are important in determining mechanical behavior:

1. Temperature
2. Time, frequency, rate of stressing or straining
3. Pressure
4. Stress and strain amplitude
5. Type of deformation (shear, tensile, biaxial, etc.)
6. Moist treatments or thermal history
7. Nature of surrounding atmosphere, especially moisture content

There is a strong dependence on temperature and time of the properties of polymers compared to those of other materials such as metals. This strong dependence of properties on temperature and on how fast the material is deformed (time scale) is a result of the viscoelastic nature of polymers. Viscoelasticity implies behavior similar to both viscous liquids in which the rate of deformation is proportional to the applied force and to purely elastic solids in which the deformation is proportional to the applied force. In viscous systems, all the work done on the system is dissipated as heat, whereas in elastic systems all the work is stored as potential energy, as in a stretched spring. It is this dual nature of polymers that makes their behavior so complex and at the same time so interesting. The great variety of mechanical tests and the numerous factors listed above would make study of the mechanical properties of polymers very complex if it were not for some general phenomena and principles that underlie all of these various properties and determine the outcome of various test or use conditions. These principles organize and systematize the study, understanding, and prediction or estimation of this complex array of properties, including interdependences. They do this with just a very few equations (or functions) and a few characteristic parameters.

## II. MECHANICAL TESTS

There are a bewildering number of mechanical tests and testing instruments. Most of these tests are very specialized and have not been officially recognized as standardized tests. Some of these tests, however, have been standardized and are described in the publications of the American Society for Testing and Materials (1). Many of the important tests for plastics are given as ASTM standards in a series of volumes. The important volumes (parts) covering polymeric materials are listed in Table 1. Although many tests have been standardized, it must be recognized that a standardized test may be no better than one that is not considered a standard. One objective of a standardized test is to bring about simplicity and uniformity to testing, and such tests are not necessarily the best for generating the most basic information or the special type of information required by a research problem. The tests may not even correlate with practical use tests in some cases.

Besides the ASTM standard tests, a number of general reference books have been published on testing and on the mechanical properties of polymers and viscoelastic materials (2-7). Unfortunately, a great variety of units are used in reporting values of mechanical tests. Stresses, moduli of elasticity, and other properties are given in such units as MK.S (SI), cgs, and English units. A table of conversion factors is given in Appendix II.

### A. Creep Tests

Creep tests give extremely important practical information and at the same time give useful data on those interested in the theory of the mechanical properties of materials. As illustrated in Figure 1, in creep tests one mea-

Table 1 ASTM Standards

| Part No. | Materials covered  |
|----------|--|
| 15       | Paper, packaging   |
| 16       | Structural sandwich constructions, wood, adhesives         |
| 20       | Paint: Materials specifications and tests                  |
| 21       | Paint: Tests for formulated materials and applied coatings |
| 24       | Textiles: Yarns and fabrics                                |
| 25       | Textiles: Fibers   |
| 26       | Plastics: Specifications                                   |
| 27       | Plastics: Methods of testing                               |
| 28       | Rubbers  |
| 29       | Electrical insulating materials                            |

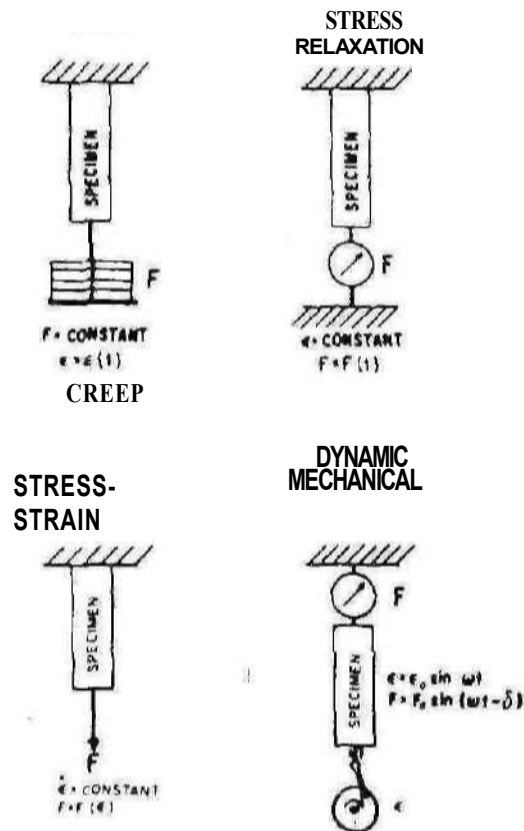


Figure 1 Schematic diagrams of various types of tensile tests  $F$ , force;  $e$  strain or elongation.

ures over a period of time the deformation brought about by a constant load or force, or for a true measure of the response, a constant stress. *Creep* tests measure the change in length of a specimen by a constant tensile force or stress, but creep tests in shear, torsion, or compression are also made. If the material is very stiff and brittle, creep tests often are made in flexure but in such cases the stress is not constant throughout the thickness of the specimen even though the applied load is constant. Figure 2 illustrates the various types of creep tests. In a creep test the deformation increase with time. If the strain is divided by the applied stress, one obtains a quantity known as the compliance. The compliance is a time-dependent reciprocal modulus, and it will be denoted by the symbol  $J$  for shear compliance and  $D$  for tensile compliance (8).

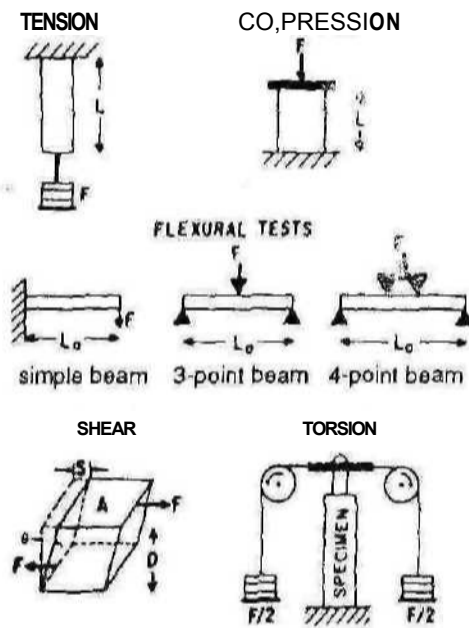


Figure 2 Types of creep tests,

If the load is removed from a creep specimen after some time, there is a tendency for the specimen to return to its original length or shape. A recovery curve is thus obtained if the deformation is plotted as a function of time after removal of the load,

## B. Stress-Relaxation Tests

In stress-relaxation tests, the specimen is quickly deformed a given amount, and the stress required to hold the deformation constant is measured as a function of time. Such a test is shown schematically in Figure 1. If the stress is divided by the constant strain, a modulus that decreases with time is obtained. Stress-relaxation experiments are very important for a theoretical understanding of viscoelastic materials. With experimentalists, however, such tests have not been as popular as creep tests. There are probably at least two reasons for this: (1) Stress-relaxation experiments, especially on rigid materials, are more difficult to make than creep tests; and (2) creep tests are generally more useful to engineers and designers.

### C. Stress-Strain Tests

In stress-strain tests the buildup of force (or stress) is measured as the specimen is being deformed at a constant rate. This is illustrated in Figure I. Occasionally, stress-strain tests are modified to measure the deformation of a specimen as the force is applied at a constant rate, and such tests are becoming commonplace with the advent of commercially available load-controlled test machines. Stress-strain tests have traditionally been the most popular and universally used of all mechanical tests and are described by ASTM standard Tests such as D638, D882, and D412. These tests can be more difficult to interpret than many other tests because the stress can become nonhomogeneous (i.e., it varies from region to region in the specimen as in cold-drawing or necking and in crazing). In addition, several different processes can come into play (e.g., spherulite and/or lamella breakup in crystalline polymers in addition to amorphous chain segment reorientation). Also, since a polymer's properties are time dependent, the shape of the observed curve will depend on the strain rate and temperature. Figure 3 illustrates the great variation in stress-strain behavior of polymers as measured at a constant rate of strain. The scales on these graphs

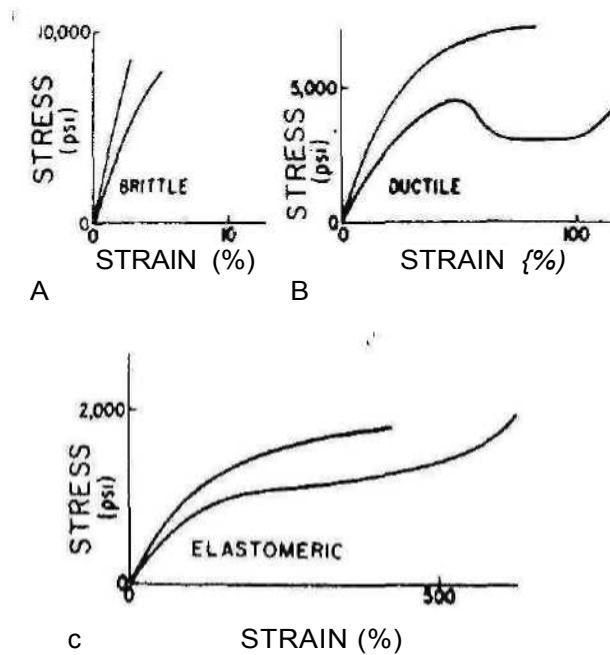


Figure 3 General types of stress-strain curves.

are not exact but are intended to give an order-of-magnitude indication of the values encountered. The first graph (A) is for hard, brittle materials. The second graph (B) is typical of hard, ductile polymers. The top curve in the ductile polymer graph is for a material that shows uniform extension. The lower curve in this graph has a yield point and is typical of a material that cold-draws with necking down of the cross section in a limited area of the specimen. Curves of the third graph (C) are typical of elastomeric materials.

Figure 4 helps illustrate the terminology used for stress-strain testing. The slope of the initial straight-line portion of the curve is the elastic modulus of the material. In a tensile test this modulus is Young's modulus,

$$E = \frac{d\sigma}{d\epsilon} \quad (1)$$

The maximum in the curve denotes the stress at yield  $\sigma_y$  and the elongation at yield  $\epsilon_y$ . The end of the curve denotes the failure of the material, which is characterized by the tensile strength  $\sigma_b$  and the ultimate strain or elongation to break  $\epsilon_b$ . These values are determined from a stress-strain curve while the actual experimental values are generally reported as load-deformation curves. Thus the experimental curves require a transformation of scales to obtain the desired stress-strain curves. This is accomplished by the following definitions. For tensile tests:

$$\text{stress } \sigma = \frac{\text{force or load } F}{\text{cross-sectional area } A} \quad (2)$$

If the cross-sectional area is that of the original undeformed specimen, this is the engineering stress. If the area is continuously monitored or known

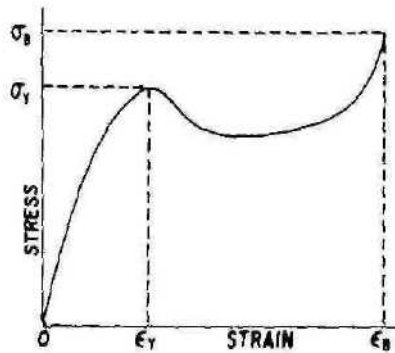


Figure 4 Stress-strain notation.

during the test, this is the true stress. For large strains (i.e. Figure 3.B and C) there is a significant difference.

The strain  $\epsilon$  can be defined in several ways, as given in Table 2, but for engineering (and most theoretical) purposes, the strain for rigid materials is defined as

$$\epsilon = \frac{L - L_0}{L_0} = \frac{\Delta L}{L_0} \quad (3)$$

The original length of the specimen is  $L_0$  and its stretched length is  $L$ . At very small deformations, all the strain definitions of Table 2 are equivalent. For shear tests (see Figure 2)

$$\text{shear stress } \sigma_s = \frac{\text{shear force } F}{\text{area of shear face } A} \quad (4)$$

$$\text{shear strain } \gamma = \frac{\text{amount of shear displacement } S}{\text{distance between shearing surfaces } D} = \tan \theta \quad (5)$$

for shear of a rod the strains are not uniform, but for small angular displacements under a torque  $AT$ , the maximum stress and strain occur

Table 2 Definitions of Tensile Strain

| Definition   | Name                         |
|--|------------------------------|
| $\epsilon = \frac{L - L_0}{L_0} = \frac{\Delta L}{L_0}$                                | Cauchy (engineering)         |
| $\epsilon = \frac{L - L_0}{L}$   |                              |
| $\epsilon = \ln \frac{L}{L_0}$   |                              |
| $\epsilon = \frac{1}{3} \left[ \frac{L}{L_0} - \left( \frac{L_0}{L} \right)^2 \right]$ | kinetic theory of rubberlike |
| $\epsilon = \frac{1}{2} \left[ \left( \frac{L}{L_0} \right)^2 - 1 \right]$             | elasticity                   |
| $\epsilon = \frac{1}{2} \left[ 1 - \left( \frac{L_0}{L} \right)^2 \right]$             | Kirchhoff                    |
| $\epsilon = \left[ \left( \frac{L}{L_0} \right)^n - 1 \right]$                         | Murnaghan                    |

seth (n is Variable)



at the surface and are given by

$$\text{shear stress (maximum)} = \frac{2F}{\pi R^3}$$

$$\text{shear strain (maximum)} = \frac{Qd}{h}$$

if Hooke's law holds, the elastic moduli are defined by the equations

$$\sigma = E\epsilon \quad (\text{tensile tests}) \quad (6)$$

$$\sigma_s = G\gamma \quad (\text{shear tests}) \quad (7)$$

where E is the Young's modulus and G is the shear modulus.

Tensile stress-strain tests give another elastic constant, called Poisson's ratio,  $\nu$ . Poisson's ratio is defined for very small elongations as the decrease in width of the specimen per unit initial width divided by the increase in length per unit initial length on the application of a tensile load:

$$\nu = \frac{-\epsilon_T}{\epsilon} = -\frac{d \ln \epsilon_T}{d \ln \epsilon} \quad (8)$$

In this equation  $\epsilon$  is the longitudinal strain and  $\epsilon_T$  is the strain in the width (transverse) direction or the direction perpendicular to the applied force. It can be shown that when Poisson's ratio is 0.50, the volume of the specimen remains constant while being stretched. This condition of constant volume holds for liquids and ideal rubbers. In general, there is an increase in volume, which is given by

$$\frac{\Delta V}{V_0} = (1 - 2\nu)\epsilon \quad (9)$$

where  $\Delta V$  is the increase in the initial volume  $V_0$  brought about by straining the specimen. Note that  $\nu$  is therefore not strictly a constant. For strains beyond infinitesimal, a more appropriate definition is (9)

$$\nu = -\frac{\ln \lambda_T}{\ln \lambda} = -\frac{\ln(1 + \epsilon_T)}{\ln(1 + \epsilon)} \quad (10)$$

Moreover, for deformations other than simple tension the apparent Poisson's ratio  $-\epsilon_T/\epsilon$  is a function of the type of deformation.

---

Poisson's ratio is used by engineer's in place of the more fundamental quality desired, the bulk modulus. The latter is in fact determined by  $\nu$  for linearly elastic systems—the widespread use of  $\nu$  engineering equation for large deformations, however, where the Strain is not proportional to the stress, a single value of the bulk modulus may still suffice even when the value of  $\nu$  is not constant,

### D, Dynamic Mechanical Tests

A fourth type of test is known as a dynamic mechanical test. Dynamic mechanical tests measure the response of a material to a sinusoidal or other periodic stress. Since the stress and strain are generally not in phase, two quantities can be determined: a modulus and a phase angle or a damping term. There are many types of dynamic mechanical test instruments. One type is illustrated schematically in Figure 1. The general type of dynamic mechanical instruments are free vibration, resonance forced vibration, non-resonance forced vibration, and wave or pulse propagation instruments (3,4). Although any one instrument has a limited frequency range, the different types of apparatus are capable of covering the range from a small fraction of a cycle per second up to millions of cycles per second. Most instruments measure either shear or tensile properties, but instruments have been built to measure bulk properties.

Dynamic mechanical tests, in general, give more information about a material than other tests, although theoretically the other types of mechanical tests can give the same information. Dynamic tests over a wide temperature and frequency range are especially sensitive to the chemical and physical structure, of plastics. Such tests are in many cases the most sensitive tests known for studying glass transitions and secondary transitions in polymers as well as the morphology of crystalline polymers.

Dynamic mechanical results are generally given in terms of complex moduli or compliances (3,4). The notation will be illustrated in terms of shear modulus  $G$ , but exactly analogous notation holds for Young's modulus  $F$ . The complex moduli are defined by

$$G^* = G' + iG'' \quad (11)$$

where  $G^*$  is the complex shear modulus,  $G'$  the real part of the modulus,  $G''$  the imaginary part of the modulus, and  $i = \sqrt{-1}$ .  $G'$  is called the storage modulus and  $G''$  the loss modulus. The latter is a damping or energy dissipation term. The angle that reflects the time lag between the applied stress and strain is  $\delta$ , and it is defined by a ratio called the loss tangent or dissipation factor:

$$\tan \delta = \frac{G''}{G'} \quad (12)$$

$\tan \delta$ , a damping term, is a measure of the ratio of energy dissipated as heat to the maximum energy stored in the material during one cycle of oscillation. For small to medium amounts of damping,  $G'$  is the same as the shear modulus measured by other methods at comparable time scales. The loss modulus  $G''$  is directly proportional to the heat  $H$  dissipated per

**Mechanical Tests and Polymer Transitions** 11cycle as given by

$$H = \pi G'' \gamma_0^2 \quad (13)$$

$$J^* = J' - iJ'' \quad (14)$$

$$\eta^* = \eta' - i\eta'' \quad (15)$$

Some of the interrelationships between the complex quantities are

$$G' = \omega \eta' \quad \text{and} \quad G'' = \omega \eta'' \quad (16)$$

$$G' = \frac{J'}{J^2} \quad \text{and} \quad J' = \frac{G'}{G''} \quad (17)$$

$$\frac{G''}{G'} = \frac{J''}{J'} \quad (18)$$

where

$$G^2 = G'^2 + G''^2 \quad \text{and} \quad J^2 = J'^2 + J''^2 \quad (19)$$

where  $\gamma_0$  is the maximum value of the shear strain during a cycle. Other dynamic mechanical terms expressed by complex notation include the complex compliance  $J^*$  and the complex viscosity  $\eta^*$ .

and  $\omega$  is the frequency of the oscillations in radians per second. Note that the real part of the complex viscosity is an energy-dissipation term, just as is the imaginary part of the complex modulus.

Damping is often expressed in terms of quantities conveniently obtained with the type of instrument used. Since there are so many kinds of instruments, there are many damping terms in common use, such as the logarithmic decrement  $\Delta$ , the half-width of a resonance peak, the half-power width of a resonance peak, the Q factor, specific damping capacity  $\eta'$ , the resilience  $R$ , and decibels of damping dB.

The logarithmic decrement  $\Delta$  is a convenient damping term for free-vibration instruments such as the torsion pendulum illustrated in Figure 5 for measuring shear modulus and damping. Here the weight of the upper sample **champ** and the inertia bar are supported by a compliant torsion wire suspension or a magnetic suspension (10) to prevent creep of the specimen if it had to support them. As shown in the bottom of this figure, the successive amplitudes  $A_n$  decrease because of the gradual dissipation of the elastic energy into heat. The logarithmic decrement is defined by

$$\Delta = \ln \frac{A_1}{A_2} = \ln \frac{A_2}{A_3} = \dots = \frac{1}{n} \ln \frac{A_1}{A_{1+n}} \quad (20)$$

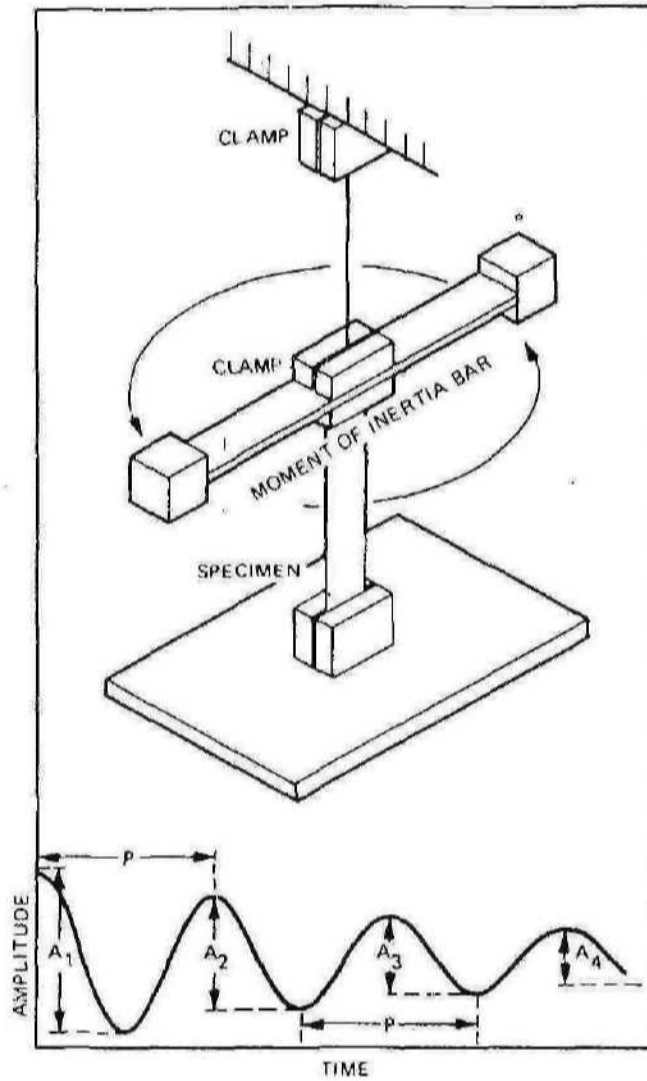


Figure 5 Schematic diagram of a torsion pendulum and a typical damped oscillation curve. |Modified from L. E. Nielsen,

It is related to the dissipation factor approximately by

$$\Delta \approx \pi \frac{G''}{G'}$$
(21)

This equation is accurate at low damping ( $A < 1$ ), but the error becomes large at high damping. More exact equations have been discussed by Struik (11) and Nielsen (4). The standard ASTM test is D2236-69.

Damping may be obtained from forced resonance vibration instruments from plots of amplitude of vibration versus frequency through the resonance peak. Figure 6 illustrates such a plot of a resonance peak. Using the notation shown in this figure, the damping may be expressed, as

$$\frac{f_2 - f_1}{f_R} \approx \sqrt{3} \frac{E''}{E'}$$
(22)

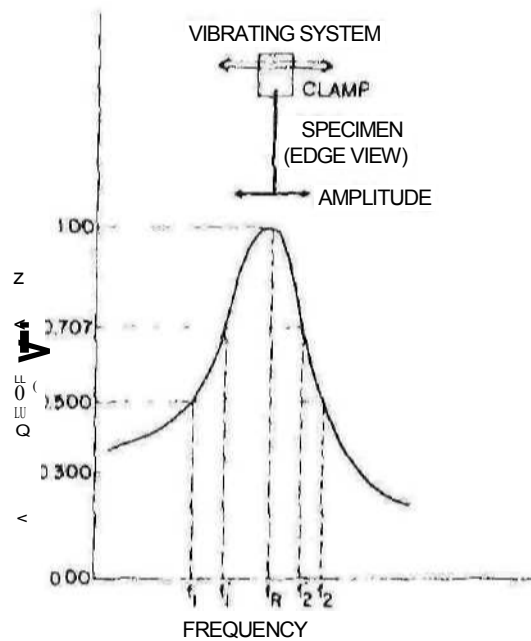


Figure 6 Typical amplitude-frequency curve obtained with a vibrating reed apparatus. [From L. E. Nielsen,

form the half-height width or

form the root mean square (rms) height peak, width. The damping is expressed in this case by  $E''/E'$  rather than as  $G''/G'$  since in the case illustrated, Young's modulus is determined instead of the shear modulus. Other common damping terms may be expressed in terms of the dissipation factor in the following parameters and equations:

reciprocal  $Q$

loss dB

sometimes it is desirable to be able to estimate damping values in shear form measurements made in tension, or vice versa, As a first approximation, very appropriate to rubbery, incompressible materials.

$$\frac{E''}{E'} \approx \frac{G''}{G'} \quad (28)$$

More exact equations, such as

$$\frac{E''}{E'} = \frac{G''}{G'} \frac{1}{1 + (G''/3K)[1 + (G''/G')^2]} \quad (29)$$

show that  $G''/G'$  is equal to or slightly greater than  $E''/E'$ . (12,13). in equation (29).  $K$  is the bulk modulus.

There are many other types of mechanical tests in common use. One of the most important of these tests is the impact strength of materials. Impact tests measure resistance to breakage under specified conditions when the test specimen is struck at high velocity. Such tests are some measurement of the toughness of the polymer. They are very important practical tests, especially where an experience base has been built up over time. However, as usually done, they are difficult to define and analyze in scientific terms, and hence it has been difficult to employ the results directly in designs. However, instrumental impact testers are now commercially available together with greatly improved analysis techniques (14), and the situation is improving rapidly. The three most widely used impact testers are the falling ball or dart testers (4.5.15), Izod tester (16.18), and Charpy tester (16), high-speed tensile stress-strain testers (19.20) may also be considered as impact or toughness testers.

For a quantitative measure of toughness, which can be used to relate the apparent toughness values observed in the different practical tests or conducting a stress analysis of functional parts, the fracture toughness test is used (14,21-23). Fracture toughness is a measure of the ability of a material to resist extension of a pre-existing crack, despite the stress concentration that is built up there. In these tests, the ends of a precracked specimen are pulled apart in a direction perpendicular to the plane of the crack (called a mode I test), or parallel but transverse to the plane of the crack (mode II). In a third mode, the plane of the crack is sheared by a sliding motion in the direction of the crack. ASTM E399-83 gives sample dimensions and procedures.

In contrast to the impact tests, these can be analysed; toughness is reported as the critical energy release rate ( $G_c$ ), or the stress concentration factor  $K_{Ic}$ . Values may range from 5000 J/m<sup>2</sup> for a tough nylon or polycarbonate down to 350 J/m<sup>2</sup> for brittle unmodified polystyrene. The values can be sensitive to rate and temperature.

Except for a few thermoset materials, most plastics soften at some temperatures. At the softening or heat distortion temperature, plastics become easily deformable and tend to lose their shape and deform quickly under a load. Above the heat distortion temperature, rigid amorphous plastics become useless as structural materials. Thus the heat distortion test, which defines the approximate upper temperature at which the material can be safely used, is an important test (4.5.7.24). As expected, for amorphous materials the heat distortion temperature is closely related to the glass transition temperature, but for highly crystalline polymers the heat distortion temperature is generally considerably higher than the glass transition temperature. Fillers also often raise the heat distortion test well above

the glass transition temperature. Other common mechanical tests include hardness, scratch resistance, friction, abrasion, tear, and fatigue tests (1,4,5).

### III. GLASS TRANSITIONS

Most polymers are either completely amorphous or have an amorphouslike component even if they are crystalline. Such materials are hard, rigid glasses below a fairly sharply defined temperature known as the glass transition temperature  $T_g$ . At temperatures above the glass transition temperature, at least at slow to moderate rates of deformation, the amorphous polymer is soft and flexible and is either an elastomer or a very viscous liquid. Mechanical properties show profound changes in the region of the glass transition. For example, the elastic modulus may decrease by a factor of over 1000 times as the temperature is raised through the glass transition region. For this reason,  $T_g$  can be considered the most important material characteristic of a polymer as far as mechanical properties are concerned. Many other physical properties change rapidly with temperature in the glass transition region. These properties include coefficients of thermal expansion (25,26), heat capacity (25,27), refractive index (28), mechanical damping (4), nuclear magnetic (29) and electron spin resonance behavior (30,31), electrical properties (32-35), and tensile strength and ultimate elongation in elastomers (36,37). In view of the great practical importance of the glass transition temperature, a table of  $T_g$  values for many common polymers is given in Appendix III. An extensive compilation is given in Ref. 38. Elastomeric; or rubbery materials have a  $T_g$ , or softening temperature value, below room temperature. Brittle, rigid polymers have a  $T_g$  value above room temperature. Glass transitions vary from  $-143^\circ\text{C}$  for poly(diethyl siloxane) rubber (39) to  $100^\circ\text{C}$  for polystyrene and on up to above  $300^\circ\text{C}$  or above the decomposition temperature for highly cross-linked phenol-formaldehyde resins and polyelectrolytes (40,41).

In addition to its practical importance,  $T_g$  has important theoretical implications for the understanding of the molecular origin of polymer mechanical behavior (3,4,6,35,42-45) and plays a central role in establishing the framework, mentioned above, which relates the properties of different polymers to each other (3;46,47).

The glass transition temperature is generally measured by experiments that correspond to a time scale of seconds or minutes. If the experiments are done more rapidly, so that the time scale is shortened, the apparent  $T_g$  value is raised. If the time scale is lengthened to hours or days, the apparent  $T_g$  value is lowered. Thus, as generally measured,  $T_g$  is not a true constant but shifts with the time scale of the experiment or observation. Moreover,  $T_g$  is masked by experimental difficulties, compounded by multiple and often inaccurate definitions of  $T_g$  in the literature. The least



ambiguous and soundest one is that temperature at which the volumetric thermal expansion coefficient undergoes a step change at heating and cooling rates of 1 C/min. Increasing the time scale by a factor of 10 will shift the apparent  $T_g$  by roughly 3°C [volumetric measurements (3)] to 7°C (maximum in  $\tan \delta$  plot) for a typical polymer.

The explicit nature of the glass transition is not clear, and many theories, some conflicting, have been proposed (25,42-45,48-53). It represents an interrupted approach to a hypothetical thermodynamic state of zero configurational entropy and close-ordered segmental packing. This state cannot be reached because the molecular motions that permit rearrangement to better packing and lower entropy become exponentially slower with decreasing temperature. Finally, at some rather small temperature range,  $T_g$ , the rate of further change exceeds the time scale of measurement. The hypothetical glass temperature is the polymeric equivalent of 0 K. for an ideal gas and lies roughly 50 K below the volumetric  $T_K$ . Thus  $T_g$  is an operational reference temperature for the onset of segmental rearrangements. The volume required for rearrangements is called the free volume. Although the theoretical nature of the glass transition is subject to debate, the practical importance of  $T_g$  cannot be disputed.

### A. Chemical Structure and $T_g$

Several factors related to chemical structure are known to affect the glass transition temperature. The most important factor is chain stiffness or flexibility of the polymer. Main-chain aliphatic groups, ether linkages, and dimethylsiloxane groups build flexibility into a polymer and lower  $T_g$ . Aliphatic side chains also lower  $T_g$ , (the effect of the length of aliphatic groups is illustrated by the methacrylate series (4,38):

---

Methyl ester  
Ethyl n-Propyl  
n-Butyl

*n-Octyl*

+Thus  $T_g$  is sensitive to the nature of the polymer chain structure such as the maximum in  $\tan \delta$  are not only sensitive to the frequency of the transition (which should always be stated) but also to extraneous features such as the degree of crosslinking, the amount of filler present, and the presence of a second phase (e.g., crystallinity), all of which can significantly change the value of the temperature at which  $\tan \delta$  is observed. In fact, when the dilatometric  $T_g$ , which is insensitive to such features, remains unaltered, it is often not coincidental.

On the other hand, large or rigid groups such as substituted aromatic structures and pendant tertiary butyl groups raise the glass transition temperature. The effect of decreasing molecular flexibility by the substitution of bulky side groups onto a polymer chain is illustrated by the polystyrenes ( $T_g = 100^\circ\text{C}$ ) and poly(2,6-dichlorostyrene) ( $T_g = 167^\circ\text{C}$ ). However it is the flexibility of the group, not its size, that is the factor determining  $T_g$ . Thus increasing the size of an aliphatic group can actually lower the glass transition temperature, as illustrated in the methacrylate series above.

A second factor important in determining  $T_g$  value is the molecular polarity or the cohesive energy density of the polymer. Increasing the polarity of a polymer increases its  $T_g$ . Thus in the series polypropylene ( $T_g = 10^\circ\text{C}$ ), poly(vinyl chloride) ( $T_g = 85^\circ\text{C}$ ), and polyacrylonitrile ( $T_g = 101^\circ\text{C}$ ) the size of the side groups is about the same, but the polarity increases. The effect of cohesive energy density or the strength of intermolecular forces is further illustrated by the series poly(methyl acrylate) ( $T_g = 3^\circ\text{C}$ ), poly(acrylic acid) ( $T_g = 106^\circ\text{C}$ ), and poly(zinc acrylate) ( $T_g > 400^\circ\text{C}$ ). In this series, the strong hydrogen bonds in poly(acrylic acid) greatly increase the intramolecular forces over those found in the methyl ester polymer. The intramolecular forces are increased more in the zinc compound by the even stronger ionic bonds, which have many of the characteristics of cross-links.

A third factor influencing the value of  $T_g$  is backbone symmetry, which affects the shape of the potential wells for bond rotations. This effect is illustrated by the pairs of polymers polypropylene ( $T_g = 10^\circ\text{C}$ ) and polyisobutylene ( $T_g = -70^\circ\text{C}$ ), and poly(vinyl chloride) ( $T_g = 87^\circ\text{C}$ ) and poly(vinylidene chloride) ( $T_g = -19^\circ\text{C}$ ). The symmetrical polymers have lower glass transition temperatures than the unsymmetrical polymers despite the extra side group, although polystyrene ( $100^\circ\text{C}$ ) and poly( $\alpha$ -methylstyrene) are illustrative exceptions. However, tacticity plays a very important role (54) in unsymmetrical polymers. Thus syndiotactic and isotactic poly(methyl methacrylate) have  $T_g$  values of 115 and 45  $^\circ\text{C}$  respectively.

The flexibility and cohesive energy density or polarity of each group are nearly independent of the other groups in the molecule to which they are attached (55-60). Because of this, each group can be assigned an apparent  $T_g$  value, and the  $T_g$  value of a polymer becomes the sum of the contri-

tutions of all the groups, that is.

$$T_g = \sum_i T_{gi} n_i \quad (30)$$

where  $n_i$  is the mole fraction of group  $i$  in the polymer.

A somewhat more complex treatment of group contributions (61) utilizes the fact that the total cohesive energy density,  $E(\text{coh})$  of the chain unit can be determined from Fedors' table of group contributions (62); the ratio of  $E(\text{coh})$  to the effective number of freely rotating groups per unit,  $\sum a_i$  is proportional to  $T_g$ . That is.

$$T_g = \frac{AE(\text{coh})}{\sum a_i} + C \quad (31)$$

where  $A = 0.0145 \text{ K mol}^{-1} \text{ J}^{-1}$  and  $C = 120 \text{ K}$ .

The strong dependence of  $T_g$  on free volume, (or an equivalent factor) is shown by a simple empirical rule and by the pressure dependence of  $T_g$ . The empirical rule is (63,64)

$$(\alpha_g - \alpha_g) T_g = 0.113 \pm 0.003 \quad (32)$$

where  $a_i$  and  $a_g$  are the volume coefficients of thermal expansion above and below  $T_g$ , respectively, and the term  $a_g - a_i$  is taken to be the expansion coefficient of the free volume. Pressure increases  $T_g$  (3,65-69). O'Reilly (65) found that pressure increases the  $T_g$  value of poly(vinyl acetate) at the rate of 0.22 K/MPa (0.22 C/atm). The  $T_g$  value of poly(vinyl chloride) increases by 0.14 K/MPa (0.14 C/atm), while the rate of increase is 0.18 K/MPa (0.18 C/atm) for poly(methyl methacrylate) (66). For polystyrene the rate of increase is about 0.17 K/MPa (0.017 C/bar) (67), and for polypropylene it is 0.20 K/MPa (0.020 C/kg cm<sup>-2</sup>) (68). Zoeller (69) has carried out extensive measurements of pressure effects on  $T_g$ . Theoretically, the  $T_g$  value should increase with pressure as a function of the ratio of the compressibility to the thermal coefficient of expansion of the polymer. Other thermodynamic relations concerning  $T_g$  have been reviewed by McKenna (70).

Most polymers show small secondary glass transitions below the main glass transition (3,37,71-76). These secondary transitions can be important in determining such properties as toughness and impact strength. These transitions are discussed in more detail in later chapters.

## B. Structural Factors Affecting $T_g$

The glass transition increases with number-average molecular weight  $M_n$ , to a limiting asymptotic value of  $T_g$  for infinite molecular weight, in the

practical range of molecular weights,  $T_g$  is given by (50.51.77.78)

$$T_g = T_g^\infty - \frac{K}{M_n} \quad (33)$$

where  $K$  is a constant characteristic of each polymer. For polystyrene  $K = 1.75 \times 10^5$ , so its  $T_g$  value increases from about 83°C for a molecular weight of  $10^4$  to 100°C for infinite molecular weight. The change in  $T_g$  arises from the ends of the polymer chains, which have more free volume

than the same number of atoms in the middle of the chain. Cowie (79.) and Boyer (80,81) suggest that a better representation, valid over a wider range in  $M_n$  is

$$T_g = T + k \log(M_n - M_{n(\max)}) \quad (34)$$

where  $k$  and  $M_{n(\max)}$  are again characteristic of each polymer and  $M_{n(\max)}$  defines a value above which  $T_g$  ceases to be molecular-weight dependent.

Cross-linking increases the glass transition of a polymer by introducing restrictions on the molecular motions of a chain (61.82-92). Low degrees of cross-linking, such as found in normal vulcanized rubbers, increase  $T_g$  only slightly above that of the uncross linked polymer. However, in highly cross-linked materials such as phenol-formaldehyde resins and epoxy resins.  $T_g$  is markedly increased by cross-linking (61,84,87,89-92). Two effects must be considered: (1) the cross-linking per se, and (2) a copolymer effect taking into account that a cross-linking agent generally is not chemically the same as the rest of the polymer (83). The chemical composition changes as cross-linking increases, so the copolymer effect can either raise Or lower the  $T_g$  value.

Nielsen (88) averaged the data in the literature and arrived at the approximate empirical equation

$$T_g - T_{g0} \approx \frac{3.9 \times 10^4}{M_c} \quad (35)$$

The number-average molecular weight between cross-linked points is  $M_n$  while  $T_{g0}$  is the glass transition temperature of the uncross-linked polymer having the same chemical composition as the cross-linked polymer; that is,  $T_g - T_{g0}$  is the shift in  $T_g$  due only to cross-linking after correcting for any copolymer effect of the cross-linking agent. Kreibich and Bauer (61) have amended and extended this expression and shown that the constant can be related to  $E(\text{coh})$  [cf. equation (31)].

DiMarzjo (93), Nielsen (88), DiBenedetto (94), and others (89) have derived theoretical equations relating the shift in  $T_g$  en used by cross-linking\*

DiBenedetto's equation is

$$\frac{T_g - T_{g0}}{T_{g0}} \doteq \frac{KX_c}{1 - X_c} \doteq \frac{2K}{n_c} \quad (36)$$

The mole fraction of the monomer units that are cross-linked in the polymer is  $X_c$ , and  $n_c$  is the number-average number of atoms in the polymer backbone between cross-links. The temperature should be expressed in absolute degrees in this equation. The constant  $K$  is predicted to be between 1.0 and 1.2; it is a function of the ratio of segmental mobilities of cross-linked to uncross-linked polymer units and the relative cohesive energy densities of cross-linked and uncross-linked polymer (88). The theoretical equation is probably fairly good, but accurate tests of it are difficult because of the uncertainty in making the correction for the copolymer effect and because of errors in determining  $n_c$ .

The degree of cross-linking has been expressed by many different quantities. For vinyl-type polymers, where there are two backbone atoms per monomer unit.

$$\frac{X_c}{1 - X_c} \doteq \frac{2}{n_c} = \frac{M_0}{M_c} \quad (37)$$

where  $M_0$  is the molecular weight of the monomer.

Plasticizers are low-molecular-weight liquids that lower the glass transition temperature of a polymer. A typical example is the use of dioctyl phthalate in poly(vinyl chloride) to convert the polymer from a rigid material to a soft, flexible one. If the glass transition of the two components  $A$  and  $B$  are known, an estimate can be made of the  $T_g$  value of the mixture by one or the other of the equations

$$T_g \doteq T_{gA}\phi_A + T_{gB}\phi_B \quad (38)$$

$$\frac{1}{T_g} \doteq \frac{W_A}{T_{gA}} + \frac{W_B}{T_{gB}} \quad (39)$$

The glass transition of the polymer is  $T_g$ , while that of the plasticizer is  $T_{gH}$ , the volume fraction of plasticizer is  $\phi_B$ , and its weight fraction is  $W_B$ . Typical values of  $T_g$  are between  $-50$  and  $-100^\circ\text{C}$ . To calculate more accurate values of  $T_g$  additional information must be available, such as the  $T_g$  value of a known mixture or the coefficients of thermal expansion ( $\alpha_A$  and  $\alpha_B$ ) of the pure components in both their liquid and glassy states (51,95). For each component  $i$

$$\alpha_i = \alpha_{iL} - \alpha_{iG} \quad (40)$$

where  $\alpha_{iL}$  is the volume coefficient of expansion above  $T_g$  and  $\alpha_{iG}$  is the coefficient below  $T_g$  for many polymers  $\alpha_A = 4.8 \times 10^{-4} \text{ K}^{-1}$ . The  $T_g$

value of plasticized polymers is then given by (51.96)'

$$T_g = \frac{T_{gA} + (KT_{gB} - T_{gA})\phi_B}{1 + (K - 1)\phi_B} \quad (41)$$

where A" is either an empirical constant of

$$K = \frac{\alpha_B}{\alpha_A} \quad (42)$$

Equation (41) becomes equation (38) if  $K = 1$ , and it is often close to equation (39) if  $K = 2$ .

An equation that usually fits experimental data better than equations (38) or (39) is the general mixture rule for two-component mixtures, in which there is a single phase; that is, the components are miscible (97)

$$T_g = T_{gA}X_A + T_{gB}X_B + lX_AX_B \quad (43)$$

where  $l$  is an interaction term and  $X_A$  and  $X_B$  are the mole fractions of polymer and plasticizer. The interaction term is usually positive if there is strong interaction of the plasticizer with the monomeric units of the polymer. If the packing of the plasticizer and polymer is poor,  $l$  may be negative, and the concentration variable probably should be volume fraction instead of mole fraction. This equation also has been used with the weight fraction as the concentration variable (98.99). The interaction constant has been used mostly as an empirical constant determined from experimental, but some attempts have been made to estimate it theoretically. Fox (100) has developed a complex theory that predicts a universal curve for  $T_g/T_{gA}$  as a function of plasticizer concentration.

The glass transition temperatures of copolymers are very analogous to those of plasticized materials if the comonomer B is considered to be a plasticizer for homopolymer A. Equations (38), (39), (41), and (43) are still applicable except that  $k$  is generally assumed to be an empirical constant (51.96.101.102).

Equation (43) has been used many times for the  $T_g$  value of copolymers (97.103.104). In copolymers, the distribution of AA, BB, and AB sequences is important in determining  $T_g$  (103.105.109). Random copolymers generally do not have the same  $T_g$  values as copolymers of the same overall composition but with the maximum possible number of AB sequences.

There is considerable confusion as to how the glass transition is affected by molecular orientation. In some experiments orientation lowers the apparent  $T_g$  value in the direction parallel to the orientation (110.113). The  $T_g$  value in the direction perpendicular to the orientation, on the other hand, may be increased (111). Others find that orientation increases the  $T_g$  value (114.115). Still others find no change in  $T_g$  value with stretching.

of rubbers (116). These  $T_g$  values were determined by varying experimental methods, so they are not always comparable. In any event, the effect is small.

#### IV. CRYSTALLINITY

Many polymers are not completely amorphous but are more or less crystalline. The degree of *Crystallinity* and the morphology of the crystalline material have profound effects on the mechanical behavior of polymers, and since these factors can be varied over a wide range, the mechanical properties of crystalline polymers take on a bewildering array of possibilities.

The nature of the mechanical property changes is discussed in subsequent chapters. The degree of crystallinity is generally measured by x-ray diffraction techniques (117, 119) or by measuring density (117, 120, 121), but some mechanical tests are the most sensitive indicators of Crystallinity (4). Morphological structure, including length of chains between folds in crystals and spherulitic structure, may be studied by light scattering (122, 123) small-angle x-ray scattering (119, 121, 124), and electron microscopy (125).

Highly crystalline polymers such as polypropylene have a complex morphological structure. The polymer chains generally appear to fold into lamellar structures on the order of 100 Å thick (125-129), with most chains turning and reentering the lamina from which they emerged. Figure 1. These lamellae stack together in layers to form ribbon-like structure\*. Between the layers are amorphous-like chain folds and some chains that go from one layer to the next to tie the entire structure together. Between the ribbons is more amorphous material. The lamellae often are part of a more complex spherulitic structure in which twisted lamellar ribbons radiate from a nucleation center (125, 127, 124, 130). Slow growth of the crystallites and annealing emphasize spherulitic structure, whereas quenching minimizes it. Figures 8 and 9 illustrate schematically some of the possible chain arrangements in crystalline polymers (131-133).

If the ordered, crystalline regions are cross sections of bundles of chains and the chains go from one bundle to the next (although not necessarily in the same plane), this is the older fringe-micelle model. If the emerging chains repeatedly fold back and reenter the same bundle in this or a different plane, this is the folded-chain model. In either case the mechanical deformation behavior of such complex structures is varied and difficult to unravel unambiguously on a molecular or microscopic scale. In many respects the behavior of crystalline polymers is like that of two-phase systems as predicted by the fringed-micelle model illustrated in Figure 7, in which there is a distinct crystalline phase embedded in an amorphous phase (134).

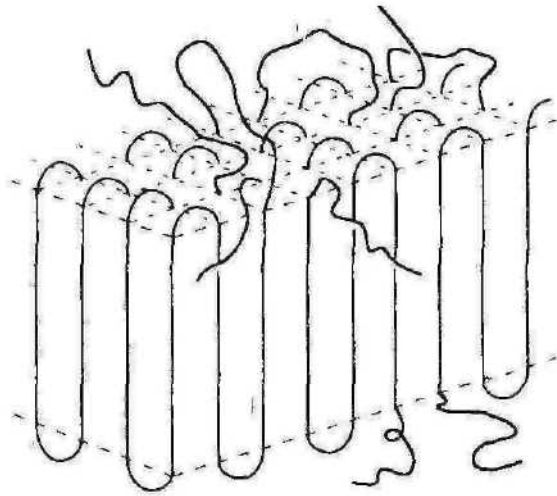


Figure 7 Chain folding in a polymer crystallite. The number of *re*-entrant folds per unit surface area would be much higher than sketched here.

A long polymer chain can go through several crystallite and amorphous regions.

#### A. Melting Points

Crystalline polymers do not have sharp melting points. Some of the crystallites, which are small or imperfect, melt before the final melting point is reached. An equilibrium theory giving the degree of Crystallinity as a function of temperature for crystallizable copolymers has been developed by Flory (135). A nonequilibrium theory that may be applicable for some quenched polymers has been proposed by Wunderlich (136). In the crystallization of copolymers, the longest segments of the crystallizable component crystallize first at the highest temperature. At lower temperatures the shorter segments crystallize. This is expected since low-molecular-weight homopolymers melt at lower temperatures than do high-molecular-weight homopolymers, as given by (137..138)

$$\frac{1}{T_m} - \frac{1}{T_m^*} = \frac{2RM_0}{\Delta H_u M_n} \quad (44)$$

In this equation  $T_m$  is the melting point in Kelvin of polymers with a number\* average molecular weight  $M_n$ . Polymer of infinite molecular weight melts at  $T_m^*$ . The molecular weight of the monomeric unit is  $M_0$ ,  $R$  the gas



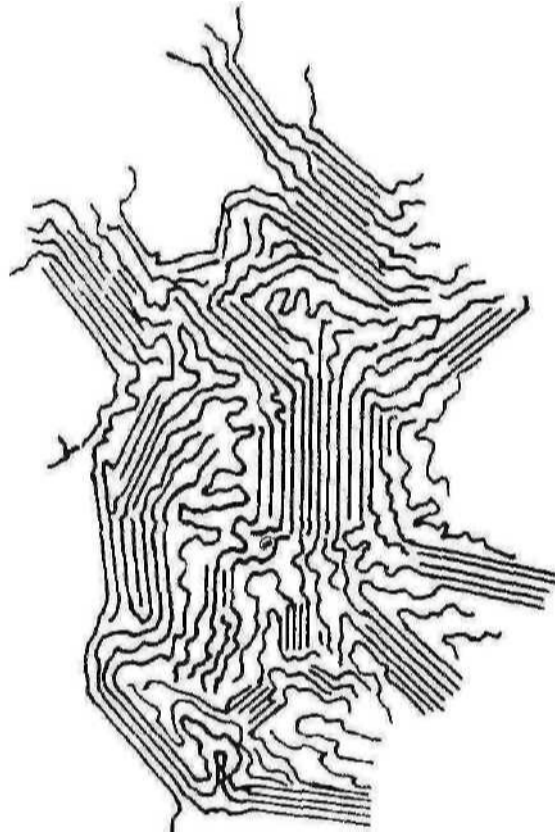


Figure 8 Fringe-micelle model of crystalline polymers. (Pram Ref. 131, )

constant, and  $\Delta H_u$  the heat of fusion per mole of crystalline polymer repeating unit.

Copolymerization usually lowers the melting point by shortening the length of crystallizable sequences. *For random copolymers the lowering of the melting point is* (138)

$$\frac{1}{T_m} - \frac{1}{T_m^0} = \frac{-R}{\Delta H_u} \ln X_A \quad (45)$$

where  $X_A$  is the mole fraction of the crystallizable comonomer  $A$  in the copolymer. Solvents and plasticizer also lower the melting point according

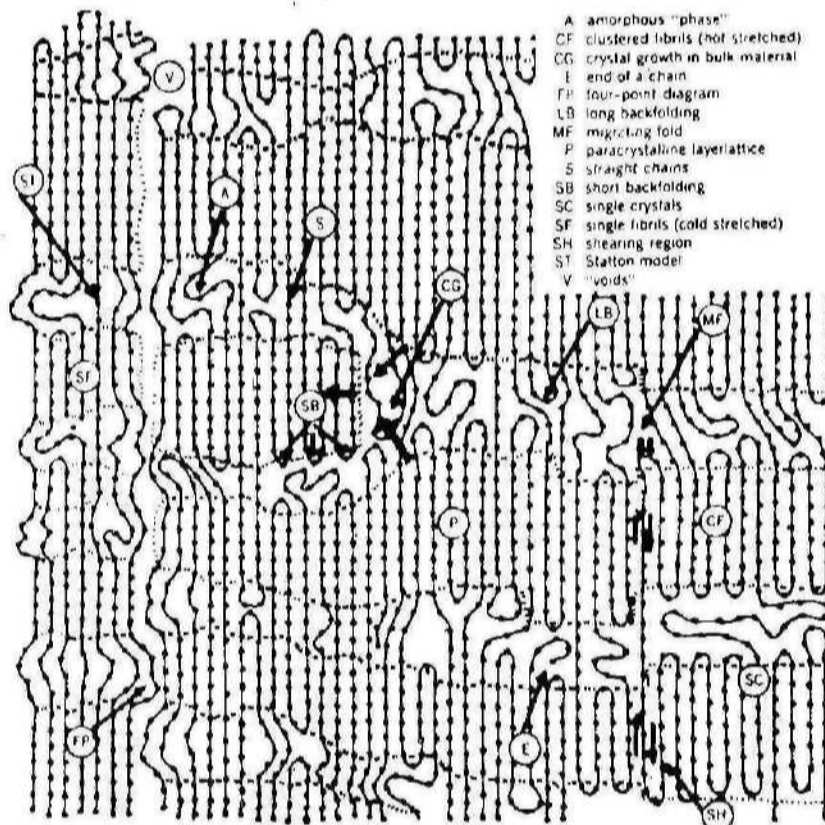


Figure 9 Types of chain ordering and folding which are possible within and between lamellae and between ribbon surfaces. In real, well-crystallized polymers, these variations are relatively far apart and the forms SC, CF, SB, and A predominate. (From Kef, 132.)

to the equation (138.140)

$$\frac{1}{T_m} - \frac{1}{T_m^0} = \frac{RV_u}{\Delta H_u V_s} (\phi_1 - \chi_1 \phi_1^2) \quad (46)$$

The molar volume of the polymer repeat unit is  $V_u$ ,  $V_s$  is the molar volume of the solvent,  $\phi_1$  is the volume fraction of the solvent, and  $\chi_1$  is an interaction term defining how good the solvent is for the polymer. The term  $\chi_1$  is negative for very good solvents and goes to about 0.55 for the limiting

case of very poor solvents. Good solvents lower the melting point more than do poor solvents.

Appendix III lists the melting points of many common polymers. More complete tables of melting points and heats of fusions may be found in Refs. 4, 38, 140, and 141.

Chemical structure factors affect the melting point and glass transition temperature in much the same manner. A good empirical rule for many polymers is (142-144)

$$\frac{T_g}{T_m} \doteq \frac{2}{3} \pm 0.04 \quad (47)$$

where the temperatures are given in Kelvin. Symmetrical molecules such as poly(vinylidene chloride) tend to have ratios about 0.06 smaller than unsymmetrical molecules such as polypropylene.

### PROBLEMS

1. Plot the various definitions of strain as defined in Table 2 as a function of  $AL/L_{it}$  from  $AL/L_{it} = 0$  to  $AL/L_{it} = 2$ .
2. Polystyrene has a shear modulus of  $1.25 \times 10^{11}$  dyn/cm<sup>2</sup> and a Poisson's ratio of 0.35 at 25°C. What is its Young's modulus in pounds per square inch?
3. A rubber has a shear modulus of  $10^7$  dyn/cm<sup>2</sup>. What is its modulus in the following units? (a) psi; (b) pascal, or newtons/m<sup>2</sup> (SI); (c) kg/cm<sup>2</sup>.
4. A load of 100 lb is applied to a specimen that has a length of 4 in. between grips, a width of 1 in., and a thickness of 0.10 in. If the Young's modulus of the material is  $3.5 \times 10^{11}$  dyn/cm<sup>2</sup>, how much will the specimen elongate when the load is applied?
5. A parallel-plate viscometer with a geometry such as shown in the lower left corner of Figure 2 is filled with a polymer melt of 10" P. What force is required to move the plates parallel to one another at a velocity of 1 cm/s if the spacing of the plates is 0.1 in. and their area is 1 in.<sup>2</sup>?
6. Derive the equation  $(V - V_u)/V_0 = (1 - 2\nu)e$ .  $V_0$  is the volume of the unstretched specimen.
7. What is the percent volume increase per percent elongation in a specimen when  $\nu = 0.3$ ? When  $\nu = 0$ ?
8. Plot  $(T'_x - T^{\wedge})$  as a function of cross-linking using DiBenedetto's equation for poly(1,4-butadiene) and for polystyrene.

- y. Plot  $T_K$  as a function of volume fraction of vinyl acetate for vinyl chloride/vinyl acetate copolymers using equations (38), (39), and (41), assuming that  $R = 2$ .
- Monomer  $A$  melts at  $200^\circ\text{C}$  with a heat of fusion of  $20 \text{ cal/mol}$  of repeat unit. What is the expected melting point of a random copolymer containing 10 mol % of a comonomer  $B$ , which does not enter into the crystal lattice?
- [1] Toluene behaves as a plasticizer for polystyrene. Estimate the  $T_g$  value of a polystyrene containing 20 vol % (toluene,

## REFERENCES

1. *ASTM Standards*, American Society for Testing and Materials, 1916 Race St., Philadelphia, PA. The corresponding European standards are the *DIN Standards*. DIN Deutsche Institut für Normung, eV (German Standards Institute, Inc), Beith, Berlin.
1. T. Alfrey, Jr., *Macromolecular Behavior of High Polymers*. Interscience, New York, 1948.
3. J. D. Ferry, *Viscoelastic properties of Polymers*, 3rd ed., Wiley, New York, 1980.
4. I. N. Nielsen, *Mechanical Properties of Polymers*. Van Nostrand Reinhold, New York, 1962.
5. J. V. Schinitz, ed., *Testing of Polymers*, 4 vols., Interscience, New York, 1955 and later years.
6. A. V. Tobolsky, *Properties and Structure of Polymers*, Wiley, New York, 1956.
7. K. Nilsson and K. A. Wolf, eds., *Struktur und physikalisches Verhalten der Kunststoffe*, Vols. 1 and 2, Springer-Verlag, Berlin, 1963 and 1964.
8. J. M. Healy, *Rheol.* 28, 141 (1984). 9. J. Blatz, *Rubber Chem. Technol.*, 36, 1467 (1963). 10. J. Blatz, *J. Polymer Sci.* A2, 6, 621 (1968).
11. L. C. E. Sruik, *Rheol. Acta*, 6, 119 (1967).
12. W. S. Cramer, *J. Polymer Sci.*, 26, 57 (1957).
13. A. J. Slaverman and P. Schwarzl, in *Die Physik der Hochpolymeren*, Vol. 4, H. A. Stuart, Ed., Springer-Verlag, Berlin, 1956, Chap. 1.
14. J. G. Williams, *Fracture Mechanics of Polymers*. Wiley, New York, 1974.
15. *ASTM Standard D1709-67*, American Society for Testing and Materials, Philadelphia.
16. *ASTM Standard D256-50*, American Society for Testing and Materials, Philadelphia.
17. J. Telfair and U. K. Nason, *Mod. Plastics*, 20, 85 (July 1941).
18. D. R. Morey, *Ind. EnR. Chem.*, 37, 255 (1945).
19. *ASTM Standards D122-6H and D22H9-W*, American Society for Testing and Materials, Philadelphia.

20. S. Strella, in *High Speed Testing*, Vol. 1, A. G. H. Dietz and F. R. Eirich, Interscience, New York, 1960, See also articles in succeeding volumes of this yearly series.
21. G. R. Irwin, *J. Appl. Mech.*, 61, A49 (1939).
22. S. Mosioyov and H. J. Ripling, *J. Appl. Polymer Sci.*, 10, 1351 (1966).
23. *ASTM Standards*, 31, 1099 (1969). ASTM STP 463. 249 (1970).
24. *ASTM Standards D648-56, D/535-65T, and D1637-61*, American Society for Testing and Materials, Philadelphia.
25. W. Kiiuzmunn, *Chem. Rev.*, 43, 219 (1948).
26. N. Bekkedahl, *Res. Nail. fiur. Sid.*, 13, 4 j 1 (1934).
27. B. Ke, *Newer Methods of I'ohrih-r Characterization*, Interscience, New York,
28. R. II. Wiley and G. M. BHUKT, *J. Polymer Sci.*, 3, 647 (1948).
29. J. A. Sauer and A. E. Woodward, *Rev. Mod. Phys.*, 32, HS (1960).
30. L. Monnerie, *NATO Adv. Study Inst. Scr., Sar. C, Static Dynamic Prop, Polymer Solid State*, 94, 271 (1982).
31. F. D. Tsay, S. D. Hong, J. Moacanin, A, Gupta, *J. Polymer Sci. Polymer Phys. Ed.*, 20, 763 (1982).
32. R. M. Fuoss, *J. -4m. Chem. Soc.*, 63, 369, 378 (1941).
33. T. H. Sutherland and B. L. Funt, *J. Polymer Sci.*, **II**, 177 (1953).
34. H. Thurn and F. Wuerstlin, *Kolloid Z.*, **145**, 133 (1956).
35. N. G. McCrum, B. E. Read, and G. Williams, *Anelastic and Dielectric Effects in Polymeric Solids*, Wiley, New York, 1967.
36. R. F. Landel and R. F. Fedors, in *Fracture Processes in Polymeric Solids*, B. Rosen, Ed., Wiley, New York, 1964, p. 361.
37. T. L. Smiih, in *Rheology*, Vol. 5, F. R. tirich, Ed., Academic Press, New York, 1969, p. 127.
38. J. Dranderup and L. II. imuiergut, lids., *Polymer Handbook*, 2nd ed., Wiley, New York, 1975, P;tit MI. pp. 179-192.
39. C. L. Ueatty Mui K I. . Kara?./, *J. Polymer Sci. (Phys.)*, 13, 971 (1975).
40. W. U. Fitzgerald and L. li. Nielsen, *proc. Roy. Soc.*, **A282**, 137 (1964).
41. J. F. Mark, A, Iilisenber^, W. \V Graessley, L. Mandelkern, and J. Koenig, *P/ivsical Properties of Polymers*, American Chemical Society, Washington, D.C., 1984.
- J. II. Gibbs and E. A. DiMarzio, *J. Chem. Phys.*, **28**, 373 (1958).
- G. Adams and J. II. Gibbs, *J. Chem. Phys.*, 43, 139 (1965).
- M. II. Cohen and D. Tumbull, *J. Chem. Phys.*, 31, 1164 (1959).
45. M. Goldstein and R. Siniha, Eds., *The Classy Transition and the Nature of the Glassy State. Ann. N.Y. Acad. Sci.*, **279** (1976).
46. R. F. Landel and R. F. Fedors, *Mechanical Behavior of Materials*, Vol. **III**, Society of Materials Science, Kyoto, Japan, 1972, p. 496,
47. D. H. Kaellhle, *Computer-Aided Design of Polymers ami Composites*, Marcel Dekker, New York, 1985; *Physical Chemistry of Adhesion*, Wiley, New York, 1971.

- AH. R. (■'- Rover and H. S. Spcnu^r. *Adwmvs in Colloid Satwe*, Vni, 2, suieitL<sup>1\*</sup>; New York. W4ft. p. I.
- \*W M. UIMMCH. 7 < *hvm. I'hvs.*, J9, W) (1W». &l T. Ct K>\.iml I<sup>1</sup>. J. Fiory. / /,4/ip/. /Viv.c.. 21. SKI (WI). 51. I<sup>1</sup>. HHH.vK\ I'hvsiti! I'rojHTiin of *Polymers*. Inierscienvt;. New York. I<sup>1</sup> S2T. M t\ Shetland A. tisenlx-rp. *Rubber Chen, Technol. {Rubber Rev.}*: 43,,
- ;t. A. UisenluTj! am) M. CSIwrn. *Ruhfrer Chcm. Tec-hnol. Itiuhk'r Rev.*, 4J,, ISh(IV7IJJ. -54 .l. Hirov,. T. L.uinc. I. Tncnv;il. and J. Pouchly. *Colloid failymrr Scf.*, 26^ 27(iyN2).
- S5. K. A, Hiiytr-./ *Appl. Pnlvmcr Set.*, 5, 318 (1W>1). 5{v W. A. Liw iirnl .I. 11. Sovcll. ./■ M/P" iWywr Sri , 12. 1.^7 (IWKI-57' W. A. l.c-c. V. /p/vinir,Vi., A2. 8. 555 (147(iJ. ■&\*: 19. !\*■ Wvituui,./ .1/)/). rnlynu-rSd.. II, 143<sup>1</sup>M1%7]. «>. H (i. I'dlk-r.,/ Mai-nwniL Sn. [t'hyx.l. IS. 5<sup>1</sup>/5 I I'HSI, ■NL. I), K. Wilt. M S Allicri. inU I. J. Croitlturb, ./- I'VIVHHT.Sci, (Z/iw.). 23, 1li>5 (I'iss)
- HI ll I KIL-ihull iiiiid M li;ii/iT. *Anxvw Mukroiiu'l. (Jinn . Ki. 57 ( W, R F, Ivtni-^ .I'niymvr luifl. .V.r. 14, 147. -472 (1\*J74). •to}. K. Siillliil .iml K I , |ln>vr. J. Clwm. I'hvs.. H. HH)3 (I^ilh m. J. Miiiivvinni jimf K, Simliii. ./ T/K-N; /a.v.. 45, <sup>1</sup>JW (I'Jtm1. ft? .! M OKnIK../ ri'Irnia \ti.. 57. 42'J (IWOi. lrt\ I<sup>1</sup> IU-vilt:nnuin .uul I I - IJ Ciiiiifkiiiiji. *Knthiul /... IW. Ui (I'Kvi). (>7, M, S, Piiler^m, ./ Apftl. t'Jivl.. 35, 17fi (I^«i4).**
- hK. IT. Pfi^ijilia iiml O- M. M. iriin. ./ ««. ,V,;r/. *fiur. Std.*, A6H. 273 (|W ti4, I', ZufkT. ./ I'ntvmvr Sn. f/Vm\). 20. 13N5 (WX2). 3i,t. G. H\_ McKciinii. in *i'otnprt'lu/nivc Polymer Scirncr. Vol. 2. fhilvnrw fttiVs.C* Hintli iuiil t". Price. I-ds.. Ptrgamnn Press, Oxford. 14X9. 71
- A, K WWIwarviiind J. \*l. *Sxucf. Adv. Polymer SKI..* 1. 114.(1^58). 72. J. M\*;;illoor. *Plnusoj NwhiTysHiiitnt Solid.<sup>1</sup>*, North-i iolland, Amstc 1\*5. p 23L
- 7.1. K. V, Hover. *Pnfymrr A'n.i\**. &l. fi. Ifi l 1 |%H), 74. J. A. SaiK-r-i- *Pnlwnn Sn . (TJ2. W ll<\*71). 7.S, ,l Mftf|b(K'r- in Wnlvoultu Basis nf Tnmsiutms and HrlaSHimh'i.l^: J, I-i'J... Cionltin .mil firci^li. Nuw York. 1\*>7« p- 75. 7ft. II W. SiarkvH- Milicr. Jr.. iintl T. Avukkm. *MmmiiUrntto.il. 77. T. (i Kw and I\*. J. ROFV, J. Polymer Sci.. 14. .U5 (1<sup>1</sup>>54). IH, K. lixhi-rreiUT ;uul I). Khode-Liehenmi, *Mukruml Chcm.*. 49. |M 7U. J. M. C.J. fuwTic. /-'wr. *Polymer J.*, M. 2<sup>c</sup>>7 (1<sup>1</sup>J7M, WL k. f. lieiwr. *MucrmnolreulcA. 7. 142 (|J74|. K1. K. I\*, ROVLT. r.'uvilopciiia of Polymej Sfirnce ami Tn'tmafoav, Veil. Wiley. NL-vv York. 1%(). p. 4dl.***
- H2\* K- I'L-bLTTCiicr :inO fi. Kanip. *J Ch<>in. Phys.* IK. >W (1^50), M. T. ti, hiXijjuJIS, U^h:\ekr.7. *Polynwi-Sri.*, IS. 371. 3'J1

- R4. M. h. Drumm, C W, H. Drtiljte, and U E. Nielsen. MW. /:\*£. *Chetn.* 48.
- SS. G M. Martin and L. Miuxlojk-jm. / . *Res. Null. Hut. Sid.* 62. 141 (1459)..
- H6. II. V. Tk-mzc. K. Schmn-iki. \*i. Schnell. and K. A. Wolf, *Rubber Chem.; Terhnn}*.. 35. 776 (1%?).
87. A. S. Kenyon and L. li Nielsm. 7. *Mucromttl, Sa* . A3. 27? (1\*^9),
- K#. L. P.. Nielsen, / . *Mwronwt. Sa Hew MiUwmni ('hem.,* 3. 69 (1969).
- Jty. Y. Diam;inl. S. Welner, »nd D. Kalz. *Polymer. II* . 4% (1970.),
90. J- P. Bell. y. /!V^ rnh-rmr Sr^ . 14, 1901 (1970).
- 91- H. A. Flockc *Kunwioff.*- . <(>. *MX n%6»*-
- W: W. Fiwh. W. Htifm;inn. .mil H. Sch.miti. / . *Aj?nl, I'tflv. W'r Sci., U.* 2\$\$
93. E, A. Di'Miirz.io, / . *Res. Nntl, Iht. Std.* . **AtiS.** til 1
94. A. T- DiB-L'ncik'ltiv. unpuNislieil private comiiiumcatimi,
95. F. N. Kelky and F. Hucchi: . 7 *Polymer Sci.* . 14.
- 9ft. M- Climltin iitid .l S, Taylor. 7. *App! Chen., (I. tuition).* I. 493 (IM52)-97.
- L. [■. NiiMk'U. *Pmiii'ti'ifl the Properties of Mixtures'*, Maavl D.L'Lkkt?r. Ncw York. W7H.
99. M,~> ('In.7. *Polymer S<i i'heHi.*). IJ. 17 fi 7 (1W1L
- 1(10. T. S. Chfjw, *Miicrntmlrvth's*. II. 3(j2 1 I^WM
- L. A.. Wo.HI. *J. Polymer Sd.* . 28. 319 (195S}.
- K. II, I1lcis. / . *rU'kfr, \*rhrm* . 70. 353 (IWi).
- M. Ilirouka JIHK) T. K;U". 7. *Polymer Su li e n* , 12, 31 | 1\*>74.Y,
- K, Miiruinctn ;uid A, Rom.nun-, *Polymrr. 1C>*. 173. 177 (1975).
- N- W. Jolinsttm.y *Man-nmnl. Sri.* . CM, 2!5 (1"7ft)
- D. ft. Rtailcy and P. M. MUIHML'Iis. 7. *P"!vi>icrSi i. (Cheni.)*, 16, IJi'
- 1(17. N. W. JolmjiUm. 7, *Mutrnmdl. Sci.*, A7. 531 (1973).
- A. fi. Tonelli. *Matromolenite* \, 8, 544 (1975).
- P. R, CoiK-hmiin. *Macwwnlearics*. 15. 770 (1VW).
- L. H. NivKL-H nnd R. Budni.ihl, 7. 4p; i' fflw., 21. 4K« (1950).
111. K. I; , Polm.-intecr. J, A.'lhonn;, and J. I). Iklitter. *Rttbber ('hem.* 39. 1403 (IWi).
112. K. II. HL'IIWL'^L^1. R. Kai^L-i. .mii! K-- Kupluil. *Kolloitl %.*- . 157. 27 (
113. E. Ho urul T. Iliilakfyamn. 7. *Polymer Sn. [Phyx.]*. 12. 1477 (1974).
114. W, O, Sran.nK 7. *puymej .SV/..CZO. II7* (1%7) . .
115. Ci. (iec, P, N. I Ian Icy. .l, H M I icrlx-n, amt [. { . A. Ljjincelii-y, Psfeja^F\* L. 365 (I^M).
116. W. V. Jnhmt.in iiiiid M. Shen. / . *Polymer .fir.* . Aj, 7. I9K3 (Mfflfr.
- 117- R. I. Miller, *lncvflopctltti o\ Polymer Scie/ice mid Tecfuolofiy*, Vol. 4, Wiley. New York. I^Wi. p -M9, UK. R. L Miller, in *Crystalline Olffin Polymers*. Pan I. R, A, V. Raff and K, W, Doak, Kdy. liituivifiHL'. Ni-w >'ork. IW^ p, 577.

19. I. S. Chirk, in *Methods of Experimental Physics*, Vol. 16, Part B. *Polymers; Crystal Structure and Morphology*, R. Fieschi, ed., Academic Press, New York, 1978, Chap. 6.2, p. 1.
20. F. P. Price, *J. Chem. Phys.*, 19, 973 (1951).
21. J. L. Wang and I. R. Harrison, in *Methods of Experimental Physics*, Vol. 16, Part B. *Polymers: Crystal Structure and Morphology*, R. Fava, Ed., Academic Press, New York, 1980, Chap. 6.2, p. 128.
22. M. B. Rhodes and R. S. Stein, *J. Appl. Phys.*, 36, 2344 (1965).
23. R. S. Stein, *Polymer Fractionation*, 9, 320 (1968).
24. J. Pommeroy, *Polymer Sci.*, 2(3), 363 (1961).
25. J. L. Wang, *Single Crystals of Polymers*, Interscience, New York, 1961, p. 11.
26. P. H. Tilton, *J. Polym. Sci.*, 24, 301 (1957).
27. A. Keller, *Mikrochim. Acta*, 1171 (1957).
28. B. W. Fisher, *Naturforsch.*, 12A, 753 (1957).
29. P. H. Geil, *Encyclopedia of Polymer Science and Technology*, Vol. 9, Interscience, New York, 1968, p. 204.
30. H. I. Kilb and F. J. Padden, Jr., *Polymer Sci.*, 41, 525 (1959).
31. W. M. H. Bryan, *J. Polymer Sci.*, 2, 547 (1947).
32. R. L. Wainman, *Polymer J.*, 349 (1972).
33. H. W. Kilsch, *Polymer J.*, 17, 307 (1985).
34. K. I. Timm, O. Genigross, and W. Abi-Zur, *Phys. Chem.*, 69, 371 (1965).
35. J. H. N. W. Fulcher, *J. Chem. Phys.*, 29, 1395 (1958).
36. J. Flory, *J. Polym. Sci.*, 7, 684 (1947); 17, 223 (1949).
37. J. Flory, *Principles of Polymer Chemistry*, Cornell University Press, Ithaca, N.Y., 1953, Chap. 13.
38. M. M. Perlman, *Firm Rev.*, 56, 903 (1956).
39. I. M. Kolthoff, *Constitution of Polymers*, McGraw-Hill, New York, 1964, p. 1.
40. R. I. Miller and I. I. NicK, *Polymer Sci.*, 55, M3 (1961).
41. K. I. Timm, *J. Polym. Sci.*, 9, 471 (1952).
42. R. I. W. Fulcher, *J. Appl. Phys.*, 25, K25 (1954).
43. W. A. Pryor and J. K. Stille, *J. Polym. Sci.*, 2, 7 (1970).



# 2

## Elastic Moduli

### I. ISOTROPIC AND ANISOTROPIC MATERIALS

#### A. Isotropic Materials

Elastic moduli measure the resistance to deformation of materials when external forces are applied. Explicitly, moduli  $M$  are the ratio of applied stress  $\sigma$  to the resulting strain  $\epsilon$ :

$$M = \frac{\sigma}{\epsilon} \quad (1)$$

In general, there are three kinds of moduli: Young's moduli  $E$ , shear moduli  $G$ , and bulk moduli  $K$ . The simplest of all materials are isotropic and homogeneous. The distinguishing feature about isotropic elastic materials is that their properties are the same in all directions. Unoriented amorphous polymers and annealed glasses are examples of such materials. They have only one of each of the three kinds of moduli, and since the moduli are interrelated, only two moduli are enough to describe the elastic behavior of isotropic substances. For isotropic materials

$$E = \frac{9GK}{3K + G} \quad (2)$$

It is not necessary to know the bulk modulus to convert  $E$  to  $G$ . If the transverse strain,  $\epsilon_r$ , of a specimen is determined during a uniaxial tensile test in addition to the extensional or longitudinal strain  $\epsilon_l$ , their ratio, called Poisson's ratio,  $\nu$  can be used:

$$\nu = -\frac{\epsilon_r}{\epsilon_l} \quad (3)$$

$$E = 2G(1 + \nu) = 3K(1 - 2\nu) \quad (4)$$

For soft elastic solids  $\nu = \frac{1}{2}$ ; for glassy polymers  $\nu$  is in the range 0.3 to 0.4—often about 0.33.

## B. Anisotropic Materials

Anisotropic materials have different properties in different directions (1-7). Examples include fibers, wood, oriented amorphous polymers, injection-molded specimens, fiber-filled composites, single crystals, and crystalline polymers in which the crystalline phase is not randomly oriented. Thus anisotropic materials are really much more common than isotropic ones. But if the anisotropy is small, it is often neglected with possible serious consequences. Anisotropic materials have far more than two independent elastic moduli—generally, a minimum of five or six. The exact number of independent moduli depends on the symmetry in the system (1-7). Anisotropic materials will also have different contractions in different directions and hence a set of Poisson's ratios rather than one.

Theoreticians prefer to discuss moduli in terms of a mathematical tensor that may have as many as 36 components, but engineers generally prefer to deal with the so-called engineering moduli, which are more realistic in most practical situations. The engineering moduli can be expressed, however, in terms of the tensor moduli or tensor compliances (see Appendix IV).

Note that in all of the following discussions the deformations and hence the strains are assumed to be extremely small. When they are not (and this can often happen during testing or use), more complex treatments are required (5-7).

A few examples of the moduli of systems with simple symmetry will be discussed. Figure 1A illustrates one type of anisotropic system, known as uniaxial orthotropic. The lines in the figure could represent oriented segments of polymer chains, or they could be fibers in a composite material. This uniaxially oriented system has five independent elastic moduli if the lines (or fibers) are randomly spaced when viewed from the end. Uniaxial systems have six moduli if the ends of the fibers are packed in a pattern such as cubic or hexagonal packing. The five engineering moduli are il-

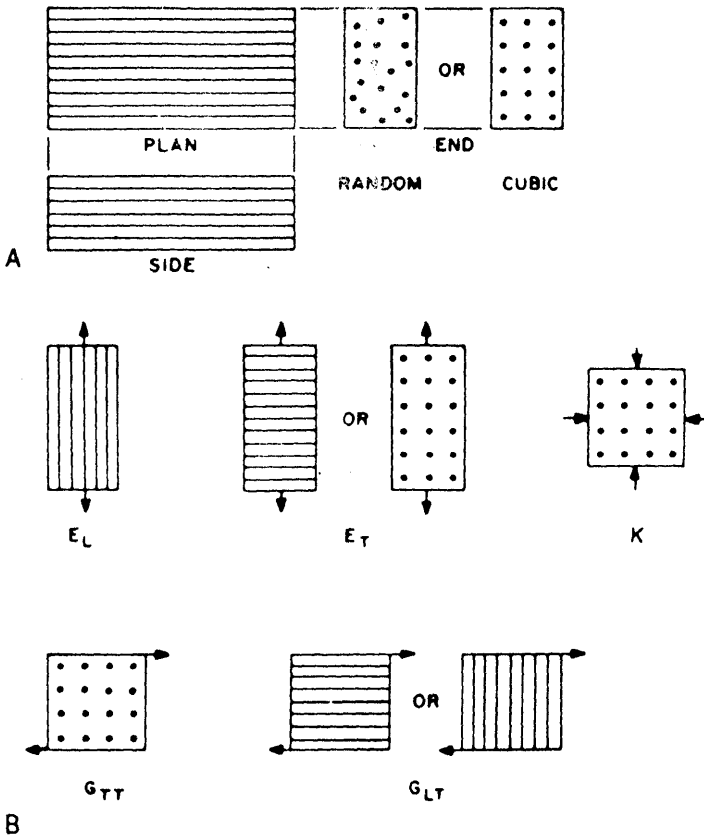


Figure 1 (A) Uniaxially oriented anisotropic material. (B) The elastic moduli of uniaxially oriented materials.

illustrated in Figure 1B for the case where the packing of the elements is random as viewed through an end cross section. There are now two Young's moduli, two shear moduli, and a bulk modulus, in addition to two Poisson's ratios. The first modulus,  $E_L$ , is called the longitudinal Young's modulus; the second,  $E_T$ , is the transverse Young's modulus; the third,  $G_{TT}$ , is the transverse shear modulus, and the fourth,  $G_{LT}$ , is the longitudinal shear modulus (often called the longitudinal-transverse shear modulus). The fifth modulus is a bulk modulus  $K$ . The five independent elastic moduli could be expressed in other ways since the uniaxial system now has two

Poisson's ratios. One Poisson's ratio,  $\nu_{ir}$ , gives the transverse strain  $\epsilon_r$  caused by an imposed strain  $\epsilon_i$  in the longitudinal direction. The second Poisson's ratio,  $\nu_{ri}$ , gives the longitudinal strain caused by a strain in the transverse direction. Thus

$$\nu_{i,r} = \begin{cases} \frac{-\epsilon_r}{\epsilon_i} & \text{for a longitudinal force} \\ \frac{-\epsilon_i}{\epsilon_r} & \text{for a transverse force} \end{cases} \quad (5)$$

where the numerators are the strains resulting from the imposed strains that are given in the denominators.

The most common examples of uniaxially oriented materials include fibers, films, and sheets hot-stretched in one direction and composites containing fibers all aligned in one direction. Some injection-molded objects are also primarily uniaxially oriented, but most injection-molded objects have a complex anisotropy that varies from point to point and is a combination of uniaxial and biaxial orientation.

A second type of anisotropic system is the biaxially oriented or planar random anisotropic system. This type of material is illustrated schematically in Figure 2A. Four of the five independent elastic moduli are illustrated in Figure 2B; in addition there are two Poisson's ratios. Typical biaxially oriented materials are films that have been stretched in two directions by either blowing or tentering operations, rolled materials, and fiber-filled composites in which the fibers are randomly oriented in a plane. The mechanical properties of anisotropic materials are discussed in detail in following chapters on composite materials and in sections on molecularly oriented polymers.

## II. METHODS OF MEASURING MODULI

### A. Young's Modulus

Numerous methods have been used to measure elastic moduli. Probably the most common test is the tensile stress-strain test (8-10). For isotropic materials, Young's modulus is the initial slope of the true stress vs. strain curve. That is,

$$E = \left. \frac{d\sigma_i}{d\epsilon} \right)_{\epsilon \rightarrow 0} = \left. \frac{F/A}{(L - L_0)/L_0} \right)_{L \rightarrow L_0} \quad (6)$$

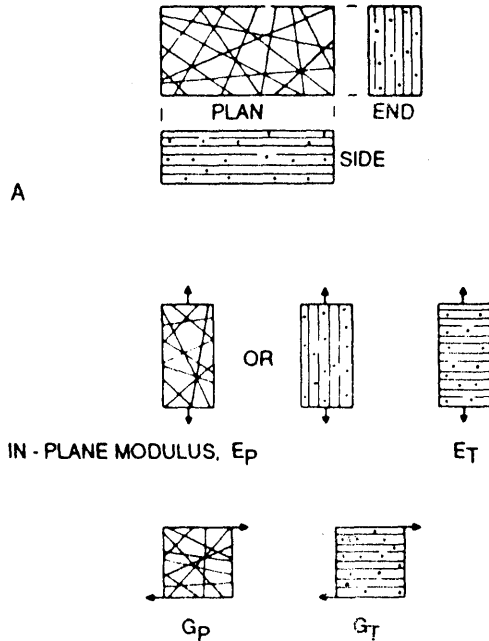


Figure 2 (A) Biaxial or planar random oriented material. (B) Four of the moduli of biaxially oriented materials.

where  $F/A$  is the force per unit cross-sectional area,  $L$  the specimen length when a tensile force  $F$  is applied, and  $L_0$  the unstretched length of the specimen. Equation (6) also applies to and gives one of the moduli of anisotropic materials if the applied stress is parallel to one of the principal axes of the material. The equation does not give one of the basic moduli if the applied stress is at some angle to one of the three principal axes of anisotropic materials.

It is also possible to run tensile tests at a constant rate of loading. If the cross-sectional area is continuously monitored and fed back into a control loop, constant-stress-rate tests can be made. In this case the initial slope

$\dagger F/A_0$ , where  $A_0$  is the initial area, is often called the engineering stress,  $\sigma$ ; the force per unit actual or deformed area,  $F/A$ , is called the true stress,  $\sigma_r$ . For polymeric materials, where strains can be large, the difference between  $\sigma$  and  $\sigma_r$  can be considerable. Defining the stretch ratio  $\lambda$  as  $L/L_0 (= 1 + \epsilon)$ ,  $\sigma_r = \lambda\sigma$  for incompressible materials.

of the strain-stress curve is the compliance

$$D = \frac{d\epsilon}{d\sigma} = \frac{(L - L_0)/L_0}{F/A} \quad (7)$$

Note that the usual testing mode for compliance is constant load or constant loading rate, so to obtain truly useful data, some means must be taken to compensate for the change in area.

Young's modulus is often measured by a flexural test. In one such test a beam of rectangular cross section supported at two points separated by a distance  $L_f$  is loaded at the midpoint by a force  $F$ , as illustrated in Figure 1.2. The resulting central deflection  $V$  is measured and the Young's modulus  $E$  is calculated as follows:

$$E = \frac{FL_0^3}{4CD^3Y} \quad (8)$$

where  $C$  and  $D$  are the width and thickness of the specimen (11,12). This flexure test often gives values of the Young's modulus that are somewhat too high because plastic materials may not perfectly obey the classical linear theory of mechanics on which equation (8) is based.

Young's modulus may be calculated from the flexure of other kinds of beams. Examples are given in Table 1 (11,12). The table also gives equations for calculating the maximum tensile stress  $\sigma_{\max}$  and the maximum elongation  $\epsilon_{\max}$ , which are found on the surface at the center of the span for beams with two supports and at the point of support for cantilever

**Table 1** Young's Modulus from Flexure of Beams

| Beam geometry, support, and loading  | $E$                          | $\sigma_{\max}$          | $\epsilon_{\max}$      |
|--|------------------------------|--------------------------|------------------------|
| 1. Rectangular beam, center loaded, two supports (three-point bend)                                  | $\frac{FL_0^3}{4CD^3Y}$      | $\frac{3FL_0}{2CD^2}$    | $\frac{6DY}{L_0^2}$    |
| 2. Rectangular beam, two supports, two equal loads $F/2$ at $L_0/4$ and $3L_0/4$ . (four point bend) | $\frac{11FL_0^3}{64CD^3Y}$   | $\frac{3FL_0}{4CD^2}$    | $\frac{48DY}{11L_0^2}$ |
| 3. Rectangular cantilever beam fixed at one end with load at other end                               | $\frac{4FL_0^3}{CD^3Y}$      | $\frac{6FL_0}{CD^2}$     | $\frac{3DY}{2L_0^2}$   |
| 4. Rod of diameter $D$ with two supports, center loaded  | $\frac{4FL_0^3}{3\pi D^4Y}$  | $\frac{8FL_0}{\pi D^3}$  | $\frac{6DY}{L_0^2}$    |
| 5. Cantilever beam of circular cross section fixed at one end with load at other end; $D$ = diameter | $\frac{64FL_0^3}{3\pi D^4Y}$ | $\frac{32FL_0}{\pi D^3}$ | $\frac{3DY}{2L_0^2}$   |

beams. In these equations  $F$  is the applied force or load,  $Y$  the deflection of the beam, and  $D$  the thickness of specimens having rectangular cross section or the diameter of specimens with a circular cross section.

Young's modulus may also be measured by a compression test (see Figure 1.2). The proper equation is

$$E = \frac{\sigma}{\epsilon} = \frac{F/A}{(L_0 - L)/L_0} = \frac{F}{\lambda} \ln \frac{L_0}{L} \quad (9)$$

Generally, one would expect to get the same value of Young's modulus by either tensile or compression tests. However, it is often found that values measured in compression are somewhat higher than those measured in tension (13-15). Part of this difference may result from some of the assumptions made in deriving the equations not being fulfilled during actual experimental tests. For example, friction from unlubricated specimen ends in compression tests results in higher values of Young's modulus. A second factor results from specimen flaws and imperfections, which rapidly show up at very small strains in a tensile test as a reduction in Young's modulus. The effect of defects are minimized in compression tests.

In any type of stress-strain test the value of Young's modulus will depend on the speed of testing or the rate of strain. The more rapid the test, the higher the modulus. In a tensile stress relaxation test the strain is held constant, and the decrease in Young's modulus with time is measured by the decrease in stress. Thus in stating a value of the modulus it is also important to give the time required to perform the test. In comparing one material with another, the modulus values can be misleading unless each material was tested at comparable time scales.

In creep tests the compliance or inverse of Young's modulus is generally measured. However, Young's modulus can be determined from a tensile creep test since the compliance is related to the reciprocal of the modulus (16,17). Whereas stress-strain tests are good for measuring moduli from very short times up to time scales on the order of seconds or minutes, creep and stress relaxation tests are best suited for times from about a second up to very long times such as hours or weeks. The short time limit here is set by the time required for the loading transient to die out, which takes a period about 10 times longer than the time required to load or strain the specimen. When corrections are applied, however (18), the lower limit on the time scale can also be very short. The long time limit for creep and stress relaxation is set by the stability of the equipment or by specimen failure.

Although creep, stress relaxation, and constant-rate tests are most often measured in tension, they can be measured in shear (19-22), compression (23,24), flexure (19), or under biaxial conditions. The latter can be applied

by loading or straining flat sheets in two directions (25-30), by simultaneous axial stretching and internal pressurization of tubes (31-34), or by simultaneously stretching and twisting tubes or rods (although the variation of the shear strain along the radius, noted above, must be remembered here) (35-40). Creep and stress relaxation have been measured in terms of volume changes, which are related to bulk moduli (41-44).

## B. Young's and Shear Moduli from Vibration Frequencies

### *Free Vibrations*

The natural vibration frequency of plastic bars or specimens of various shapes can be used to determine Young's modulus or the shear modulus. Figure 3 illustrates four common modes of free oscillation. In Figure 3A and B the effect of gravity can be eliminated for bars in which the width is greater than the thickness by turning the bar so that the width dimension is in the vertical direction. The equations for the Young's moduli of the four cases illustrated in Figure 3 are given in Table 2 for the fundamental frequency. The shear modulus for the natural torsional oscillations of rods of circular and rectangular cross section are also given in Table 2 (45). Dimensions without subscripts are in centimeters; dimensions with the subscript *in* are in inches. The moduli are given in  $\text{dyn}/\text{cm}^2$ . In the table,  $R$  is the radius,  $p$  a shape factor given in Table 3 (8,46),  $C$  the width,  $D$  the thickness,  $\rho$  the density of the material making up the beam of total mass  $m$ ,  $P$  the period of the oscillation,  $f_H$  the frequency of the vibrations in hertz or cycles per second, and  $I$  the rotary moment of inertia in  $\text{g} \cdot \text{cm}^2$ .

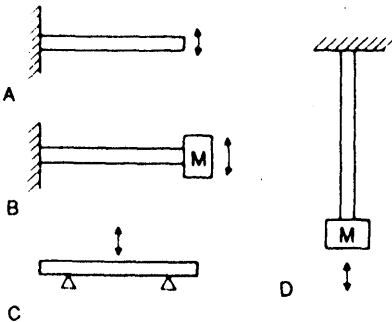


Figure 3 Vibrating systems for measuring Young's modulus.



Table 2 Equations for Dynamic Moduli from Free and Resonance Vibrations

| Method and specimen  | Modulus (dyn/cm <sup>2</sup> )  |
|--|---|
| 1. Torsion pendulum, rectangular cross section                                     | $G' = \frac{64\pi^2 LI}{CD^3 \mu P^2} = \frac{38.54IL_{in}}{C_{in} D_{in}^3 \mu P^2}$ |
| 2. Torsion pendulum, circular cross section  | $G' = \frac{8\pi LI}{R^4 P^2} = \frac{1.531IL_{in}}{R_{in}^4 P^2}$                    |
| 3. Vibrating cantilever reed, rectangular cross section                            | $E' = \frac{38.24\rho L^4}{D^2} f_R^2$  |
| 4. Vibrating cantilever reed, circular cross section                               | $E' = \frac{16\pi^2 \rho L^4}{(1.875)^4 R^2} f_R^2$                                   |
| 5. Vibrating rectangular cantilever reed of mass $m$ with mass $M$ on end          | $E' = \frac{16\pi^2 (M + 0.23m)L^3}{CD^3} f_R^2$                                      |
| 6. Free-free vibration of rod supported at nodal points, circular cross section    | $E' = \frac{16\pi^2 \rho L^4 f_R^2}{(22.0)^2 R^2}$                                    |
| 7. Free-free vibration of rod supported at nodal points, rectangular cross section | $E' = \frac{48\pi^2 \rho L^3 f_R^2}{(22.0)^2 D^2}$                                    |
| 8. Longitudinal vibrations of circular rod of mass $m$ with large mass $M$ on end  | $E' = \frac{4\pi L (M + m/3) f_R^2}{R^2}$   |
| 9. Longitudinal vibrations of rectangular rod of mass $m$ with mass $M$ on end     | $E' = \frac{4\pi^2 L (M + m/3) f_R^2}{CD}$  |

### Forced Vibrations

Free and resonance vibrations do not permit the facile measurement of  $E$  or  $G$  over wide ranges in frequency at a given temperature, although with careful work, resonance responses can be examined at each of several harmonics (47,48). In general, to obtain three decades of frequency, the specimen dimensions and the magnitude of the added mass must be varied over a considerable range.

In driven dynamic testing an oscillating strain (or stress) is applied to a specimen. This is almost always sinusoidal for ease of analysis. In this case

$$\epsilon = \epsilon_0 \sin \omega t \quad (10)$$

The stress thus produced is out of phase with the input by an amount  $\delta$ :

$$\sigma = \sigma_0 \sin(\omega t + \delta) = (\sigma_0 \cos \delta) \sin \omega t + (\sigma_0 \sin \delta) \cos \omega t \quad (11)$$

so that  $\sigma_0 \cos \delta$  is the component of the stress in phase with the strain and  $\sigma_0 \sin \delta$  is the component exactly  $90^\circ$  out of phase with the strain. Since the in-phase component is exactly analogous to that of a spring, and the out-of-phase component to that of a viscous response, the ratio of the

Table 3 Shape Factor  $\mu^*$ 

| Width $C$     | $\mu$ |
|---------------|-------|
| Thickness $D$ |       |
| 1.00          | 2.249 |
| 1.20          | 2.658 |
| 1.40          | 2.990 |
| 1.60          | 3.250 |
| 1.80          | 3.479 |
| 2.00          | 3.659 |
| 2.25          | 3.842 |
| 2.50          | 3.990 |
| 2.75          | 4.111 |
| 3.00          | 4.213 |
| 3.50          | 4.373 |
| 4.00          | 4.493 |
| 5.00          | 4.662 |
| 7.00          | 4.853 |
| 10.00         | 4.997 |
| 20.00         | 5.165 |
| 50.00         | 5.266 |
| 100.00        | 5.300 |
| $\infty$      | 5.333 |

\* $\mu = 5.333 (1 - 0.63D/C)$  if  $C/D > 2$ .

components to the maximum strain  $\epsilon_0$  are called the storage and loss moduli, respectively. Using the symbol  $M$  here to denote a generalized modulus, then:

$$\text{storage modulus } M' = \frac{\sigma_0}{\epsilon_0} \cos \delta \quad (12)$$

$$\text{loss modulus } M'' = \frac{\sigma_0}{\epsilon_0} \sin \delta \quad (13)$$

so the tangent of the loss angle is  $M''/M'$ . The two moduli are also called the real and imaginary components of the complex modulus, where  $M^* = M' + iM''$  (see Problem 7). Here  $M$  can be  $E$ ,  $G$ , or  $K$ , depending on the experiment, i.e., depending on whether a tensile, shear, or volumetric strain was applied. (Note however that the letter  $M$  is usually reserved for and intended to indicate the longitudinal modulus.)  $H$  stress is applied and strain is measured, compliance is being determined, not modulus. It would

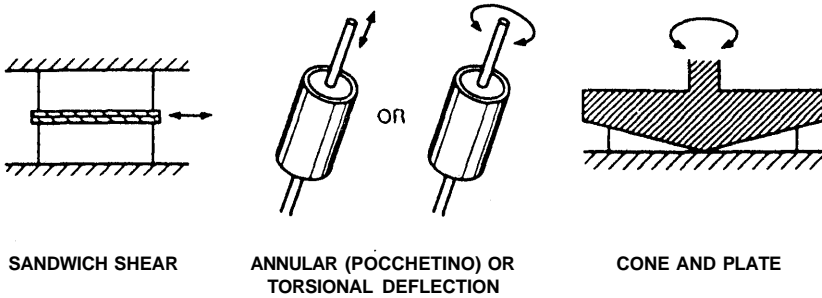


Figure 4 Some test modes for measuring shear response. Arrows indicate direction of the force or displacement applied to that surface.

be denoted as  $D$  for tensile compliance,  $J$  for shear, and  $B$  for bulk. The compliance-modulus relationships for elastic materials have been given in equations (1.16) to (1.18); those for viscoelastic materials are given in subsequent chapters.

If a disklike specimen is sheared between two end plates by rotation of one over the other to obtain the shear modulus, then at any moderate twist angle the strain (and strain rate) vary along the radius, so only an effective shear modulus is obtained. For better results the upper plate is replaced with a cone of very small angle. Figure 4 shows fche cone-and-plate and two other possible test geometries for making shear measurements.

At high frequencies of  $10^4$  to  $10^7$  Hz, Young's modulus of fibers and film strips can be measured by wave propagation techniques (16,49-53). An appropriate equation when the damping is low is

$$E = \rho v^2 \quad (14)$$

where  $p$  is the density of the material and  $v$  is the velocity of the ultrasonic wave in it.

### III. RELATIONS OF MODULI TO MOLECULAR STRUCTURE

The modulus-time or modulus-frequency relationship (or, graphically, the corresponding curve) at a fixed Temperature is basic to an understanding of the mechanical properties of polymers. Either can be converted directly to the other. By combining one of these relations (curves) with a second major response curve or description which gives the temperature dependence of these time-dependent curves, one can either predict much of the response of a given polymer under widely varying conditions or make rather

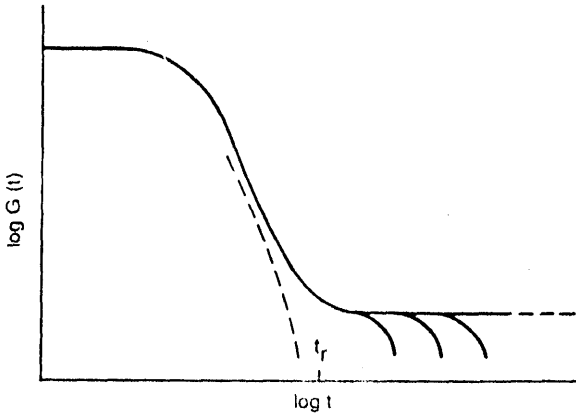
detailed comparisons of the responses of a set of polymers (7,16,54-56). These frequency/time response curves serve to delineate the effects of changes in backbone structure (i.e., the type of polymer or copolymer), molecular weight and molecular weight distribution, degree of cross-linking, and of Plasticization. For two-phase and multiphase systems such as semi-crystalline polymers and polymer blends, morphology and interaction between the phases or components both play significant and complex roles in determining the response. Here the ability to predict response from just a knowledge of the response of the amorphous component or from the responses of the individual blend constituents is still rather poor. Nevertheless, great insight can be obtained into the response that is observed.

In the past it has often been the custom to measure the temperature dependence of the dynamic modulus and loss tangent at a single frequency rather than the frequency dependence at a single or set of temperatures. Although the modulus-temperature measurement is very useful in ascertaining qualitative features of response and the effect of the foregoing molecular and compositional factors on it, it cannot be used for quantitative estimates of the response under other test or use conditions. Moreover, the results can be misleading if not used with care. The modulus-time measurement does not have these problems. However, examples of both methods of presenting polymer response are described here. (Similar instructive generalizations of compliance-time/frequency and compliance-temperature can also be made (16,57,58), although on the experimental side single-frequency measurements akin to Figure 5B are seldom made and there is no equivalent to the characteristic time of Figure 5A).

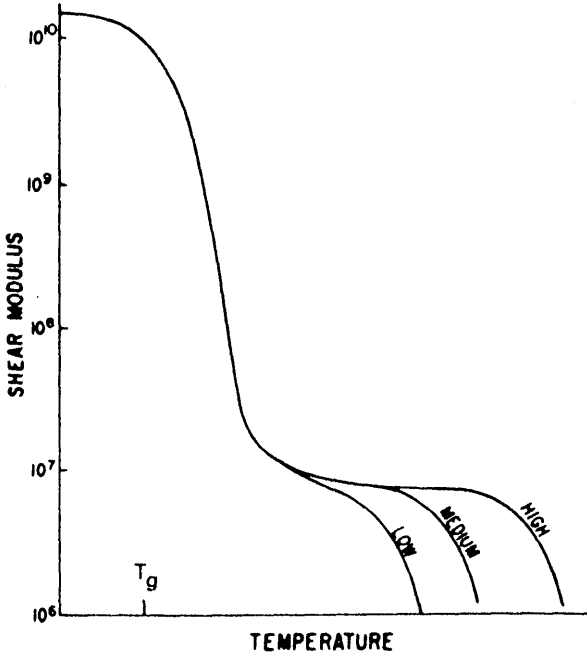
In this section we summarize the effect of structural and compositional factors on the modulus of the simplest of amorphous polymers. Actual polymers are usually more complex in behavior than the generalized examples shown here. In later chapters we discuss more complex systems in detail.

### A. Effect of Molecular Weight

Figure 5A (solid line) shows the modulus-time curve for three different molecular weights of an amorphous polymer such as normal atactic polystyrene. The modulus in the glassy region, about  $10^{10}$  dyn/cm<sup>2</sup> is slightly frequency dependent at very short times (not shown). It drops about three decades in the glass-to-rubber transition region; the slope of the transition zone in  $G(t)$  is about -1 on such a log-log plot. The response then levels out to a nearly constant plateau of the rubbery modulus, about  $10^6$  dyn/cm<sup>2</sup>, and finally drops to zero at very long times or extremely low frequencies. Beyond this point the material acts as a purely viscous liquid.



A



B

Figure 5 (A) Relaxation modulus at a fixed temperature of a polymer sample: (1) of very low molecular weight (dashed line on left), (2) of moderate to high molecular weight (solid lines), and (3) when cross-linked (dashed line on right). (B) Effect of molecular weight on the modulus-temperature curve of amorphous polymers. Modulus is given in  $\text{dyn/cm}^2$ . The characteristic or reference time is  $t_r$ , the reference temperature,  $T_K$ .

The length of the rubbery plateau increases with molecular weight, as indicated: the longer the plateau, the higher the steady-flow viscosity. If the polymer is cross-linked, the response levels off at the true rubbery modulus. In this case the height of the final plateau increases with increasing degree of cross-linking.

The complete curve for the response of an uncross-linked polymer at a fixed temperature, depicted here, covers so many decades of time that it has only been measured at a single temperature on a very few low-molecular-weight polymers. The experimental results seen in the literature are actually a composite of data taken at several temperatures over a limited time scale. The effect of a temperature rise is to translate the main transition in the curve of Figure 5A to the left, toward shorter time, with essentially no change in shape.

The response at a single low frequency (or a fixed time of observation in stress relaxation) as a function of temperature is depicted in Figure 5B. If the time scale of the experimental technique is about 1 s, the drop in modulus at the transition zone takes place near the (dilatometric) glass transition temperature of the polymer. The initial decrease starts below  $T_g$  and the midpoint of the change occurs above  $T_g$ . If this drop in modulus occurs above room temperature, the polymer is a rigid glass; if well below room temperature, the polymer is a viscous liquid or an elastomer. For a high-frequency measurement the transition would start and end at the glassy and rubbery plateaus, but the slope would be much less.

Thus to contrast the responses of two polymers, one can either compare their time-frequency response at a fixed temperature (e.g., at room or some other operating temperature), so that their characteristics during use under the same conditions are compared, or they can be compared at equivalent temperature (e.g.,  $T^*$  or  $T^* + \Delta T$ ), so that the nature of their responses are compared. Just as there is a temperature of reference in Figure 5B,  $T_v$ , there is also a virtually unused time or frequency of reference in Figure 5A.  $t_i$  is essentially the time at which  $G'$  drops to a value of  $10^{7.5}$  dyn/cm<sup>2</sup> (or  $C' = 10^7 \times 10^7$ ) (16). The magnitude of this reference time or frequency is determined by the rate at which segments of the polymer chain can diffuse past one another (i.e., by a very local viscosity (16.5<sup>^</sup>)- This time scale also depends on structural features of the chain segment, such as the monomer molecular weight  $M_1$ , the effective bond length of bonds along the backbone chain  $a$ , and other molecular features unique to and characteristic of any given chain;  $T_{ref} \ll (a/M_u) \xi_0 - k \xi_0$ ,  $k \approx 1$  cm/dyn. However, the prime factor, and the one used to characterize this time scale, is the average friction that a monomer-sized segment offers to motion. Table 4 lists some representative values of this monomeric friction factor,  $\xi_0$ , (16). Since  $\xi_0$  is a measure of and related to a viscosity,

Table 4 Monomeric Friction Coefficients of Selected Polymers

| Polymer                                   | $T_r$<br>k | $M_0$<br>g/mol | $a \times 10^8$<br>cm | log $\zeta_0$ (dyn·s/cm) at: |                   |                           |
|---|------------|----------------|-----------------------|------------------------------|-------------------|---------------------------|
|   |            |                |                       | 298°C                        | $T_r$             | $T_r + 100^\circ\text{C}$ |
| Methacrylate polymers                     |            |                |                       |                              |                   |                           |
| Methyl                                    |            | 100            | 6.9                   | 0.66 (398°)                  |                   |                           |
| Ethyl                                     | 335        | 114            | 5.9                   |                              | 6.22              | -4.40                     |
| <i>n</i> -Butyl                           | 300        | 142            | 6.4                   |                              | 3.81              | -4.77                     |
| Rubbers                                   |            |                |                       |                              |                   |                           |
| Hevea rubber <sup>a</sup>                 | 200        | 68             | 6.8                   | -6.41                        | 4.47              | -6.49                     |
| 1,4-Polybutadiene <sup>b</sup>            | 172        | 54             | 6.0                   | -6.75                        | 0.83              | -6.16                     |
| 1,2-Polybutadiene                         | 261        | 54             | 7.55                  | -4.11                        | 2.38              | -7.01                     |
| Styrene-butadiene copolymer <sup>c</sup>  | 210        | 65.5           | 6.7                   | -6.14                        | —                 | -6.55                     |
| Butyl rubber <sup>d</sup>                 | 205        | 56             | 5.9                   | -4.16                        | 3.57              | -4.46                     |
| Ethylene-propylene copolymer <sup>e</sup> | 242        | 39.9           | 5.5                   | -4.50                        | 3.10              | -6.23                     |
| General                                   |            |                |                       |                              |                   |                           |
| Polyisobutylene                           | 205        | 56             | 5.9                   | -4.35                        | 3.47              | -4.67                     |
| Polystyrene                               | 373        | 104            | 7.4                   |                              | 2.06              | -6.95                     |
| Poly(vinyl acetate)                       | 305        | 86             | 6.9                   |                              | 4.29              | -6.32                     |
| Poly(vinyl chloride)                      | 347        | 62.5           | 6                     |                              | 4.05 <sup>f</sup> | -7.46                     |
| Poly(dimethyl siloxane)                   | 150        | 74             | 6.2                   | -8.05                        | -3.60             | -7.50                     |
| Poly(ethylene oxide)                      |            | 44             |                       |                              |                   |                           |

Source: Adapted from Ref. 16.

<sup>a</sup>Lightly vulcanized with dicumyl peroxide.

<sup>b</sup>Cis/trans/vinyl = 43:50:7, lightly vulcanized with dicumyl peroxide.

<sup>c</sup>Random copolymer, 23.5% styrene.

<sup>d</sup>Lightly cross-linked with sulfur.

<sup>e</sup>Ethylene/propylene = 16:84, by mole.

<sup>f</sup>Difficult to estimate reliably because  $C_1^*$  and  $C_2^*$  uncertain; based on "universal" values.

it is temperature dependent. Hence its value is always given at a characteristic or reference temperature, either  $T^\wedge$ , itself or  $T_H \mp KM$ . Although poly(dimethyl siloxane) has the lowest value of  $\epsilon_0$  and  $T_y$  shown and poly(methyl methacrylate) has the highest, there is no consistent correlation of  $\epsilon_0$  and  $1/\eta$ .

Plazek has questioned the variation of  $\wedge$  with  $t_K$  (60). He suggests that  $tag$  is a universal constant (of unspecified magnitude) that is independent of structure and that the variation with  $T^\wedge$  in Table 4 is an artifact due to the lack of good data around  $T^\wedge$  and the consequent need to make an unreliable extrapolation from higher temperature data. Nevertheless, the

high temperature variation remains, which is of more practical use to engineers needing to compare the responses of different polymers.

In general, then, an examination of the effects of the operational variables temperature and frequency and of changes in the nature of the polymer is closely tied to  $T_K$  and  $\xi_{(A)}$ , which set the location of the transition zone in plots such as Figure 5B and A, respectively.

Molecular weight has practically no effect on the modulus from the glassy state through the transition region and into the plateau. If the molecular weight is high enough to be of interest for most applications where mechanical properties are important, neither  $\tau^*$  nor the reference time of the response is affected by further changes in molecular weight. However, the width of the plateau and the manner in which it drops off with time or temperature are strongly influenced by both the molecular weight and the molecular weight distribution. Broader distributions lead to broader, slower dropoffs. At a characteristic molecular weight,  $M_e$ , which is polymer specific, the plateau disappears. For  $M < M_e$  both the characteristic time of Figure 5A and  $\tau^*$  of Figure 5B are decreased and the curves shift to the left, as shown.

The rubbery plateau is caused by molecular entanglements (16,54-56, 61-63). Entanglements were formerly thought to consist of polymer chains looping around one another. These widely spaced entanglement points then serve as virtual cross-links. Since a typical polymer has a molecular weight between entanglement points,  $A_e$ , of roughly 20,000, most molecules will have several entanglements, and the number of entanglements will increase with molecular weight. Viscous flow occurs when a large fraction of the entanglements move permanently to relieve the stress on them during the time scale of the experiment. A progressively higher molecular weight requires a correspondingly longer time or higher temperature before viscous flow dominates the response. The modulus then takes another drop from about  $10^7$  dyn/cm<sup>2</sup> to zero. Thus the length of the rubbery plateau is a function of the number of entanglements per molecule,  $M/M_e$  (10,54,56,64,65).

A more appropriate picture (66-71) considers that a randomly coiled chain embedded in its randomly coiled neighbors is restricted from diffusing laterally because most of the adjoining segments that it contacts, being randomly oriented, will be transverse to it. Hence it is trapped in a tubelike cage of its neighbors and can move only (or move primarily) by diffusing along its own length.  $M_e$  is now a measure of the tube diameter. Disentanglement and the resulting flow then represents the diffusion out of this tube by a snakelike motion called reptation (63) rather than a slipping through the imagined entanglement loops. The net effect is the same, however, in that while the magnitude of rubbery plateau is still independent



of molecular weight, the higher the molecular weight, the longer it takes, in Figure 5A, or the higher the temperature, in Figure 5B, before viscous flow occurs.

For molecular weights below  $M_m$ , both the monomeric friction factor and  $T_K$  are less than the asymptotic values found at higher molecular weight. The decrease in friction factor shifts the modulus curve to the left, as shown in Figure 5A by the dashed line, even though the samples are being compared at equivalent temperatures (i.e.,  $T_K + \Delta T$ ). The  $\gamma$  effect means that this curve would be shifted still farther toward shorter times if the results for the high- and very low-molecular-weight samples were compared at the same temperature.

## B. Effect of Cross-Linking

A small number of chemical cross-links act about the same as entanglements, but the cross-links do not relax or become ineffective at high temperatures. Thus cross-linked elastomers show rubberlike elasticity and recoverable deformation even at high temperatures and for long times after being stretched or deformed. The modulus in the rubbery region increases with the number of cross-link points or, equivalently, as the molecular weight between cross-links  $M_c$  decreases. This behavior is illustrated in Figure 6. The modulus actually increases slightly with temperature as long as the kinetic theory of rubber elasticity is valid (see Chapter 3).

In addition to raising the rubbery modulus, cross-linking produces three other effects (72-74). First, when the cross-link density becomes fairly high, the glass transition temperature is increased, so the drop in the modulus becomes shifted to higher temperatures or longer times. Second, the transition region is broadened, with the modulus dropping at a lower rate and plateauing at a higher level. At least part of the broadening of the transition region is due to the heterogeneity in the molecular weight between cross-links (73). Widely spaced cross-links produce only slight restrictions on molecular motions, so the  $T_g$  tends to be close to that of the uncross-linked polymer. As the cross-link density is increased, molecular motion becomes more restricted, and the  $T_K$  of the cross-linked polymer rises.

The final reason for the broadening is that the nature of the polymer backbone has changed and the highly cross-linked system has become a copolymer. A homopolymer consisting of just the cross-link structure would have a higher  $\xi$ , value and go through its transition at a much higher temperature, and the results observed reflect this. Cross-linking has rather little effect on the magnitude of the modulus in the glassy state (i.e., at very short times or at temperatures below  $T_g$ ). Both increases and decreases

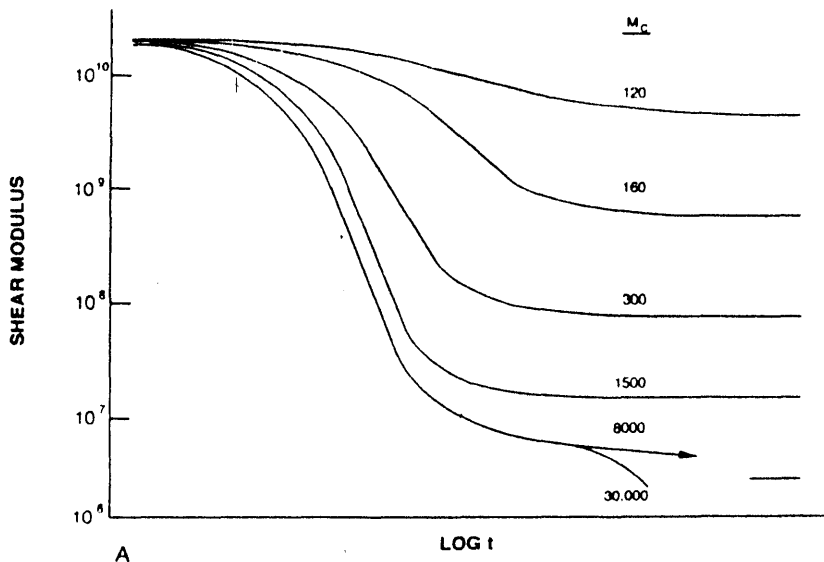
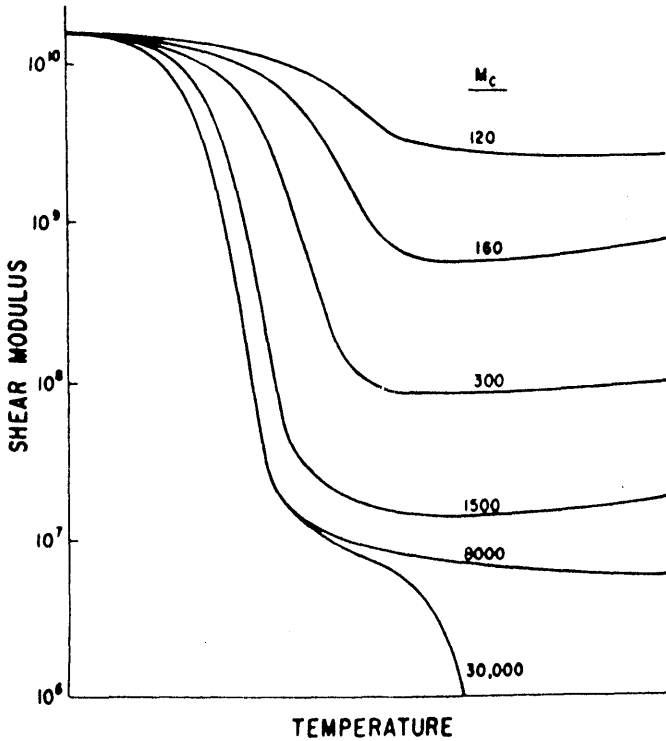


**Figure 6** Effect of cross-linking on (A) modulus-time and (B) modulus-temperature curves of amorphous uncross-linked polymers. The numbers on the curves are approximate values of  $M_c$ . The value 30,000 refers to an uncross-linked polymer with a molecular weight of roughly 30,000 between entanglement points. Modulus is given in  $\text{dyn/cm}^2$ .

has been observed. If perfect network structures could be made, large increases in modulus should theoretically occur at extremely high degrees of cross-linking, such as in diamonds.

### C. Effect of Crystallinity

Crystallinity in a polymer modifies the modulus curve of an amorphous polymer above its  $T_K$  point by at least two mechanisms (75,76). First, the crystallites act as cross-links by tying segments of many molecules together. Second, the crystallites have very high moduli compared to the rubbery amorphous parts, so they behave as rigid fillers in an amorphous matrix. Hard particles will stiffen a soft matrix far more than they will a hard matrix. Since a glass has a modulus nearly as great as that of an organic crystal (77), Crystallinity has only a slight effect on the modulus below  $T_{gy}$  while the stiffening effect is most pronounced in the normally rubbery



B

region of response. Here the modulus increases very rapidly with the degree of Crystallinity. The effects of Crystallinity are illustrated in Figure 7. The cross-linking and filler effects of the crystallites last up to the melting point. The melting point will generally increase some as the degree of Crystallinity increases. Above the melting point, behavior typical of an amorphous polymer is found.

Between  $T_g$  and the melting point, the modulus—temperature curves often have an appreciable negative slope. This gradual change in modulus is due partly to some melting of small or imperfect crystallites below the melting point, which reduces both the rigid filler effect and the cross-linking effect, and due partly to a loosening of the structure as a result of thermal expansion.

The effect of Crystallinity on the time-scale plot is rather complex and not readily sketched. If the crystallites were thermally stable, the isothermal

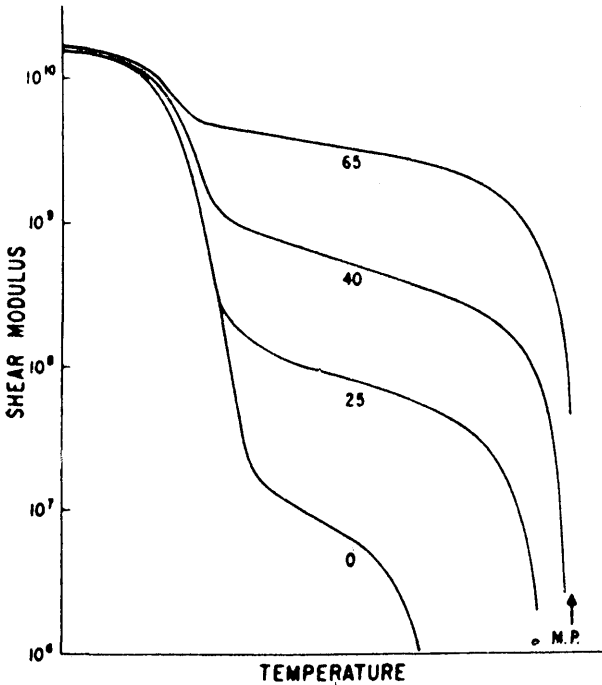


Figure 7 Effect of crystallinity on the modulus-temperature curve. The numbers on the curves are rough approximations of the percent of crystallinity. Modulus is given in dyn/cm<sup>2</sup>.

curves for varying percent crystallinities would resemble those for varying cross-link density (Figure 6B). Raising the temperature would merely shift the curves to the left, to shorter times. Since the crystallites do melt, however, there is an additional drop in the plateau modulus at each temperature, until the crystallites no longer serve as cross-links and the modulus drops rapidly toward that of the amorphous state.

Crystallinity often has little if any effect on  $T_K$ , but with some polymers crystallized under certain conditions, the  $T_K$  value is raised (78,79). The increase appears to be caused either by polymer being restricted to short amorphous segments between two crystallites or by stresses put on the amorphous chain sequences as a result of the crystallization process. In either case the mobility is restricted, so higher temperatures are required to restore it. Thus quench cooling tends to increase  $T_K$ , whereas annealing reduces  $T_K$  back to the value typical of the amorphous polymer.

The morphology of the crystallite structures present is also important in determining the mechanical properties.

## D. Copolymerization and Plasticization

Plasticizer and Copolymerization change the glass transition temperature as discussed in Chapter 1. Plasticizers have little effect on  $\epsilon_{\infty}$ . Copolymerization can change  $\epsilon_{\infty}$ , although less strongly than  $T_g$ . As a result, the basic modulus-temperature and modulus-time curves are shifted as shown in Figure 8 for different compositions. The shift in the modulus-temperature curve is essentially the same as the shift in  $T_g$ . The shift in the modulus-time curve includes this plus the effect of any change in  $\epsilon_{0j}$ .

Copolymers and plasticized materials often show another effect—a broadening of the transition region with a decrease in the slope of the modulus curve in the region of the inflection point. This effect is most pronounced with plasticizer which are poor solvents for the polymer (80-84). Heterogeneous copolymers, in which there is a change in overall chemical composition in going from one molecule to another, also have broad transition regions (85-87). This heterogeneity can result from the fact that in most copolymerizations the first polymer formed tends to be richer in one component than the other, while during the last part of the polymerization reaction the molecules become richer in the other comonomer. This results in a mixture with a distribution of glass transitions and friction factors. Polymer mixtures of different chemical composition tend to be insoluble in each other, and this tendency for phase separation is another cause of the broadening of the transition region (87). If the molecules of different composition are completely soluble in one another and if the mixture is homogeneous in the sense of being thoroughly mixed, there is little if any broadening of the transition (88).

The magnitude of the rubbery modulus does not depend, strictly speaking, on  $M_f$  but on the number concentration of chains between entanglement points,  $\nu_e$  ( $\nu_e = \nu / RTIM_f$ ). Thus plasticizers can lower the plateau modulus by a simple dilution effect. Usually, the plasticizer content is too low to have any significant effect. However, the plateau can be decreased markedly within a polymer family (e.g., methyl acrylates) by copolymerizing a monomer with long side-chain branches (e.g., dodecyl methacrylate). The decrease occurs because the degree of polymerization between available cross-links  $\bar{P}_c (= AV_{\text{monomer}} \text{ molecular weight } M_f)$  is insensitive to structure (62) and nearly constant. Hence increasing  $M_o$  raises the effective  $M_e$  significantly, with a corresponding decrease in the rubbery plateau.

Plasticizers and Copolymerization also shift the glass transition responses of the amorphous phase of crystalline polymers. In addition, the degree of Crystallinity and melting point are lowered. The resulting effects on the

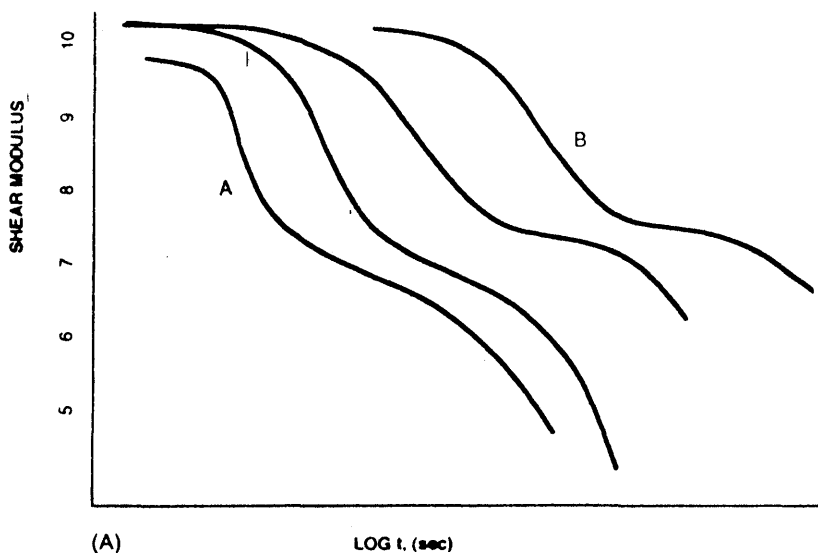


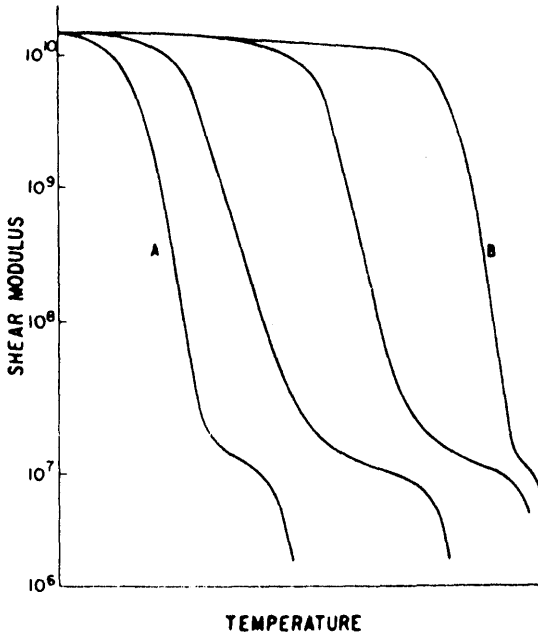
**Figure 8** Effect of plasticization or copolymerization on (A) the modulus-time and (B) modulus-temperature curves. The curves correspond to different plasticizer concentrations or to different copolymer compositions. Curve B is unplasticized homopolymer; A is either a second homopolymer or plasticized B.

modulus-temperature curves are as expected from the previous discussion. There are also other subtle effects, which are discussed in detail in later chapters.

### E. Block and Graft Polymers and Polyblends

In a few cases mixtures of two polymers are soluble in one another, where there is a close match of the solubility parameters or strong polymer-polymer interactions. They form single-phase systems. Two examples of compatible blends are polystyrene with poly(2,6-dimethyl phenylene oxide) (89) and poly(methyl methacrylate) with highly chlorinated (>50%) polyethylene (90). The mechanical properties of compatible blends resemble those of random copolymers, having a single  $T^{\wedge}$  value and modulus transition zone.  $T_K$  varies rather regularly with composition, often following the simple rule of mixtures. The rubbery plateau and steady-flow viscosity are less apt to vary regularly.

Generally, however, mixtures of two polymers are insoluble in one another and form two-phase systems (91-104). Block and graft polymers, in



(B)

which there are long sequences of each homopolymer, also are two-phase systems (105-114). Thus in block and graft polymers there is the unique situation in which a single molecule can be in two phases simultaneously.

Incompatibility and phase separation can be difficult to determine. Most often the inhomogeneity renders the product turbid or at least milky. However, systems with closely matching indices of refraction or with a very small domain size can be quite transparent. While differential scanning calorimetry, density, dilatometric  $\Delta$ , dielectric, and x-ray measurements have all been applied to determining compatibility, modulus measurements and scanning electron microscopy (in cases where one phase can be stained) have proven to be the most sensitive to phase separation (115). In two-phase systems where the phases are well separated, there are two glass transitions instead of the usual one. Each transition is characteristic of one of the homopolymers. The resulting modulus-temperature curve has two steep drops, as shown in Figure 9. The value of the modulus in the plateau region between the two glass transitions depends on the ratio of the components and on which phase tends to be the continuous phase and which is the dispersed phase, and on the morphology of the discontinuous phase

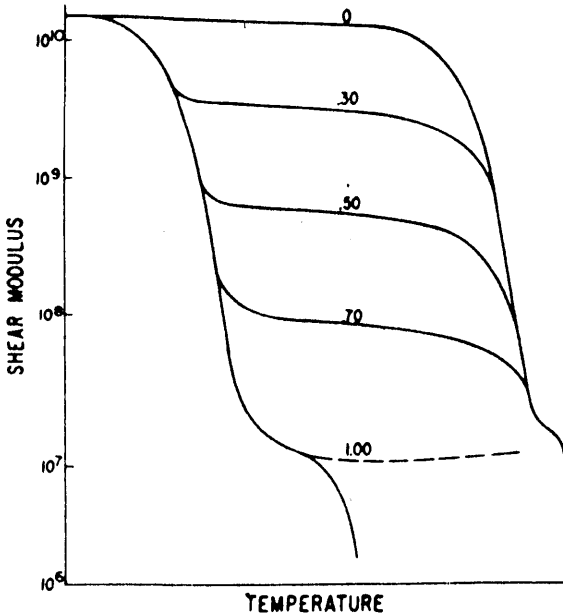


Figure 9 Modulus-temperature curves of two-phase polyblends and block polymers of widely different  $T_g$  values. The numbers on the curves are rough estimates of the volume fraction of the component with the lower  $T_g$  value, which is shown both as an amorphous and as a cross-linked material (dashed line). Modulus is given in dyn/cm<sup>2</sup>.

(104,116,117). A corresponding isothermal  $\log E(t)$  versus  $\log t$  plot would look very similar if it could be measured over the full glass-to-flow region. However, the width of the intermediate plateau would decrease strongly with increasing temperature.

## PROBLEMS

1. What is the shear modulus of a polymer specimen as measured in a torsion pendulum with a period of 1.0 s if the specimen is 4 in. long, 0.40 in. wide, and 0.030 in. thick? The moment of inertia of the system is 5000 g·cm<sup>2</sup>.
2. What is the Young's modulus of the polymer in Problem 1 if Poisson's ratio is 0.35?



3. A nylon fiber has uniaxial orientation in which the polymer chains are parallel to the fiber axis. Is  $E_L$  greater than  $E_T$ ? Is  $G_{TT}$  greater than  $G_{LT}$ ? Why?
4. A beam of polystyrene is supported at each end. A load of 10 lb is applied to the middle. How much will the beam deflect if it is 1 ft long with a square cross section 1 in. to the side? The Young's modulus is  $3.5 \times 10^{10}$  dyn/cm<sup>2</sup>.
5. If the beam of Problem 4 were a cantilever beam with the load on the end, what would the deflection of the end be?
6. A bar of polystyrene with a Young's modulus of  $3.5 \times 10^{10}$  dyn/cm<sup>2</sup> is dropped on the floor. As it rebounds into the air, it vibrates as a free-free beam. What is the frequency of the sound it emits if it is 8 in. long and has a diameter of 0.5 in?
7. A sinusoidal input,  $\epsilon = \epsilon_0 \sin \omega t$  [see equation (10)], can also be written as  $\epsilon = \epsilon_0 e^{i\omega t}$ . Show that  $\sigma/\epsilon$ , called  $M^*$ , then leads to  $M^* = M' + iM''$ . Show that for a compliance, the sign is reversed (e.g., in shear,  $J^* = J' - iJ''$ ).
8. Although mixtures of most polymers form two-phase systems with two glass transitions, some mixtures do form one phase with a single  $T_g$ . An example of a single-phase mixture is poly(vinyl acetate) ( $T_g = 35^\circ\text{C}$ ) and poly(methyl acrylate) ( $T_g = 14^\circ\text{C}$ ). What is the approximate  $T_g$  value of a mixture containing equal volumes of the two polymers?
9. The modulus of a crystalline polymer changes from  $1.3 \times 10^{10}$  dyn/cm<sup>2</sup> below  $T_g$  to  $10^9$  dyn/cm<sup>2</sup> just above the glass transition region. What is the approximate degree of crystallinity? On raising the temperature to the region of the melting point, the modulus drops to  $10^8$  dyn/cm<sup>2</sup>. What is the degree of crystallinity at this higher temperature?
10. Give several possible ways of telling the difference between an uncross-linked polymer of very high molecular weight and one that has a very low degree of cross-linking.
11. Using only mechanical tests, how can a crystalline polymer be distinguished from a cross-linked one?
12. A glass fiber mat in which the fibers appear to be randomly oriented is impregnated with a thermosetting resin and cured. Strips are cut from the sheet in different directions, and their Young's modulus is measured. The Young's moduli are not the same in different directions. If the differences are much greater than the expected experimental errors, what is the most probable cause of the difference in moduli?

13. A uniaxial composite consists of aligned glass fibers in a polymer matrix. If the modulus of the fibers is 20 times that of the polymer, is the longitudinal Young's modulus greater or less than the transverse Young's modulus? Is  $G_{LT}$  greater than  $G_{TT}$ ?
14. A beam with a square cross section of thickness  $D$  is to be compared with a circular beam of diameter  $D$ . If the two beams of the same length are supported on their ends and are center loaded with a weight  $W$ , which beam will deflect the most? What is the ratio of their center deflections if both beams have the same modulus?
15. Two beams of the same material are clamped at one end to form a cantilever beam. One beam has a square cross section of thickness  $D$ , and the other beam has a circular cross section of diameter  $D$ . The beams are set in vibration by a tap near the free end. If the length of the beams is the same, which beam will have the higher frequency of vibration? What is the ratio of their frequencies?
16. The Young's modulus of a polymer is to be measured by the frequency of vibration of a cantilever beam. The beam is 4 in. long, 0.5 in. wide, and 0.025 in. thick. The density of the polymer is 1.0. If the resonance frequency is 20 Hz, what is the Young's modulus?

## REFERENCES

1. R. F. Hearmon, *Introduction to Applied Anisotropic Elasticity*, Oxford University Press, Oxford, 1961.
2. J. E. Ashton and J. M. Whitney, *Theory of Laminated Plates*, Technomic, Lancaster, Pa., 1970.
3. J. F. Nye, *Physical Properties of Crystals: Their Representation by Tensors and Matrices*, Oxford University Press, Oxford, 1957.
4. I. M. Ward, in *Polymer Systems: Deformation and Flow*, R. E. Wetton and R. W. Whorlow, Eds., Macmillan, London, 1968, p. 1.
5. R. M. Christensen, *Mechanics of Composite Materials*, Wiley, New York, 1979.
6. R. M. Jones, *Mechanics of Composite Materials*, Scripta, Silver Spring, Md., 1975.
7. I. M. Ward, *Mechanical Properties of Solid Polymers*, 2nd ed., Wiley, New York, 1983.
8. L. E. Nielsen, *Mechanical Properties of Polymers*, Van Nostrand Reinhold, New York, 1962.
9. W. D. Harris, in *Testing of Polymers*, Vol. 4, W. E. Brown, Ed., Interscience, New York, 1969, p. 399.
10. *ASTM Standards D638, D882, and D412*, American Society for Testing and Materials, Philadelphia.

11. R. J. Roark, *Formulas for Stress and Strain*, 3rd ed., McGraw-Hill, New York, 1954.
12. H. S. Loveless, in *Testing of Polymers*, Vol. 2, J. V. Schmitz, Ed., Interscience, New York, 1966, p. 321.
13. *Technical Data on Plastics*, Manufacturing Chemists' Association, Washington, D.C., 19
14. C. C. Hsiao and J. A. Sauer, *ASTM Bull.*, **172**, 29 (1951).
15. A. E. Moehlenpah, O. Ishai, and A. T. DiBenedetto, *J. Appl. Polymer Sci.*, **13**, 1231 (1969).
16. J. D. Ferry, *Viscoelastic Properties of Polymers*, 3rd ed., Wiley, New York, 1980.
17. I. L. Hopkins and R. W. Hamming, *J. Appl. Phys.*, **28**, 906 (1957).
18. L. J. Zapas and J. C. Phillips, *J. Res. Natl. Bur. Std.*, **A75**, 33 (1971).
19. J. Marin and G. Cuff, *Proc. ASTM*, **49**, 1158 (1949).
20. D. J. Plazek, *J. Polymer Sci.*, **A2**, **6**, 621 (1968).
21. T. Yoshitomi, K. Nagamatsu, and K. Kosiyama, *J. Polymer Sci.*, **27**, 335 (1958).
22. T. E. Morrison, L. J. Zapas, and T. W. DeWitt, *J. Polymer Sci.*, **19**, 237 (1956).
23. W. N. Findley, *Trans. Plastics Inst.*, **30**, 138 (1962).
24. D. G. O'Connor and W. N. Findley, *Trans. SPE*, **2**, 273 (1962).
25. L. R. G. Treloar, *Proc. Roy. Soc. (London)*, **A351**, 301 (1976), and further references there.
26. L. J. Zapas, *J. Res. Natl. Bur. Std.*, **A70**, 525 (1966).
27. G. W. Becker, *J. Polymer Sci.*, **C16**, 2893 (1967); G. W. Becker and O. Krüger, in *Deformation and Fracture of High Polymers*, H. H. Kausch, J. A. Hassell, and R. I. Jaffee, Eds., Plenum Press, New York, 1973, p. 115.
28. A. San Miguel, *Exptl. Mech.*, **12**, 155 (1972).
29. J. Glucklich and R. F. Landel, *J. Polymer Sci. (Phys.)*, **15**, 2185 (1977).
30. Y. Obata, S. Kawabata, and H. Kawai, *J. Polymer Sci.*, **A2**, **8**, 903 (1970); S. Kawabata and H. Kawai, *Fortschr. Hochpolymer Forsch.*, **24**, 89 (1977).
31. H. Vangerko and L. R. G. Treloar, *J. Phys. D, Appl. Phys.*, **11**, 1969 (1978).
32. M. Zaslavsky, *Polymer Eng. Sci.*, **9**, 105 (1969).
33. T. L. Smith and J. A. Rinde, *J. Polymer Sci.*, **A2**, **7**, 675 (1969).
34. L. M. Carapellucci and A. F. Yee, *Polymer Eng. Sci.*, **26**, 920 (1986).
35. E. Z. Stowell and R. K. Gregory, *J. Appl. Mech.*, **E32**, 37 (1965).
36. S. S. Sternstein and T. C. Ho, *J. Appl. Phys.*, **43**, 4370 (1972).
37. R. G. Mancke and R. F. Landel, *J. Polymer Sci. (Phys)*, **10**, 2041 (1972).
38. G. B. McKenna, in *Comprehensive Polymer Science*, Vol. 2, *Polymer Properties*, C. Bioth and C. Price, Eds., Pergamon Press, Oxford, 1989.
39. D. L. Questad, *Polymer Eng. Sci.*, **26**, 269 (1986).
40. R. K. Mittal and I. P. Singh, *Polymer Eng. Sci.*, **26** (1986).
41. A. J. Kovacs, *Trans. Soc. Rheol.*, **5**, 285 (1961).
42. A. J. Kovacs, *Adv. Polymer Sci.*, **3**, 394 (1964).
43. W. N. Findley, R. M. Read, and D. Stern, *J. Appl. Mech.*, **E34**, 895 (1967).

44. C. C. Surland, *J. Appl. Polymer Sci.*, **11**, 1227 (1967); *Exptl. Mech.*, **3**, 112 (1963).
45. J. P. Den Hartog, *Mechanical Vibrations*, 4th ed., McGraw-Hill, New York, 1956.
46. G. W. Trayer and H. W. March, *Natl. Advisory Comm. Aeronaut. Rept.* **334**.
47. W. M. Madigosky and G. F. Lee, *J. Acoust. Soc. Am.*, **73**, 1374 (1983).
48. B. Hartman, J. V. Duffy, G. F. Lee, and E. Balizer, *J. Appl. Polymer Sci.*, **35**, 1829 (1988).
49. H. A. Waterman, *Kolloid Z.*, **192**, 1, 9 (1963).
50. W. P. Mason and H. J. McSkimin, *Bell Syst. Tech. J.*, **31**(1), 121 (1952).
51. R. S. Witte, B. A. Mrowca, and E. Guth, *J. Appl. Phys.*, **20**, 481 (1949).
52. A. W. Nolle, *J. Appl. Phys.*, **19**, 753 (1948).
53. B. A. Dunell and J. H. Dillon, *Textile Res. J.*, **21**, 393 (1951).
54. F. Bueche, *Physical Properties of Polymers*, Interscience, New York, 1962.
55. A. V. Tobolsky, *Properties and Structure of Polymers*, Wiley, New York, 1960.
56. J. J. Aklonis and W. J. MacKnight, *Introduction to Polymer Viscoelasticity*, 2nd ed., Wiley, New York, 1983.
57. S. J. Orbon and D. J. Plazek, *J. Polymer Sci., Polymer Phys. Ed.*, **17**, 1871 (1979); N. Raghupathi, Ph.D. thesis, University of Pittsburgh, 1975.
58. D. J. Plazek and G. C. Berry, in *Glass: Science and Technology*, Vol. 3, *Viscosity and Relaxation*, D. R. Uhlmann and N. J. Kreidl, Eds., Academic Press, New York, 1986, p. 363.
59. P. E. Rouse, Jr., *J. Chem. Phys.*, **21**, 1272 (1953).
60. D. J. Plazek, M. J. Rosner, and D. L. Plazek, *J. Polymer Sci., Polymer Phys.*, **26**, 473 (1988).
61. G. C. Berry and T. G. Fox, *Adv. Polymer Sci.*, **5**, 261 (1968).
62. T. G. Fox, S. Gratch, and S. Loshaek, in *Rheology*, Vol. 1, F. R. Eirich, Ed., Academic Press, New York, 1956, p. 431.
63. R. S. Porter and J. F. Johnson, *Chem. Rev.*, **66**, 1 (1966).
64. J. D. Ferry, R. F. Landel, and M. L. Williams, *J. Appl. Phys.*, **26**, 359 (1955).
65. G. V. Vinogradov, E. A. Dzyura, A. Ya. Malkin, and V. A. Grechanovskii, *J. Polymer Sci.*, **A2**, **9**, 1153 (1971).
66. P.-G. De Gennes, *Nature (London)*, **282**, 367 (1979); *Scaling Concepts in Polymer Physics*, Cornell University Press, Ithaca, N.Y., 1979.
67. M. Doi and S. F. Edwards, *J. Chem. Soc. Faraday Trans. 2*, **74**, 1789, 1802, 1818 (1975).
68. M. Doi and S. F. Edwards, *J. Chem. Soc. Faraday Trans. 2*, **75**, 38 (1979).
69. D. S. Pearson, *Rubber Chem. Technol.*, **60**, 439 (1987).
70. C. F. Curtiss and R. B. Bird, *J. Chem. Phys.*, **74**, 2016, 2026 (1981).
71. R. B. Bird, O. Hassager, R. C. Armstrong, and C. F. Curtiss, *Dynamics of Polymeric Liquids*, Vol. 2, *Kinetic Theory*, 2nd ed., Wiley, New York, 1987.

72. L. E. Nielsen, *J. Macromol. Sci. Rev. Macromol. Chem.*, **3**, 69 (1969).
73. K. Ueberreiter and G. Kanig, *J. Chem. Phys.*, **18**, 399 (1950).
74. A. V. Tobolsky, D. Katz, M. Takahashi, and R. Schaffhauser, *J. Polymer Sci.*, **A2**, 2749 (1964).
75. L. E. Nielsen and F. D. Stockton, *J. Polymer Sci.*, **A1**, 1995 (1963).
76. A. V. Tobolsky, *J. Chem. Phys.*, **37**, 1139 (1962).
77. J. J. Joseph, J. L. Kardos, and L. E. Nielsen, *J. Appl. Polymer Sci.*, **12**, 1151 (1968).
78. D. W. Woods, *Nature*, **174**, 753 (1954).
79. S. Newman and W. P. Cox, *J. Polymer Sci.*, **46**, 29 (1960).
80. L. E. Nielsen, R. Buchdahl, and R. Levreault, *J. Appl. Phys.*, **20**, 507 (1949).
81. K. Wolf, *Kunststoffe*, **41**, 89 (1951).
82. K. Schmieder and K. Wolf, *Kolloid Z.*, **127**, 65 (1952).
83. F. Linhardt, *Kunststoffe*, **53**, 18 (1963).
84. R. J. Hammond and J. L. Work, *J. Polymer Sci.*, **A1**, **6**, 73 (1968).
85. L. E. Nielsen, *J. Am. Chem. Soc.*, **75**, 1435 (1953).
86. A. V. Tobolsky and I. L. Hopkins, *J. Polymer Sci.*, **A1**, **7**, 2431 (1969).
87. G. Kraus and K. W. Rollmann, *Adv. Chem. Ser.*, **99**, 189 (1971).
88. S. N. Chinai and L. E. Nielsen, *Mechanical Properties of Polymers*, Van Nostrand Reinhold, New York, 1962, p. 173.
89. R. P. Kambour and S. A. Smith, *J. Polymer Sci. (Phys.)*, **20**, 2069 (1982).
90. C. Zhikuan, S. Ruona, D. J. Walsh, and J. S. Higgins, *Polymer*, **24**, 263 (1983).
91. A. Dobry and F. Boyer-Kawenoki, *J. Polymer Sci.*, **2**, 90 (1947).
92. R. Buchdahl and L. E. Nielsen, *J. Appl. Phys.*, **21**, 482 (1950).
93. R. Ecker, *Rubber Chem. Technol.*, **30**, 200 (1957).
94. E. Jenckel and H. U. Herwig, *Kolloid Z.*, **148**, 57 (1956).
95. T. T. Jones, *Brit. Plastics*, **33**, 525 (1960).
96. G. Kraus, K. W. Rollman, and J. T. Gruver, *Macromolecules*, **3**, 92 (1970).
97. G. Cigna, *J. Appl. Polymer Sci.*, **14**, 1781 (1970).
98. K. Fujimoto and N. Yoshimura, *Rubber Chem. Technol.*, **41**, 1109 (1968).
99. S. Miyata and T. Hata, in *Proc. 5th Intern. Congr. Rheol.*, Vol. 3, S. Onogi, Ed., University of Tokyo, Tokyo, 1970, p. 71.
100. K. Fujino, Y. Ogawa, and H. Kawai, *J. Appl. Polymer Sci.*, **8**, 2147 (1964).
101. P. Zitek and J. Zelinger, *J. Polymer Sci.*, **A1**, **6**, 467 (1968).
102. S. G. Turley, *J. Polymer Sci.*, **C1**, 101 (1963).
103. P. Bauer, J. Hennig, and G. Schreyer, *Angew. Makromol. Chem.*, **11**, 145 (1970).
104. M. Takayanagi, *Mem. Fac. Eng. Kyushu Univ.*, **23**(1), 1 (1963).
105. J. A. Blanchette and L. E. Nielsen, *J. Polymer Sci.*, **20**, 317 (1956).
106. E. B. Atkinson and R. F. Eagling, *Physical Properties of Polymers*, Soc. Chem. Ind. Monogr. 5, Macmillan, New York, 1959, p. 197.
107. H. Hendus, K.-H. Illers, and E. Ropte, *Kolloid Z.*, **216-217**, 110 (1967).
108. G. Holden, E. T. Bishop, and N. R. Legge, *J. Polymer Sci.*, **C26**, 37 (1969).

109. G. M. Estes, S. L. Cooper, and A. V. Tobolsky, *J. Macromol. Sci. Rev. Macromol. Chem.*, **C4**, 313 (1970).
110. J. F. Beecher, L. Marker, R. D. Bradford, and S. L. Aggarwal, *J. Polymer Sci.*, **C26**, 117 (1969).
111. E. Perry, *J. Appl. Polymer Sci.*, **8**, 2605 (1964).
112. M. Baer, *J. Polymer Sci.*, **A2**, 417 (1964).
113. M. Buccaredda, E. Butta, and V. Frosini, *J. Polymer Sci.*, **C4**, 605 (1964).
114. R. J. Angelo, R. M. Ikeda, and M. L. Wallach, *Polymer*, **6**, 141 (1965).
115. H. Breuer, in *Polymer Blends and Mixtures*, D. J. Walsh, J. S. Higgins, and A. Macconachie, Eds., Nijhoff, Dordrecht, The Netherlands, 1985, pp. 375, 383.
116. L. E. Nielsen, *Appl. Polymer Symp.*, **12**, 249 (1969).
117. D. H. Kaelble, *Trans. Soc. Rheol.*, **15**, 235 (1971).

# 3

## Creep and Stress Relaxation

### I. INTRODUCTION

Creep and stress-relaxation tests measure the dimensional stability of a material, and because the tests can be of long duration, such tests are of great practical importance. Creep measurements, especially, are of interest to engineers in any application where the polymer must sustain loads for long periods. Creep and stress relaxation are also of major importance to anyone interested in the theory of or molecular origins of Viscoelasticity.

For elastomeric materials, extremely simple equipment can be used to measure creep or stress relaxation. For rigid materials the measurements become more difficult, and more elaborate equipment is generally required. In the creep of rigid materials, the difficulty arises from the necessity to measure accurately very small deformations and deformation rates. In the case of the stress relaxation of rigid polymers, the problem is to measure the stress and small strains accurately when the specimen is comparable in rigidity to that of the apparatus, in which case small deformations of the apparatus or slippage of the specimen in its grips can introduce very large errors. A great many instruments have been described in the literature. Instruments and techniques, together with many references, have been described in detail by Ferry (1) and Nielsen (2) and are not reviewed here. However, most modern testing laboratories have commercial "universal" testing machines that can make such measurements,

especially if electronic or optical strain gages are used properly to measure the longitudinal and lateral strain. Unfortunately, creep measurements tend to be made at constant force or load and not constant stress (whether using simple or complex test equipment). One should try to ensure that the proper data are being supplied for and used in analyses.

If the deformations and stresses are small and the time dependence is weak, creep and stress-relaxation tests are essentially the inverse of one another. Otherwise data from one kind of test can be used to calculate the other by fairly complex methods to be described later. However, to a first approximation the interconversion from creep to stress relaxation, or vice versa, is given by a simple equation (3):

$$\left( \frac{\epsilon(t)}{\epsilon_0} \right)_{\text{creep}} \approx \left( \frac{\sigma_0}{\sigma(t)} \right)_{\text{relax}} \quad (1)$$

where  $\epsilon_0$  is the initial strain in a creep test and  $\epsilon(t)$  is the creep strain after time  $t$ .  $\sigma_0$  is the initial stress measured at the beginning of a stress-relaxation test, and  $\sigma(t)$  is the stress after time  $t$ . This equation works better in regions of small time dependence (i.e., in the glassy region, in the rubbery region, or with crystalline materials). The creep response lies at longer times than does inverse stress relaxation. This small difference is accounted for in the more complex calculation methods, but should be kept in mind if equation (1) is used.

When the stresses and strains become large and the stress-strain curve becomes nonlinear, simple descriptions of the response and interconversions between creep and relaxation become increasingly less valid. Published discussions of nonlinear Viscoelasticity in melts, elastomers, and glassy solids all treat or emphasize<sup>1</sup> different aspects of nonlinearity. The problem is still under active investigation, with the greatest progress having been made with elastomers and the least progress with glassy solids. Of course, the response of two-phase systems is, by the same token, even less well understood. Despite this, such materials can be described to a useful extent by straightforward mechanics. The problem that can arise, however, is in trying to describe (1) how the materials will react to a complex stress or strain field if only knowledge of the response in simple tension or simple shear is available, and (2) what the long-time response will be. In the following section the discussion will rely on understanding gained at the linear viscoelastic level. The degree to which it can be extrapolated outside this region must be kept in mind.

## II. MODELS

Very simple models can illustrate the general creep and stress-relaxation behavior of polymers except that the time scales are greatly collapsed in the models compared to actual materials. In the models most of the in-



teresting changes occur in about one decade of time, whereas polymers show (he same total changes only over many decades of time. Nevertheless such models provide a useful mnemonic device for describing or recalling the interplay between viscous and elastic response and for the underlying simple differential equations that describe stress-strain-time relations in linear Viscoelasticity. At the same time, they provide a useful means of visualizing responses.

A simple model for stress relaxation is a Maxwell unit, which consists of a Hookean spring and a Newtonian dashpot in series as shown in the insert in Figure 1. The modulus or stiffness of the spring is  $E$ , and the viscosity of the dashpot is  $\eta$ . In a stress-relaxation experiment the model is given a definite strain  $\epsilon$  while the stress  $\sigma$  is measured as a function of time. In the strained model, the change of the elongation of the spring is compensated by an equal change in the dashpot, but the net rate of change is zero; that is.

$$\frac{d\epsilon}{dt} = \frac{1}{E} \frac{d\sigma}{dt} + \frac{\sigma}{\eta} = 0 \tag{2}$$

since  $\epsilon = \sigma/E$  for the spring and  $\sigma/\eta = d\epsilon/dt$  for the dashpot. The solution of this equation of motion is

$$\frac{\sigma}{\sigma_0} = e^{-Et/\eta} = e^{-t/T} \tag{3}$$

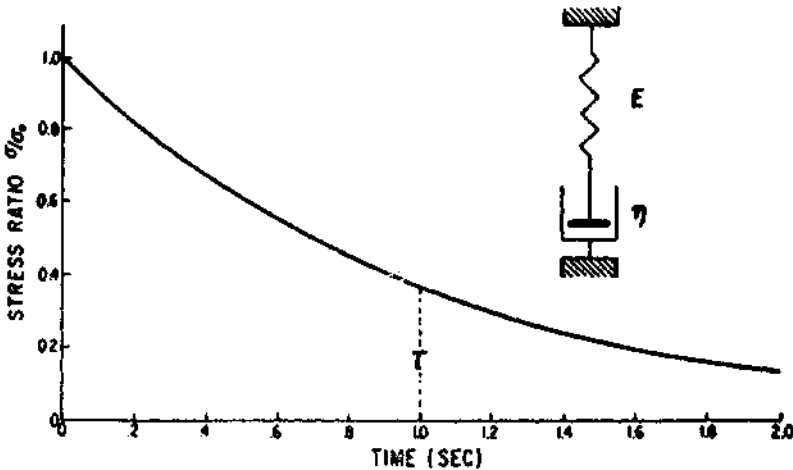


Figure 1 Stress relaxation of a Maxwell model (linear scales),  $T = 1$  s.

where

$$\tau = \frac{\eta}{E} \quad (4)$$

The quantity  $T$  is called the relaxation time.

Equation (3) is plotted with two different time scales in Figures 1 and 2 for values somewhat typical of an elastomer. All the initial deformation takes place in the spring; at a later time the dashpot starts to relax and allows the spring to contract. Most of the relaxation takes place within one decade of time on both sides of the relaxation time, but this is shown clearly only in Figure 2. On the logarithmic time scale, the stress-relaxation curve has a maximum slope at the time  $t = T$  and the stress ratio  $\sigma/\sigma_0$  is 0.3679 or  $e^{-1}$ . The stress relaxation may also be given in terms of a stress-relaxation modulus  $E_r(t)$ :

$$E_r(t) = \frac{\sigma(t)}{\epsilon} = \frac{\sigma_0}{\epsilon} e^{-t/\tau} \quad (5)$$

The model of Figure 1 cannot describe creep behavior at all. This may be illustrated by the four-element model shown in Figure 3. When a constant load is applied, the initial elongation comes from the single spring with the modulus  $E_1$ . Later elongation comes from the spring  $E_2$  and dashpot  $\eta_2$ , in parallel, and from the dashpot with the viscosity  $\eta_1$ . The total elongation

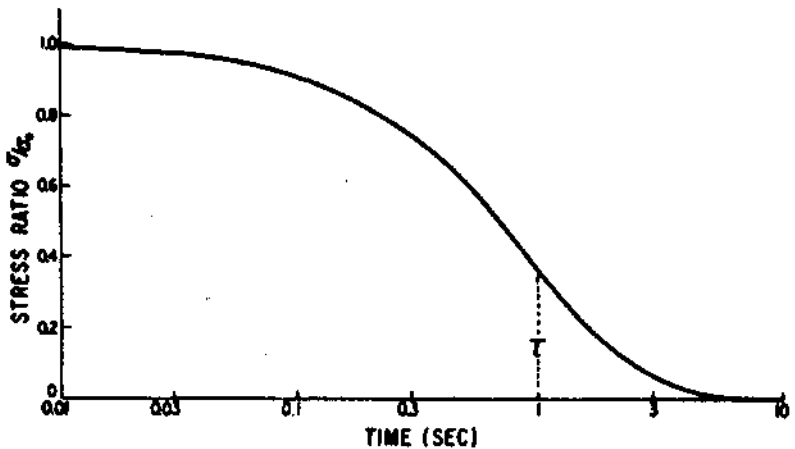


Figure 2 Stress relaxation of a Maxwell model on a logarithmic time scale. Model is the same as Figure 1.

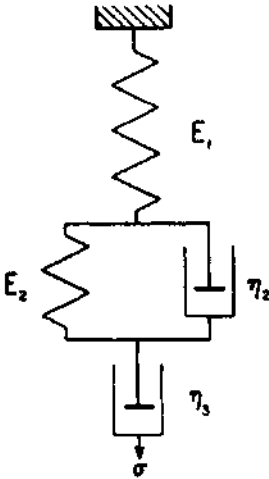


Figure 3 Four-element model for creep.

of the model is the sum of the individual elongations of the three parts. Thus

$$\epsilon = \frac{\sigma_0}{E_1} + \frac{\sigma_0}{E_2} (1 - e^{-t/\tau}) + \frac{\sigma_0}{\eta_3} t \tag{6}$$

where  $\sigma_0$  is the applied stress and the retardation time  $T$  is defined by

$$\tau = \frac{\eta_2}{E_2} \tag{7}$$

In a recovery test after all the load is removed at time  $t_1$ , the creep is all recoverable except for the flow that occurred in the dashpot with viscosity  $\eta_3$ .

The instant the load is removed there is a reduction in the elongation of the model equal to  $\sigma_0/E_2$ . The equation for subsequent creep recovery is

$$\epsilon = \epsilon_2 e^{-(t-t_1)/\tau} + \frac{\sigma_0 t_1}{\eta_3} \tag{8}$$

where

$$\epsilon_2 = \frac{\sigma_0}{E_2} (1 - e^{-t_1/\tau}) \tag{9}$$

Figure 4 illustrates the creep and recovery of a four-element model with the following constants:

$$\begin{aligned} \sigma_0 &= 10^9 \text{ dyn/cm}^2 & E_1 &= 5 \times 10^9 \text{ dyn/cm}^2 \\ \eta_2 &= 5 \times 10^9 \text{ P} & E_2 &= 10^9 \text{ dyn/cm}^2 \\ \eta_3 &= 5 \times 10^{11} \text{ P} & \tau &= 5 \text{ s} \end{aligned}$$

The creep experiment lasted 1(K) s and then the load was removed for the recovery experiment.

Figures 5 and h show how the shape of the creep curve is modified by changes in the constants of the model. The values of the constants are given in Table I. Curve I is the same as shown in Figure 4, curve II shows only a small amount of viscous creep, and in curve III, viscous flow is a prominent part of the total creep. The same data were used in Figures 5 and 6, but notice the dramatic change in the shapes of the curves when a linear time scale is replaced by a logarithmic time scale. In the model, most of the recoverable creep occurs within about one decade of the retardation time.

In Chapter 4, the response of these models to dynamic (i.e., sinusoidal) loads or strains is illustrated. In Chapter 5, the stress-strain response in constant rate experiments is described. Models with nonlinear springs and nonlinear dashpots (i.e., stress not proportional to strain or to strain rate)

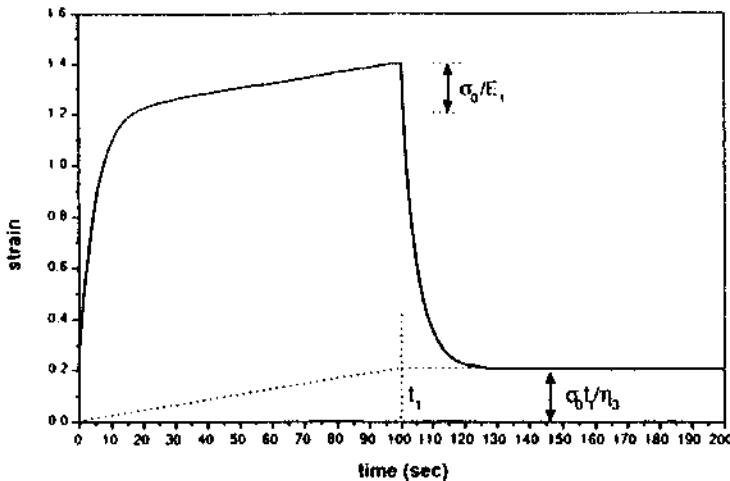


Figure 4 Creep and creep recovery of a four-element model.

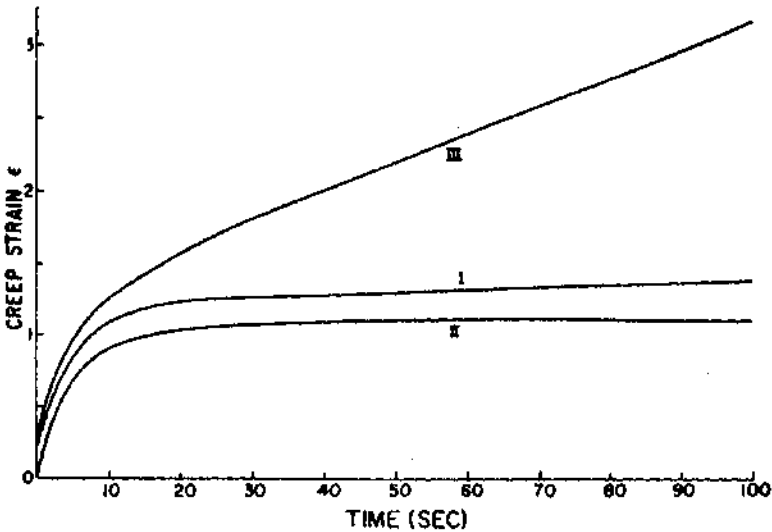


Figure 5 Creep of a four-element model with the constants given in Table 1~ Linear time scale.

in which the nonlinearity is taken to be associated with specific mechanisms such as springs with rubberlike elasticity have also been employed (4).

### III. DISTRIBUTION OF RELAXATION AND RETARDATION TIMES

In Section II, models were discussed that had only a single relaxation or retardation time. Actual polymers have a large number of relaxation or retardation times distributed over many decades of time.  $E(t)$  is then the sum of individual contributions, so equation (5) becomes

$$E(t) = \sum_{i=1}^N E_i e^{-t/\tau_i} \quad (10)$$

Models purporting to describe real material behavior with only a small number of values of  $T$  will provide illustrative calculations of the response only over a small time or temperature region. Such illustrative results can be extremely important in providing guidance as to potential trends in response. However, the models can never be used for reliable estimates of response under real use conditions over wide time or temperature ranges.

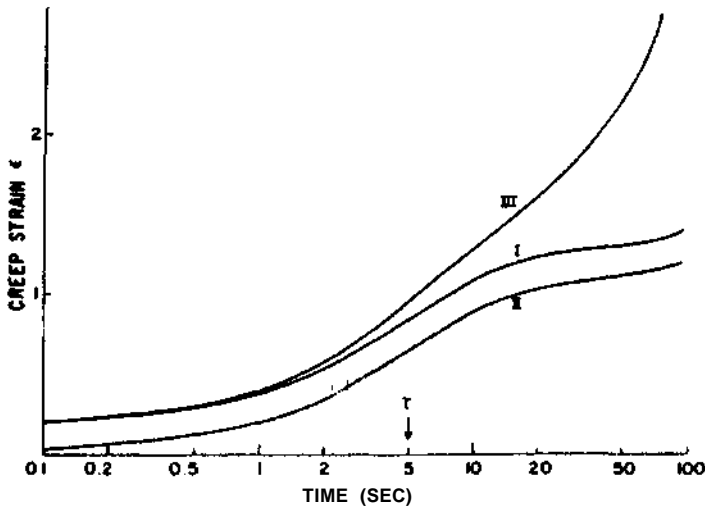


Figure 6 Creep of a four-element model with the same constants as in Figure 5 but with a logarithmic time scale.

Table 1 Constants for Four-Element Creep Model

| Curve | $E_1$           | $\eta_1$           | $E_2$  | $\eta_2$        | $\sigma_0$ |
|-------|-----------------|--------------------|--------|-----------------|------------|
| I     | $5 \times 10^9$ | $5 \times 10^{11}$ | $10^9$ | $5 \times 10^9$ | $10^9$     |
| II    | $10^{11}$       | $5 \times 10^{11}$ | $10^9$ | $5 \times 10^9$ | $10^9$     |
| III   | $5 \times 10^9$ | $5 \times 10^{10}$ | $10^9$ | $5 \times 10^9$ | $10^9$     |

For real polymers with large  $N$ , the summation passes over to an integral and  $E_i$  is replaced by a continuous set of contributions to the modulus associated with each time increment between  $\tau$  and  $\tau + d\tau$  (i.e.,  $F(d\tau)$ ):

$$E(t) = \sum_{i=1}^N E_i e^{-t/\tau_i} \rightarrow \int_0^\infty F(\tau) e^{-t/\tau} d\tau \quad (11)$$

$F(i)$  is the underlying modulus spectrum for that system. As noted above, since the time scale of relaxation is so broad, results are best depicted on a logarithmic time scale. To do this, one needs the contribution to the modulus associated with or lying in the time interval between  $\ln T$  and  $\ln T + d \ln T$ ; this incremental contribution to the modulus is designated as

$H$   $d \ln t$ , so

$$E(t) = \int_{-\infty}^{\infty} H(\ln \tau) e^{-\tau} d \ln \tau \quad (12)$$

The continuous function  $H(\ln T)$  [often simply given the symbol  $H(r)$  as in this chapter) is the continuous relaxation spectrum. Although called, by long-standing custom, a spectrum of relaxation times, it can be seen that  $H$  is in reality a distribution of modulus contributions, or a modulus spectrum, over the real time scale from 0 to  $\infty$  or over the logarithmic time scale from  $-\infty$  to  $+\infty$ .

The distribution of relaxation times  $H(r)$  can be estimated from a stress relaxation or  $E_r(t)$  curve plotted on a  $\log t$  scale by

$$H(\tau) \doteq \frac{-d[E_r(t)]}{d \ln t} \doteq \frac{-1}{2.303} \frac{d[E_r(t)]}{d \log_{10} t} \quad (13)$$

A distribution obtained by the use of equation (13) is only a first approximation to the real distribution. The corresponding distribution of retardation times is designated as  $L(T)$ . It may be estimated from the slope of a compliance curve  $D(t)$  or  $J(t)$ , for tensile or shear creep, respectively, plotted on a logarithmic time scale according to the equation (for shear creep).

$$L(\tau) \doteq \frac{d[J(t)]}{d \ln t} \doteq \frac{1}{2.303} \frac{d[J(t)]}{d \log_{10} t} \quad (14)$$

If there is any viscous flow component to the creep, it should be removed before making the calculation, so

$$L(\tau) \doteq \frac{1}{2.303} \frac{d[J(t) - t/\eta]}{d \log_{10} t} \quad (15)$$

For tensile creep,  $\eta$  would be the tensile viscosity. When the viscosity is high (e.g., when working at relatively low temperatures or with very high-molecular-weight polymers) it can be difficult to determine  $t/\eta$  accurately, so creep recovery measurements are made. Here the load is released after a given creep time and the strain is followed as the specimen shrinks back toward its new equilibrium dimensions.

Equations (13) and (14) can be used to obtain quick estimates and to visualize the response of a polymer system under investigation. In any case, unless  $D(t)$  and  $E(t)$  are varying very slowly on a  $\log$  time scale, the distributions are valid only in the time range from the minimum time of observation, plus one decade, to the maximum time of observation, less one decade. Many more accurate and complex methods of estimating  $L(r)$  and  $H(T)$  have been proposed. These methods have been summarized by

various authors, including Leaderman (5), Ferry (1), and Tobolsky (6), and presented more recently in great detail by Tschoegl (7).

To get accurate distributions of relaxation or retardation times, the experimental data should cover about 10 or 15 decades of time. It is impossible to get experimental data covering such a great range of times at one temperature from a single type of experiment, such as creep or stress relaxation.† Therefore, master curves (discussed later) have been developed that cover the required time scales by combining data at different temperatures through the use of time-temperature superposition principles.

Distributions of relaxation or retardation times are useful and important both theoretically and practically, because  $H$  can be calculated from  $L$  (and vice versa) and because from such distributions other types of viscoelastic properties can be calculated. For example, dynamic modulus data can be calculated from experimentally measured stress relaxation data via the resulting  $H$  spectrum, or  $H$  can be inverted to  $L$ , from which creep can be calculated. Alternatively, rather than going from one measured property function to the spectrum to a desired property function [e.g.,  $E(t) \xrightarrow{*} H(\tau) \rightarrow G^*(\omega)$ ], Schwarzl has presented a series of easy-to-use approximate equations, including estimated error limits, for converting from one property function to another (11).

From the practical standpoint of trying to solve stress analysis problems, however, very little use has been made of  $H(\tau)$  and  $L(\tau)$ , even when they are known. The reason is that at each step in time, integration over the whole range of  $\tau$  has to be carried out. It is easier, instead, to use  $E(\tau)$  or  $D(\tau)$ .

The exponential series in equation (10), called a Prony series, is an attractive explicit representation of  $L(t)$ , extremely useful in numerical calculation. However, although it can describe  $E(t)$  with great fidelity and accuracy if  $E_i$ ,  $\tau_i$ , and  $N$  are known, a known set of  $E(t)$  data cannot be inverted analytically to determine the coefficients. Approximate numerical techniques called collocation methods (12) have been developed which, using preselected  $\tau$  values, will fit the experimental data very well for data that vary slowly (i.e., near the rubbery or glassy region). However, they are unreliable in fitting data through a full transition region. Many people have written computer programs for these and related computations/transformations, but few appear to be commercially available.

The methods described above give continuous distributions of relaxation times. However, the molecular theories of Viscoelasticity of polymers as

---

†Combinations of experiments using dynamic testing such as described in Chapter 4 and one of the transient test modes of creep or stress relaxation have been used in a few cases to obtain wide time coverage at one temperature (8-10).



developed by Rouse (13), Zimm (14), Bueche (15,16), the Doi-Edwards (17-19) school, the Bird-Curtiss-Armstrong (20) school, and others (1,21) give a discrete spectrum of relaxation times (although over much of the range the spectral lines merge into a continuous spectrum).  $\tau_i$  of equation (10) is now completely specified. A typical equation from these theories at temperatures above  $T_g$  is that of the modified Rouse theory for an uncross-linked polymer (21)

$$\tau_i = \tau_p = \frac{6\eta M}{\pi^2 \rho R T p^2} \quad p = 1, 2, 3, \dots, N/5 \tag{16}$$

The longest relaxation time,  $\tau_1$ , corresponds to  $p = 1$ . The important characteristics of the polymer are its steady-state viscosity  $\eta$  at zero rate of shear, molecular weight  $M$ , and its density  $\rho$  at temperature  $T$ ;  $R$  is the gas constant, and  $N$  is the number of statistical segments in the polymer chain. For vinyl polymers  $N$  contains about 10 to 20 monomer units. This equation holds only for the longer relaxation times (i.e., in the terminal zone). In this region the stress-relaxation curve is now given by a sum of exponential terms just as in equation (10), but the number of terms in the sum and the relationship between the TS of each term is specified completely. Thus

$$\frac{\sigma}{\sigma_0} = \frac{5}{N} \sum_{p=1}^{N/5} e^{-t/\tau_p} = \frac{5}{N} \sum_{p=1}^{N/5} e^{-p^2 t/\tau_1} \tag{17}$$

Here  $\tau_1$  is still a ratio of a viscosity to a modulus, as in the spring-dashpot model of Figure 1, but each spring has the same (shear) modulus,  $\rho RT/M$  and the steady-flow viscosity  $\eta$  of equation (16) is the sum of the viscosities of the individual submolecules. Molecular theories are discussed more fully in Section X.

#### IV. SUPERPOSITION PRINCIPLES

There are two superposition principles that are important in the theory of Viscoelasticity. The first of these is the Boltzmann superposition principle, which describes the response of a material to different loading histories (22). The second is the time-temperature superposition principle or WLF (Williams, Landel, and Ferry) equation, which describes the effect of temperature on the time scale of the response.

The Boltzmann superposition principle states that the response of a material to a given load is independent of the response of the material to any load that is already on the material. Another consequence of this principle is that the deformation of a specimen is directly proportional to the applied stress when all deformations are compared at equivalent times

(i.e., this is the region of linear response referred to earlier). The effect of different loads is additive.

For the case of creep, if there are several stresses  $\sigma_0, \sigma_1, \sigma_2, \dots, \sigma_{i-1}$  applied at times  $0, t_1, t_2, \dots, t_i$ , the Boltzmann superposition principle may be expressed by

$$\epsilon(t) = J(t)\sigma_0 + J(t - t_1)(\sigma_1 - \sigma_0) + \dots + J(t - t_i)(\sigma_i - \sigma_{i-1}) \quad (18)$$

The creep  $\epsilon(t)$  at time  $t$  depends on the compliance function  $J(t)$ , which is a characteristic of the polymer at a given temperature, and on the initial stress  $\sigma_0$ . At a later time  $t_1$ , the load is changed to a value of  $\sigma_1$ . At still later times  $t_i$ , the load may be increased or decreased to  $\sigma_i$ , but for each additional stress, a different time scale has to be employed in  $J$  (i.e.,  $t - t_i$ ), the time over which that stress was applied. Furthermore, while  $\epsilon(t)$  for any load is given by the product  $J(t)\sigma$ , the stress of concern is the incremental added stress or  $\sigma_i - \sigma_0$ .

Figure 7 illustrates the Boltzmann superposition principle for a polymer that obeys a common type of behavior given by the Nutting equation

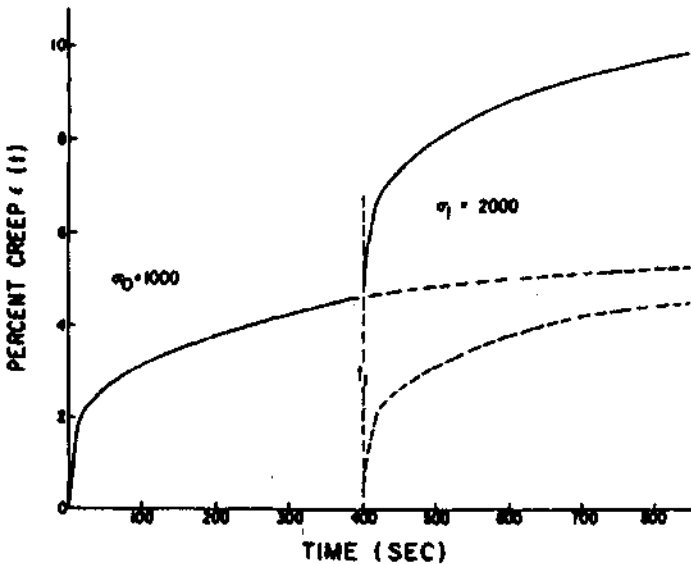


Figure 7 Creep of a material that obeys the Boltzmann superposition principle. The load is doubled after 400 s.

(23,24):

$$\epsilon(t) = K\sigma t^n \tag{19}$$

where  $K$  and  $n$  are constants that depend on the temperature. The special case illustrated in Figure 7 is given by

$$\epsilon(t) = 10^{-5}\sigma t^{0.25} \tag{20}$$

where  $\sigma$  has the units of pounds per square inch and  $t$  is in seconds. Doubling the load after 400 s gives a total creep that is the superposition of the original creep curve shifted by 400 s on top of the extension of the original curve.

A similar superposition holds for stress-relaxation experiments in which the strain is changed during the course of the experiments. The Boltzmann superposition principle for stress relaxation is

$$\sigma(t) = E_r(t)\epsilon_0 + E_r(t - t_1)(\epsilon_1 - \epsilon_0) + \dots \tag{21}$$

The initial strain  $\epsilon_0$  is changed at time  $t_1$  to  $\epsilon_1$ , and the stress is the sum of that induced by the separate strain increments.

Time-temperature superposition has been used for a long time; early work has been reviewed by Leaderman (22). Creep curves made at different temperatures were found to be superposable by horizontal shifts along a logarithmic time scale to give a single creep curve covering a very large range of times. Such curves made by superposition, using some temperature as a reference temperature, cover times outside the range easily accessible by practical experiments. The curve made by superposition is called a master curve. Subsequent advances in the time-temperature superposition principle were made by Ferry, who made the process explicit (25); by Tobolsky (6,26); and by Williams, Landel, and Ferry (1,27), who showed that the reference temperature is not arbitrary but is related to  $T_K$ .

Ferry showed that superposition required that there be no change in the relaxation/retardation mechanism with temperature and that the  $T$  values for all mechanisms must change identically with temperature. Defining the ratio of any relaxation time  $\tau$  at some temperature  $T$  to that at reference temperature  $T_0$  as  $a_T$ ,

$$a_T \equiv \frac{\tau_i}{\tau_{i0}} \tag{22}$$

so the quantity  $t/\tau_i$  in equation (10) becomes

$$\frac{t}{\tau_i} = \frac{t}{\tau_{i0}a_T} = \frac{t/a_T}{\tau_{i0}} = \frac{t_0}{\tau_{i0}} \tag{23}$$

Thus (the time scale  $t$  at  $T$ , divided by  $a_T$ , is equivalent to the scale at  $T_r$ ). On a log scale,  $\log a_T$  is thus the horizontal shift factor required for superposition. An important consequence of equation (22) is that  $a_T$ , or  $\log a_T$  is the same for a given polymer (or solution) no matter what experiment is being employed. That is, creep and stress-relaxation curves are shifted by the same amount.

For uncross-linked polymers, since  $\tau = \eta/G$

$$a_T = \frac{\eta}{\eta_r} \quad (24)$$

and  $a_T$  can be evaluated independently, from the viscosity. A more exact relation is

$$a_T = \frac{\eta}{\eta_r} \frac{T_r \rho_r}{T \rho} \quad (25)$$

where  $\rho$  and  $\rho_r$  are the densities at temperature  $T$  and the reference temperature  $T_r$ , respectively. For plasticized polymers or solutions, the density ratio is replaced by the (volumetric) concentration ratio. At  $T_K$  the viscosity is generally on the order of  $10^8$  P.

The method of relating the horizontal shifts along the log time scale to temperature changes as developed by Williams, Landel, and Ferry from equation (24) is known as the WLF method. The amount of horizontal shift of the log time scale is given by  $\log a_T$ . If the glass transition temperature is chosen as the reference temperature, the temperature dependence of the shift factor for most amorphous polymers is

$$\log a_T = \frac{C_1(T - T_g)}{C_2 + T - T_g} = \frac{-17.4(T - T_g)}{0.025/\Delta\alpha + T - T_g} \quad (26)$$

or, less accurately, using the average value of  $\Delta\alpha$  from many polymers, of  $4.5 \times 10^{-4} \text{ K}^{-1}$

$$\log a_T = \frac{-17.4(T - T_g)}{51.6 + T - T_g} \quad (27)$$

$\Delta\alpha$  is the difference between the liquid and glassy volumetric expansion coefficients and the temperatures are in kelvin. The WLF equation holds between  $T_g - 10$  K and about 100 K above  $T_g$ . Above this temperature, for thermally stable polymers, Berry and Fox (28) have shown that a useful extension of the WLF equation is the addition of an Arrhenius term with a low activation energy.

An important aspect of the WLF development is that if a temperature other than  $T_K$  is chosen as the reference temperature, an equation with the

same form as equation (26) is obtained, but with different numerical coefficients. These change in a defined manner, however:

$$C_1^0 = \frac{C_1^K C_2^K}{C_1^K + T_0 - T_K}$$

$$C_2^0 = C_2^K + T_0 - T_K \tag{28}$$

The temperature-time superposition principle is illustrated in Figure 8 by a hypothetical polymer with a  $T_K$  value of  $0^\circ\text{C}$  for the case of stress relaxation. First, experimental stress relaxation curves are obtained at a series of temperatures over as great a time period as is convenient, say from 1 min to  $10^6$  min (1 week) in (he example in Figure 8. In making the master curve from the experimental data, the stress relaxation modulus  $E_r(t)$  must first be multiplied by a small temperature correction factor  $f(T)$ . Above  $T_g$  this correction factor is  $T_{ref}/T$ , where  $T_{ref}$  is the chosen reference

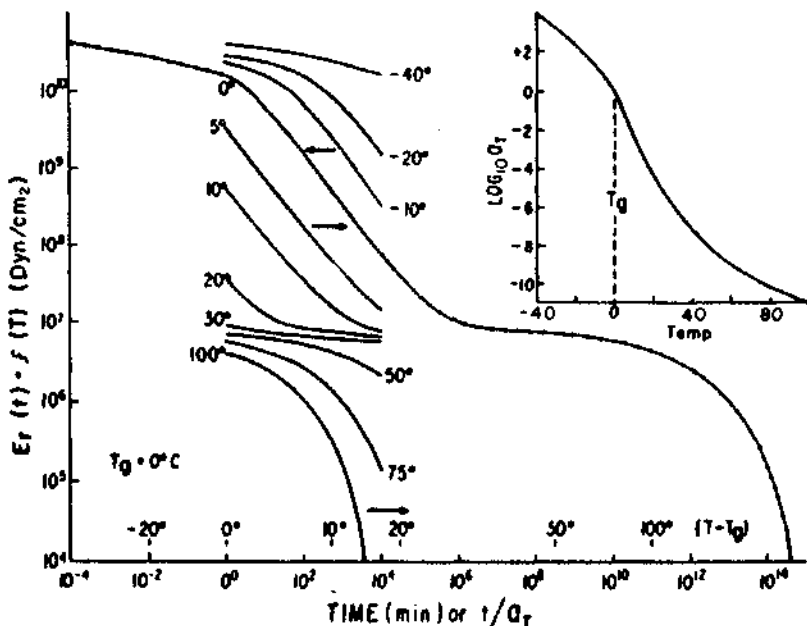


Figure 8 WLF time-temperature superposition applied to stress-relaxation data obtained at several temperatures to obtain a master curve. The master curve, made by shifting the data along the horizontal axis by amounts shown in the insert for  $a_T$ , is shown with circles on a line.

temperature: temperatures are in kelvin. This correction arises from the kinetic theory of rubber elasticity, which we discuss later. Below  $T_g$  the WLF theory is not applicable, so a different temperature correction should be used since the modulus decreases with temperature below  $T_g$  but increases with temperatures above  $T_g$ . Below  $T_g$ , it is often assumed that  $f(T) = 1$ , but McCruin et al. (29,30) and Rusch (31) have suggested a more realistic, but still small correction. Next, the corrected moduli curves are plotted as the solid curves in Figure 8. The curve at some temperature is chosen as the reference —  $T_g$  in the example.<sup>1</sup> The curves are then shifted one by one along the log time scale until they superpose. Curves at temperatures above  $T_g$  are shifted to the right, and those below  $T_g$  are shifted to the left. The shift is  $\log(1/a_T)$ . Usually, the curves do not cover a large enough  $\log E(t)$  range to permit superposition on the reference curve. In this case they are shifted to superpose with their nearest neighbor. The magnitude of such a shift is called  $\Delta \log(1/a_T)$ ; then  $\log a_T = \sum_i^n \Delta \log(1/a_T)$ . The complete master curve is shown by the line with circles in Figure 8; it covers 18 decades of time, whereas the original data covered only (our decades. For most amorphous polymers above  $T_g$  the shift factor is given quite accurately by the WLF function shown in the insert and in Table 2. Thus the stress relaxation curve at 5°C should be shifted 1.427 decades in time to the right (longer times) to superpose properly with the curve at 0°C. The master curve in this example has a prominent plateau near  $10^7$  dyn/cm<sup>2</sup>; this long plateau is characteristic of very high-molecular-weight

Table 2 WLF Shift Factors

| $T - T_g$ | Shift factor, $\log_{10} a_T$ |
|-----------|-------------------------------|
| 0         | 0                             |
| 2         | -0.6003                       |
| 5         | -1.4272                       |
| 10        | -2.6385                       |
| 20        | -4.5836                       |
| 30        | -6.0767                       |
| 50        | -8.2186                       |
| 80        | -10.251                       |
| 100       | -11.173                       |

<sup>1</sup>In practice, it is best to choose a reference temperature at the midpoint of the data and superpose the data to this temperature. A particularly apt reference temperature is  $T_g + 50^\circ$ , which has been referred to as a standard reference temperature,  $T_r$  (27). Conversion from any reference temperature to  $T_r$  can then be made via equations such as equation (28).

polymers and is due to chain entanglements, which act as temporary cross-links (see Figure 2.5). Since time and temperature are equivalent according to the superposition principle, the reduced time scale at a fixed temperature,  $t/a_T$ , can be replaced by a temperature scale at a fixed time. The equivalent temperature scale is shown above the reduced time scale on the abscissa of Figure 8 for a reference time of 1 min. Any different reference time has a different equivalent temperature scale.

Master curves are important since they give directly the response to be expected at other times at that temperature. In addition, such curves are required to calculate the distribution of relaxation times as discussed earlier. Master curves can be made from stress relaxation data, dynamic mechanical data, or creep data (and, though less straightforwardly, from constant-strain-rate data and from dielectric response data). Figure 9 shows master curves for the compliance of poly(*n*.v-isoprene) of different molecular weights. The master curves were constructed from creep curves such as those shown in Figure 10 (32). The reference temperature  $T_r$  for the

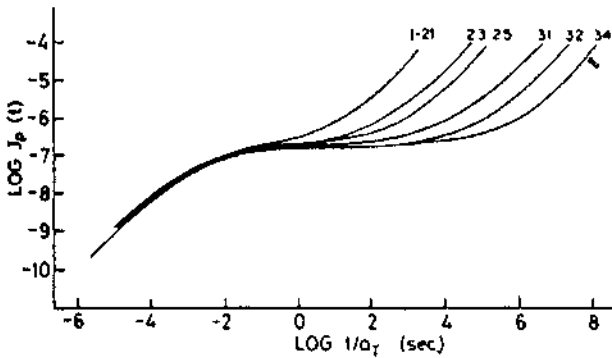


Figure 9 Master curves for creep compliance of polyisoprene of various molecular weights at a reference temperature of  $-3(0)^{\circ}\text{C}$ :

| Curve | Weight-average molecular weight |
|-------|---------------------------------|
| 1-21  | $5.76 \times 10^4$              |
| 1-23  | $1.03 \times 10^5$              |
| 1-25  | $1.59 \times 10^5$              |
| 1-31  | $3.95 \times 10^5$              |
| 1-32  | $6.20 \times 10^5$              |
| 1-34  | $1.12 \times 10^6$              |

(From Ref. 32.)

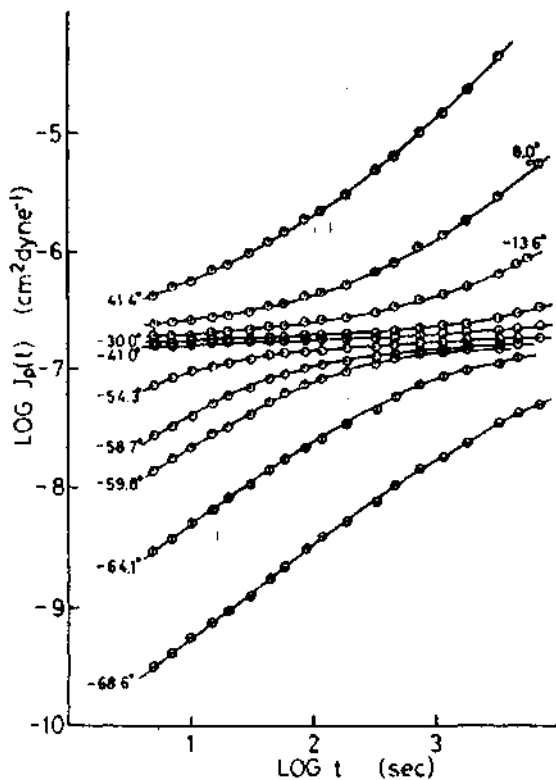


Figure 10 Creep compliance of polyisoprene at various temperatures. Data are for a fraction with a molecular weight of  $1.12 \times 10^6$ . (Prom Ref. 32.)

master curves was  $-30^\circ\text{C}$ , which is about  $43^\circ\text{C}$  above  $T_g$ . The shift factors  $a_T$  follow the WLF theory, but since the reference temperature was not  $T_g$ , equation (27) does not hold. The WLF equation for this case is

$$\log a_T = \frac{-8.20(T - T_0)}{89.5 + T - T_0} \quad (29)$$

Master curves can often be made for crystalline as well as for amorphous polymers (33-38). The horizontal shift factor, however, will generally not correspond to a WLF shift factor. In addition, a vertical shift factor is generally required which, has a strong dependence on temperature (36-38). At least part of the vertical shift factor results from the change in



modulus due to the change in degree of Crystallinity with temperature. Aging and heat treatments may also affect the shift factors. For these reasons, the vertical shift factors are largely empirical, with very little theoretical validity, and whenever they are required the resulting master curves cannot be used for reliable extrapolation to estimate the response very far from the experimental observation "window." A few references to papers discussing master curves for the creep and stress relaxation behavior of a number of polymers are given in Table 3 (39--53).

**Table 3** Master Curves for Various Polymers

| Refs.  | Test                              | Polymers  |
|--------|-----------------------------------|---|
| 39     | Creep and stress relaxation       | Polystyrene, poly(methyl methacrylate), poly(methyl acrylate)                         |
| 40     | Creep                             | Polystyrene   |
| 32     | Creep                             | Poly( <i>cis</i> -isoprene)   |
| 41     | Stress relaxation                 | Styrene-butadiene rubber  |
| 42     | Creep, stress relaxation, dynamic | Nylon 66  |
| 43     | Creep                             | Nylon 66  |
| 44     | Relaxation                        | Poly(methyl methacrylate)   |
| 45     | Relaxation                        | Poly(methyl methacrylate) and poly(methyl acrylate)                                   |
| 46     | Relaxation                        | Styrene-butadiene rubber  |
| 47     | Relaxation                        | Polyisobutylene, poly(methyl methacrylate)  |
| 26     | Relaxation                        | Polyisobutylene   |
| 48     | Creep and relaxation              | ABS, styrene-acrylonitrile copolymer, poly(vinyl chloride), poly(methyl methacrylate) |
| 49     | Creep                             | Rubber  |
| 50     | Creep                             | Polycarbonate   |
| 38, 51 | Relaxation                        | High-density polyethylene   |
| 22     | Creep                             | Many materials  |
| 8      | Creep                             | Cellulose nitrate   |
| 34     | Stress relaxation                 | Poly(vinyl alcohol) copolymers  |
| 37     | Stress relaxation                 | High-density polyethylene   |
| 36     | Stress relaxation                 | Crystalline polymers  |
| 35     | Stress relaxation                 | Low-density polyethylene  |
| 33     | Stress relaxation                 | Polypropylene, high- and low-density polyethylene                                     |
| 52     | Stress relaxation                 | Polycarbonate   |
| 53     | Stress relaxation                 | Polypropylene/vinyl chloride graft polymers   |

The WLF equation can be used to convert data from a master curve created at one temperature to that at another temperature or to find the temperature dependence of the response at a selected time scale. In the latter case, while it is easy to calculate  $\log a_T$  from the known values of  $C_1'$  and  $C_2'$ , obtain the shifted time, and read the modulus at the shifted time, Jones (54) has developed a nomographic technique that can be used to make quick estimates. The technique was developed for dynamic properties and so is discussed in Chapter 5. Nevertheless, the principle should be applicable to transient data as well.

## V. NONLINEAR RESPONSE

If the Boltzmann superposition principle holds, the creep strain is directly proportional to the stress at any given time. Similarly, the stress at any given time is directly proportional to the strain in stress relaxation. That is, the creep compliance and the stress relaxation modulus are independent of the stress and strain, respectively. This is generally true for small stresses or strains, but the principle is not exact. If large loads are applied in creep experiments or large strains in stress relaxation, as can occur in practical structural applications, nonlinear effects come into play. One result is that the response  $\epsilon(t)$  or  $\sigma(t)$ , respectively, is no longer directly proportional to the excitation ( $\sigma$  or  $\epsilon$ ). The distribution of retardation or relaxation times can also change, and so can  $a_r$ .

The problem is very complex even in cases where complications such as microcracking or phase changes (e.g., appearance of Crystallinity, as in stretching natural rubber, or change in percent Crystallinity in polyethylene) are absent. It involves unsolved problems in nonequilibrium thermodynamics, mathematical approximations (although these are rapidly being eliminated by the use of numerical methods) and the physics of any underlying processes. As a result, there is no general solution. However, in the case of amorphous elastomers, very great progress has been made in the phenomenological or descriptive approach.

### A. Strain Dependence of Stress Relaxation

For elastomers, Tobolsky (6), Thirion and Chasset (5), and Guth et al. (56) have all reported qualitative conclusions that the rate of stress relaxation is independent of the strain level for natural rubber and styrene-butadiene rubber (SBR) for strains up to 80 to 100%. Martin et al. (57)

---

\*For a single stress application; if loads had been applied at different times, the proportionality would hold only after the initial transient response had died out.

and Halpin (58) have similarly reported that the creep rate is independent of the stress level for four different types of elastomers for strains up to about 2(X)%. Landel and Stedry (59) appear to have been the first to publish explicit stress-relaxation data showing the independence of strain and time, for SBR (up to very large strains) and a polyurethane rubber, Ilavsky and Prins (60) and co-workers have presented similar explicit results for a series of polyurethane rubbers. Thus the response can be separated or factored into functions of time and of stress. Factorizability, when it holds, offers a powerful simplification to any attempt to develop theories or descriptions of polymer response, whether phenomenologically or molecularly based, as well as an often stringent test of their validity. The factorizability is easily tested since plots of  $\log \sigma(t)$  or  $\log \epsilon(t)$  versus  $\log t$  will all be linear, with the same slope. In the more general case, the curves will not be linear but they will still be parallel. A cross plot of the strains at any given time against the stress will give the resulting isochronal (constant time)  $\epsilon - \sigma$  relationship.

Using this factorizability of response into a time-dependent and a strain-dependent function. Landel et al. (61,62) have proposed a theory that would express tensile stress relaxation in the nonlinear regime as the product of a time-dependent modulus and a function of the strain:

$$\lambda \sigma(t, \lambda) = E(t) F[u'(\lambda)] = G(t) F[u'(\lambda)] \tag{30}$$

Here  $E(t)$  is the usual small-strain tensile stress-relaxation modulus as described and observed in linear viscoelastic response [i.e., the same  $E(t)$  as that discussed up to this point in the chapter]. The nonlinearity function  $F[u'(\lambda)]$  describes the shape of the isochronal stress-strain curve. It is a simple function of  $\lambda$ , which, however, depends on the type of deformation. Thus for uniaxial extension,

$$F = \lambda u'(\lambda) - \lambda^{-1/2} u'(\lambda^{-1/2}) \tag{31}$$

The underlying nonlinearity function  $u'(\lambda)$ , which is independent of the type of deformation, is very similar for different amorphous rubbers. For SBR, it is independent of the cross-link density over moderate changes in cross-link density (62) and independent of the temperature down to  $-40^\circ\text{C}$ , a temperature where the modulus has increased by a factor of 2 to 3 over the room-temperature value (61). The function  $u'(\lambda)$  is insensitive to the presence of moderate amounts of carbon black filler for strains up to about 100% (63).

Moreover, in developing and testing the theory, biaxial stress-relaxation experiments were carried out. That is, square sheets were stretched in both directions but in unequal amounts. In all cases, the stress in the major stretch direction relaxed at the same relative rate as that in the minor

stretch direction—plots of log stress versus log time were parallel. (The maximum strains attained in these experiments approached 2(K)%.) The observation of simple factorizability even under biaxial conditions (61-65) should provide a powerful simplification for future theoretical developments. Factorizability holds through the rubbery plateau but breaks down, for the particular SBR rubber used (61), at the beginning of the rubber-to-glass transition /one—in the case studied, for time scales less than 1 min at  $-40^{\circ}\text{C}$  and for time scales less than a few hundred minutes at  $-45^{\circ}\text{C}$  (61,66). Further discussions of  $u'(\lambda)$  are postponed to Chapter 5, since  $u'(\lambda)$  describes the shape of the stress-strain curve and we are dealing here with creep and stress relaxation.

Factorizability has also been found to apply to polymer solutions and melts in that both constant rate of shear and dynamic shear results can be analyzed in terms of the linear viscoelastic response and a strain function. The latter has been called a damping function (67,68).

For glassy and crystalline polymers there are few data on the variation of stress relaxation with amplitude of deformation. However, the data do verify what one would expect on the basis of the response of elastomers. Although the stress-relaxation modulus at a given time may be independent of strain at small strains, at higher initial fixed strains the stress or the stress-relaxation modulus decreases faster than expected, and the Boltzmann superposition principle no longer holds.

Tassaglia and Koppehele (69) found for cellulose monofilaments that stress relaxation depended on the initial strain—the modulus decreased as strain increased. The shape of the stress-relaxation curves changes dramatically with the imposed elongation for nylon and polyethylene terephthalate (70). Similar results were found with polyethylenes (64,71,72). Polymers such as ABS materials and polycarbonates that can undergo cold drawing show especially rapid stress relaxation at elongations near the yield point. As long as the initial elongations are low enough for the stress-strain curve to be linear, the stress relaxes slowly. However, in the region of the stress-strain curve where the curve becomes nonlinear, the stress dies down much more rapidly.

## B. Stress Dependence of Creep

For elastomers, factorizability holds out to large strains (57,58). For glassy and crystalline polymers the data confirm what would be expected from stress relaxation—beyond the linear range the creep depends on the stress level. In some cases, factorizability holds over only limited ranges of stress or time scale. One way of describing this nonlinear behavior in uniaxial tensile creep, especially for high modulus/low creep polymers, is by a power

law such as the Nutting equation (23,24),

$$\epsilon = K\sigma^\beta t^n \tag{32}$$

where  $K$ ,  $\beta$ , and  $n$  are constants at a given temperature. The constant  $\beta$  is equal to or greater than 1.0. This equation represents many experimental data reasonably accurately, but it has received little theoretical justification (52-53). Note that in the linear region,  $\beta = 1$ , equation (32) implies that  $\log D(t)$  is linear in  $\log$  time. This means that it cannot hold over the whole transition region since, experimentally,  $n$  changes with time. Hence equation (32) should be used with caution if data must be extrapolated to long times.

The hyperbolic sine function also fits many experimental simple tension data, and it has considerable theoretical foundation (77-88):

$$\epsilon = K(t) \sinh \frac{\sigma}{\sigma_c} \tag{33}$$

$K(t)$  is the function defining the time dependence of the creep. The constant  $\sigma_c$  is a critical stress characteristic of the material, and at stresses greater than  $\sigma_c$  the creep compliance increases rapidly with stress.

At small strains (i.e., in the linear region),  $K(t)/\sigma_c = D(t)$ . Figure 11 illustrates the creep dependence of a polyethylene with a density of 0.950 at 22°C (89). In this case the critical stress  $\sigma_c$ , was about 620 psi, and the

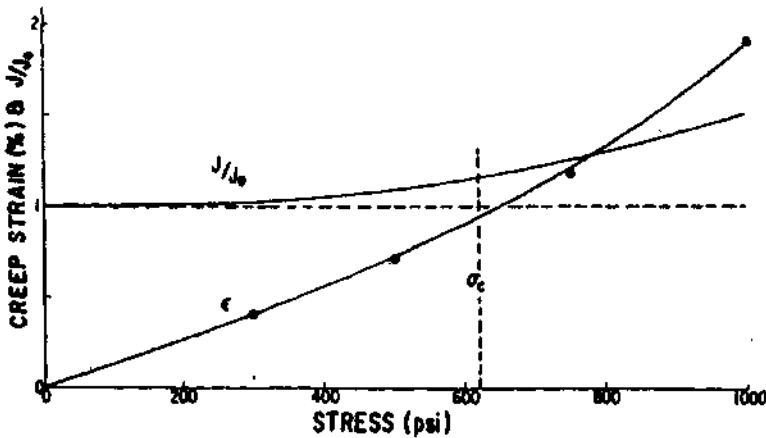


Figure 11 Shear creep  $\epsilon$  of polyethylene (density = 0.950) at different loads after 10 min, and  $J/J_0$  as a function of applied stress. Deviation from the value of 1.0 indicates a dependence of creep compliance on load.

creep was measured after 10 min. For this polyethylene the experimental data after 10 min are accurately given by

$$\epsilon(10) = 0.792 \sinh \frac{\sigma}{620} \quad (34)$$

where the strain is given in percent and the stress in psi. Similar equations hold for other times and temperatures. Plotted in the same figure is the quantity

$$\frac{J}{J_0} = \frac{\sinh(\sigma/\sigma_c)}{\sigma/\sigma_c} \quad (35)$$

where  $J_0$  is the creep compliance at very low loads. This ratio is 1.0 if the Holt/mann superposition holds. In the case of polyethylene, deviations become apparent at about 200 psi, and at a stress of 1000 psi, the compliance ratio  $J/J_0$  has increased by 50%. In practical situations where a plastic object must be subjected to loads for long periods of time without excessive deformation, the stress should be less than the critical stress  $\sigma_c$ .

Little is known about the variation of the critical stress  $\sigma_c$  with structure and temperature. For the polyethylene discussed above,  $\sigma_c$  decreased from 620 psi at 22°C to 390 psi at 60°C; this appears to be a general trend with all polymers. Turner (84) found that the value of  $\sigma_c$  for polyethylenes increased by a factor of about 5 in going from a polymer with a density of 0.920 to a highly crystalline one with a density of 0.980. Reid (80,81) has suggested that for rigid amorphous polymers,  $\sigma_c$  should be proportional to  $(T_g - T)$ . For brittle polymers, the value of  $\sigma_c$  may be related to the onset of crazing.

Equations (32) and (33) imply that factorizability holds and that an applied stress does not shift the distribution of retardation times. The shape of the creep curves when plotted as  $\log \epsilon$  vs.  $\log t$  is not changed by the stress and the curves could be superposed by a vertical shift. When plotted as  $\epsilon$  vs.  $t$  or  $\log t$ , however, the shapes are changed. However, the curves can now be superimposed by multiplying the compliance by a constant for each stress to bring about a normalization in the vertical direction. On the other hand, in some cases (often rigid polymers at high loads) stresses do change the distribution of retardation times to shorter times (43,90-93). Then a horizontal shift is required on log time plots to superimpose creep curves obtained at different stresses even if the temperature is held constant and factorizability no longer holds.

Many other data in the literature show a strong dependence of creep compliance on the applied load, although in some cases the authors did not discuss this aspect of creep. Stress dependence is found with all kinds of plastics. For example, the creep of polyethylene has been studied by

several authors (74,75,83,84,89,94-96), as has rigid poly(vinyl chloride) (80,81,83,91,93,97,98). Leaderman (99) studied plasticized poly(vinyl chloride). Polystyrene has been investigated by Sauer and others (73,100), and ABS polymers have been studied also (87,93,101). Polypropylene has also been a popular polymer (92,102,103). Sharma studied a chlorinated polyether (Penton) (104) and cellulose acetate butyrate (76). Nylon was studied by Catsiff et al. (43), nitrocellulose by Van Holde (79), and an epoxy resin by Ishai (K6). The relaxation times of an ABS polymer can be shortened by as much as four decades by high loads (105). Dilation created by the creep load is responsible for at least part of this speeded-up stress relaxation.

## VI. EFFECT OF PRESSURE

Few data are available on creep and stress relaxation at pressures other than at 1 atm. However, the data are essentially what would be expected if pressure decreases free volume and molecular or segmental mobility. For elastomers, which are nearly incompressible, very high pressures are required to change the response. Nevertheless, there is a pressure analog of the WLF equation that accounts for these changes (106). DeVries and Backman (107) found that a pressure of 50,000 psi decreases the creep compliance of polyethylene by a factor of over 10. Pressure increased the stress-relaxation modulus a comparable amount. At the higher pressures (30,000 psi), the stress continued to relax for a much longer time than it did at 1 atm; pressure seems to shift some of the relaxation times to longer times, just as in elastomers.

## VII. THERMAL TREATMENTS

Annealing of polymers increases the modulus and decreases the rate of creep or stress relaxation at temperatures below the melting point or glass transition temperature. This decrease in creep or stress relaxation of a polymer after standing for some time after the preparation of a specimen often is called "physical aging" (108). As shown in Figure 12, physical aging affects both the magnitude and rate of creep or relaxation. The general response at a fixed aging temperature is that of a change in magnitude of a property, coupled with a very large shift along the time scale. As a result, the less-aged responses can be superposed (in the log-log plots) on the well-aged response.

Below  $T_g$ , stress relaxes out faster in quenched specimens than in slowly cooled ones for amorphous polymers such as poly(methyl methacrylate) (109). Quenched specimens of the same polymer have a creep rate at high

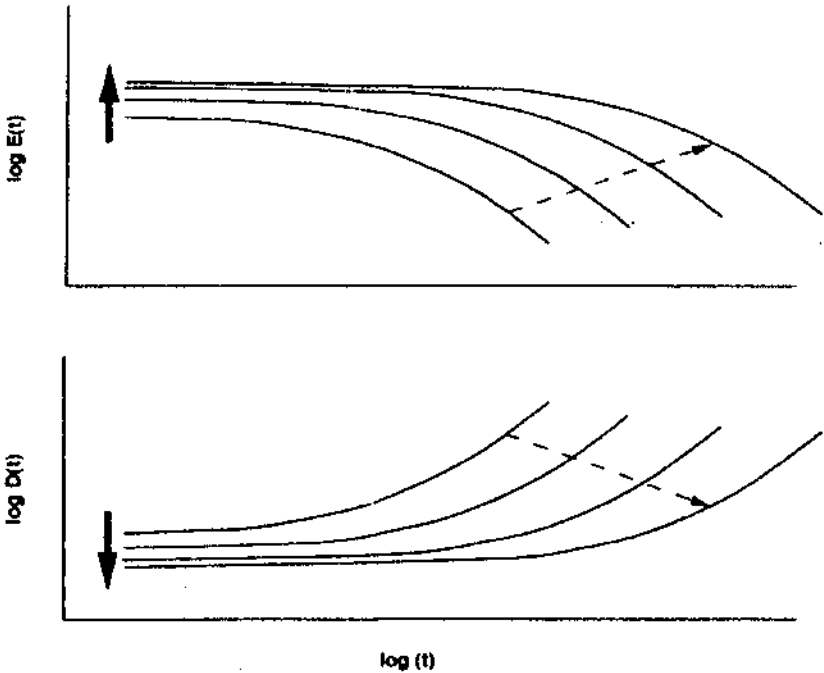


Figure 12 Effect of increasing aging or annealing time,  $t_a$ , on creep and stress relaxation. The heavy arrow indicates increasing aging time; the dashed one, the direction and amount of shifting required for superposition.

loads that is as high as 50 times the rate for specimens annealed at  $95^\circ\text{C}$  for 24 h (110). The creep rate is strongly dependent on the annealing temperature and the annealing time (108,111-115). At temperatures just below  $T_g$  most of the effects due to annealing can be achieved in a short time. However, greater effects are possible by annealing at lower temperatures, but the annealing times become very long. Annealing affects the creep behavior at long times much more than it does the short-time behavior (97). For example, unplasticized poly(vinyl chloride) annealed at  $60^\circ\text{C}$  had nearly the same creep up  $U > 1000$  s for specimens annealed for 1 h and for 2016 h. However, beyond 10,000 s, the specimen annealed for 1 h had much greater creep than the specimen that had been annealed for 2016 h (97). Findley (98) reports similar results. Principal parameters in the physical aging process are the total volume (or density) and its rate of change with time. (Here one has a volumetric creep strain instead of the usually measured tensile or shear creep strain.)



Quenched amorphous polymers typically have densities from  $10^{-4}$  to  $10^{-2}$   $\text{g/cm}^3$  less than those for annealed polymers. Thus it appears that the free volume is an important factor in determining creep and stress relaxation in the glassy state, especially at long times. However, the relationship between the free and total volume is not clear, even at small deformations. In one treatment of this relation (116) it was possible to relate the aging time to the shift along the time scale of stress relaxation in poly(methyl methacrylate) from the concurrently measured volume change (117). Tensile strains and large shear strains induce a dilation since Poisson's ratio is not 1. If the fractional free volume change, a percentage of the total volume change, is the same in creep and structural relaxation, physical aging should be reversed at large strains according to a free-volume explanation (108). Initial work in creep and stress relaxation confirmed this reversal, but work in more complex test modes disputes the reversal or the conclusion that free volume controls changes in rate of creep or relaxation (118-121).

Crazing in glassy polymers greatly increases the creep and stress relaxation (122--125). The creep is small up to an elongation great enough to produce crazing; then the creep rate accelerates rapidly. Anything that enhances crazing will increase the creep. These factors include adding low-molecular-weight polymer, mineral oil, or rubber to produce a polyblend. Even the atmosphere surrounding a specimen can change creep behavior by changing the crazing behavior (126). Immersion in some liquids can greatly enhance creep and crazing (127). The atmosphere can change the creep of rubbers even though no crazing occurs (128). The creep of natural rubber is much greater in air than in a vacuum or in nitrogen.

Annealing can reduce the creep of crystalline polymers in the same manner as for glassy polymers (89,94,102). For example, the properties of a quenched specimen of low-density polyethylene will still be changing a month after it is made. The creep decreases with time, while the density and modulus increase with time of aging at room temperature. However, for crystalline polymers such as polyethylene and polypropylene, both the annealing temperature and the test temperatures are generally between the melting point and  $T_g$ . Thus for crystalline polymers the cause of the decreased creep must be associated with the degree of Crystallinity, secondary crystallization, and changes in the crystallite morphology and perfection brought about by the heat treatment rather than with changes in free volume or density.

### VIII. EFFECT OF MOLECULAR WEIGHT: MOLECULAR THEORY

At temperatures well below  $T_g$  where polymers are brittle, their molecular weight has a minor effect on creep and stress relaxation. This independence

of properties from molecular weight results from the very short segments of the molecules involved in molecular motion in the glassy state. Motion of large segments of the polymer chains is frozen-in, and the restricted motion of small segments can take place without affecting the remainder of the molecule. If the molecular weight is below some critical value (129) or if the polymer contains a large fraction of very low-molecular-weight material mixed in with high-molecular-weight material, the polymer will be extremely brittle and will have a lower-than-normal strength. Even these weak materials will have essentially the same creep behavior as the normal polymer as long as the loads or elongations are low. At higher loads or elongations the weak low-molecular-weight materials may break at considerably lower elongations than the high-molecular-weight polymers.

Crazing occurs more easily in low-molecular-weight polymers, which can increase the creep or stress-relaxation rate before failure takes place. The dependence of crazing on molecular weight of polystyrene in the presence of certain liquids is well illustrated by the data of Rudd (130). As a result of crazing by butanol, he found that the rate of stress relaxation is much faster for low-molecular-weight polystyrene than for high-molecular-weight material. This is to be expected since there are fewer than the normal number of chains carrying the load in crazed material. In addition, craze cracks act as stress concentrators which increase the load on some chains even more. These overstressed chains tend to either break or slip so as to relieve the stress on them. Thus, in the glassy state, crazing is a major factor in stress relaxation and in creep (131,132). Crazing may also be at least part of the reason why creep in tension is generally greater than creep in compression, since little, if any, crazing occurs in compression tests (133).

In the glass transition region the creep and stress relaxation is independent of molecular weight for  $M > M_r$  and only weakly dependent on  $M$  for  $M < M_r$  when measured at a fixed value of  $T - T_r$ . It is only in the elastomeric region above  $T_r$  that the behavior becomes strongly dependent on molecular weight. The important reason for this dependence on molecular weight for uncross-linked, amorphous materials is that the mechanical response of such materials is determined by their viscosity and elasticity resulting from chain entanglements. When viscosity is the factor determining creep behavior, the elongation versus time curve becomes a straight line; that is, the creep rate becomes constant. The melt viscosity of polymers is extremely dependent on molecular weight as shown by Figure 13 (134). When the polymer chains are so short that they do not become entangled with one another, the viscosity is approximately proportional to the molecular weight. When the chains are so long that they become strongly entangled, it becomes difficult to move one chain past another. Thus the viscosity becomes very high, and it becomes proportional to the 3.4 or 3.5 power of the molecular weight (135-138). The break in

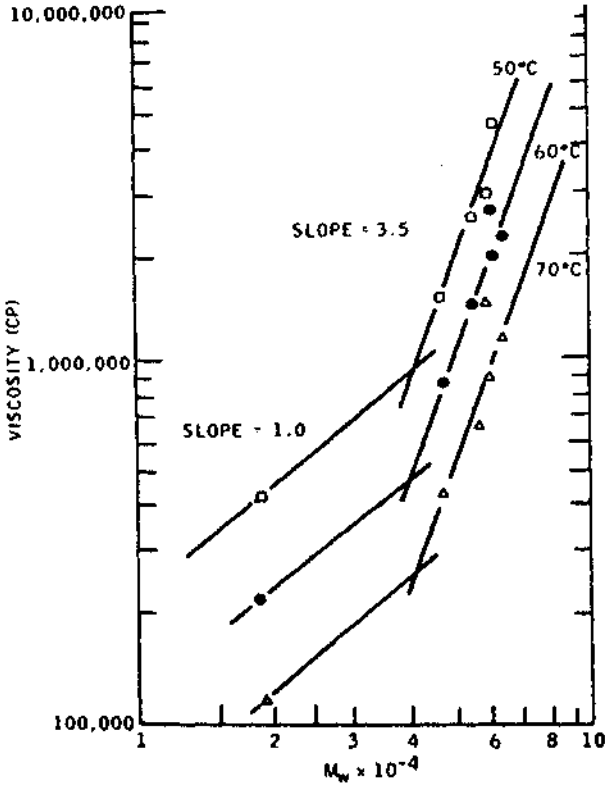


Figure 13 Melt viscosity as a function of molecular weight for butyl rubber. (From Ref. 134.)

the curve of Figure 13 gives the approximate molecular weight  $M_e$  at which entanglements can occur. The entanglements not only increase the viscosity but also act as temporary cross-links and give rise to rubberlike elasticity (28,139-141). [The value of  $M_e$  obtained from viscosity measurements is approximately twice the value calculated from the modulus equation of the kinetic theory of rubber elasticity, which will be discussed later (1,6,16). This result is what would be expected if half of a polymer chain containing only one entanglement dangles on each side of the point where the chain gets entangled with another chain.]

In general, the two sections of the curve in Figure 13 can be represented by an equation of the form (134-138,28)

$$\log \eta = \log K_1 + K_2 \log M \tag{36}$$

The constant  $K_1$  depends on the structure of the polymer and on the temperature. The constant  $K_2$  has different values below and above  $M_c$ .  $\eta_{sp}/c$  is also sensitive to temperature below  $M_c$ . For  $M \approx M_c$ , the chains are so short that the change in  $M$  strongly affects  $T_g$ . Since properties are best compared at corresponding states, they should be compared at the same  $T/T_g$ . When this is done,  $K_2$  is temperature independent and  $K_2 = 1$  (142). For  $M \gg M_c$ ,  $K_2$  is always temperature independent and  $K_2 = 3.4$  to 3.5. For sharp fractions, the value of all the molecular weight averages are nearly the same, for unfractionated polymers and polymer blends,  $M$  should be the weight-average molecular weight, or better yet, the viscosity-average molecular weight.

The molecular origins of these polymer responses and their change with the time scale or frequency of observation is now fairly well understood. Using the stress relaxation modulus as a reference, in the glassy state and the initial glass-to-rubber transition region, the response is due to the motion of very short-chain segments—one or two monomer units long. These are librational or rotational modes of motion. The elastic restoring force comes from the potential barrier to this libration or rotation. In the glassy state, the local structure is an unstable one, becoming more dense with aging time, so interaction increases and the rate of motion is reduced with aging. In the upper end of the transition zone, the structure has been modeled as a damped Debye oscillator (143) and as a less specific interaction between segment and surroundings characterized by a coupling constant  $i$  (144).

In the first model, the relaxation time is still given by the Rouse form

$$\tau_i = \tau_p = \frac{\tau_1}{p^2} \quad (37)$$

but now  $E_i$  is not a constant, so

$$E(t) = \sum_p E_p e^{-(t/\tau_p)^2} \quad (38)$$

and the modulus falls off as  $t^{-2/3}$ . In the second model,

$$\tau_p = [(1 - n)\omega_c^2 \tau_0]^{1/(1-n)} \quad (39)$$

where  $\omega_c$  is an atomic vibration frequency,  $\tau_0$  a primitive relaxation time for a motion uncoupled from its surroundings, and  $n$  a measure of the strength of coupling. This leads to a "stretched-exponential" representation of  $E(t)$  [i.e., a single exponential term but with the exponent raised to a power  $\beta$ , =  $(1 - n)$ ]:

$$E(t) = E_g \int e^{-t/\tau_p^\beta} d\tau \quad (40)$$

This form is also known as the Williams-Watts function† (145). It is a powerful yet simple form to use in fitting data, since it can accommodate any slope in the transition region. However, equation (40) cannot describe a complete master curve from glassy to rubbery state with a single value of  $\beta$ . Instead,  $\beta$  (or  $n$ ) is taken to be time (or temperature) dependent.

As the time scale of observation increases, the response of increasingly large segments is being observed. As  $E(t)$  drops below  $10^7$  to  $10^8$  Pa, two new mechanisms of behavior control the response. The local structure no longer impedes the chain segmental motion and the entropy takes over as the restoring force. That is, the chain segments have a rubberlike elasticity, with each segment of molecular weight  $M_{seg}$  having a modulus of  $kT/M_{seg}$ . When chains are disturbed from their equilibrium position as a step strain is imposed, all segments initially respond with this elastic restoring force but then begin immediately to diffuse under Brownian motion toward a new equilibrium position. This motion is impeded by the local viscosity of the surrounding chains. A description, or model, of this response was first developed by Rouse (13) and Zimm (14) for dilute solutions, but the Rouse treatment is applicable to undiluted polymer as well (17,18,21). As noted earlier, a discrete spectrum of relaxation times emerges [see equations (16) and (17)]. For molecular weight below the "entanglement" molecular weight, these equations describe the complete course of the relaxation process and the flow behavior.

If the molecular weight is above a critical value, the chain segments impede each other's motion. This entanglement effect has long been known (146) and was formerly attributed to the looping of chains around each other. The current picture is that adjoining chains and chain segments impede the lateral diffusion while diffusion along a chain's contour length is largely unmodified. The local constraints inhibiting lateral motion can be thought of as defining a tubular shell through which the chain can diffuse. Consequently, relaxational processes now involve primarily a slithering through the surrounding medium, the tube, in a snakelike motion called reptation (147). The diameter of the tube is now defined by a critical molecular length above which reptation starts. This is the same critical molecular weight as for entanglement, so the symbol  $M_e$  is retained, but "entanglement" is now given a very clear physical origin. In the Doi-Edwards (17-19) detailed description of the molecular motions involved, the Rouse-like motion passes over to the reptation-controlled motion at a time

$$\tau_p = \tau_A = \frac{N_e^2 \tau_0}{2\pi^2}$$

†This implies that  $H = E_e \tau_e^{-1} \omega^{-n}$ .

where  $N_e$  is the number of segments of size  $M_e$ . Beyond this point,  $\tau_p$  (Rouse) changes to  $\tau_p$  (reptation).

$$\tau_{1c1} = 6 \left( \frac{N}{N_e} \right)^3 \tau_1 = \frac{3N^3 \tau_0}{\pi^2 N_e} \quad (41)$$

and at the same time the modulus becomes essentially constant:

$$E(t) = \nu_{\text{int}} RT = \frac{\rho RT}{M_e} \equiv E_N \quad (42)$$

This is the entanglement plateau and the modulus is given by the concentration of Rouse submolecule chains per cubic centimeter,  $\nu_{\text{int}}$ , or the molecular weight between entanglements  $M_e$ . (This plateau region can have a slight slope, which arises because the lateral constraints to motion are themselves moving and this constraint release mechanism makes  $\nu_{\text{int}}$  a slowly decreasing function of the time scale of observation.) The plateau persists until a second critical time scale.

$$\tau_B = 2 \left( \frac{N}{N_e} \right)^2 \tau_A = \frac{N_e \tau_1}{2} \quad (43)$$

At this point both the spectrum of relaxation times and the way they contribute to the modulus change, so that

$$E(t) = \frac{8E_N}{\pi^2} \sum_{p=1}^{N_e-1} e^{-2t/\tau_p} \sum_{p,\text{odd}} \frac{1}{p^2} e^{-p^2 t/\tau_{rep}} \quad (44)$$

and

$$\tau_{rep} = 6 \left( \frac{N}{N_e} \right)^3 \tau_A = \frac{6M_e^2}{2\pi^2} \left( \frac{N}{N_e} \right)^3 \tau_0 \quad (45)$$

Beyond  $\tau_B$ , whole molecules are moving and contributing to viscous flow [i.e., equation (44) describes the long-time tail of the stress relaxation curve or the onset of the flow regime].

The Doi-Edwards reptation model thus predicts that the width of the modulus plateau varies as the square of the molecular weight, or, in comparing different polymers that have different  $M_e$  values, as  $(M/M_e)^2$ . Another way of stating this is to say that the monomeric friction factor has been increased by the factor  $(M/M_e)^2$ . Furthermore, since in general  $\eta = \tau G$ , this model predicts that at constant temperature the viscosity will be proportional to molecular weight below  $M_e$  (Rouse-like response) and proportional to  $M^3$  above it (reptation response). Experimentally, in the  $M \leq M_e$  regime, chain ends markedly reduce  $T_g$ , so the comparison must be made at equivalent states (i.e., at constant  $T - T_g$ ) (142). When this

is done, direct proportionality is indeed found [see equation (36) and Figure 13]. For  $M > M_e$ , however, the viscosity is always proportional to  $M^{3.4}$ . More detailed analyses of the tube and of the chain within the tube (18,148-151) show that the viscosity response is better modeled with the factor  $(M/M_e)^{3.2}$  replaced by  $(M/M_e)^{3.4}$  (18), which is in good agreement with experiment [equation (36)J].

In the steady flow regime, only the longest relaxation time is applicable, so equation (16) becomes

$$\eta = \frac{\pi^2 \rho R T \tau_1}{6M} = \frac{\rho N_0 a^2 M \zeta_0}{36 M_0^2} \quad (46)$$

where  $N_0$  is Avogadro's number,  $a$  an effective bond length along the backbone chain.  $M_0$  the monomer molecular weight, and  $\zeta_0$  the monomeric friction factor. The latter is a measure of the force required to pull a polymer chain through its surroundings at unit speed. It is inversely proportional to the polymer self-diffusion coefficient.

Bueche (16,152) had earlier proposed a related theory based on a spring-bead model (springs with a rubberlike elasticity spring constant coupled in a linear chain by beads whose friction factor supplies the viscous resistance). This theory as extended by Fox and co-workers (28,153) gives

$$\eta = \rho \frac{N_0}{6} \left( \frac{\langle s_0^2 \rangle}{M} z_w \right) \left( \frac{z_w}{z_r} \right)^a \zeta \quad (47)$$

where

$$a = 1 \quad \text{for } z_w < z_r$$

$$a = 3.5 \quad \text{for } z_w > z_r$$

In this equation  $z_w$  is the weight-average number of atoms in the backbone of the polymer chains,  $z_r$  the average number of atoms in the backbone of the polymer chains between entanglements,  $\zeta$  the friction factor per backbone chain atom (rather than the chain monomer as in the Rouse theory), and  $\langle s_0^2 \rangle$  the mean-square radius of gyration of the polymer chains. The chain length  $z_w$  may be calculated from the molecular weight  $M_w$  and the molecular weight of the monomer  $M_0$  for monomers that have two backbone atoms per monomer unit by

$$z_w = \frac{2M_w}{M_0} \quad (48)$$

The radius of gyration  $\langle s_0^2 \rangle$  of polymers is generally determined from light-scattering measurements on dilute polymer solutions and  $\langle s_0^2 \rangle / M$  is a constant for a given polymer. Values for many polymers are tabulated in Ref. 154.

The monomeric friction factors  $\zeta_0$  and  $\zeta$  have a temperature dependence given by the Williams-Landel-Ferry (WLF) relation, equation (27):

$$\log \frac{\zeta_0}{\zeta_r} = \log \frac{\eta}{\eta_r} \approx \frac{-17.44(T - T_r)}{51.6 + T - T_r} \quad (49)$$

where  $\zeta_r$  is the value of the friction coefficient at  $T_r$ . Apparently for all polymers,

$$\frac{(\eta_0^*)}{M} \frac{z_r}{V} \approx 4.7 \times 10^{-15} \quad (50)$$

The molecular weight distribution, as well as the average molecular weight, affects the viscosity, creep compliance, and the stress relaxation modulus (1,155-- U>0). For a broad molecular weight distribution the plateau regions in creep and relaxation become less flat and the stress relaxation in the terminal zone becomes broad. The steady-state creep compliance is extremely sensitive to the high-molecular-weight tail of the molecular weight distribution. Thus the modified Rouse theory would predict (1), for a most probable molecular weight distribution.

$$J_e \approx \frac{2M_w}{5M_n \rho R T}$$

For blends made up of two fractions of different molecular weight, the viscosity of the blend  $\eta_b$  is at a given temperature in some cases approximated by

$$\eta_b \approx \phi_1 \lambda_1 \eta_1 + \phi_2 \lambda_2 \eta_2 \quad (51)$$

where the subscripts refer to fractions 1 and 2,  $\phi_i$  is the volume fraction of fraction 1,  $\eta_i$  the corresponding viscosity, and  $\lambda$  a concentration weight factor that in some cases is given by (159)

$$\lambda_i \approx \left( \frac{\bar{M}_{wb}}{\bar{M}_{wi}} \right)^{2.5} \quad i = 1, 2 \quad (52)$$

Here  $\bar{M}_{wb}$  is the weight-average molecular weight of the blend, and  $\bar{M}_{wi}$  is the weight-average molecular weight of component  $i$ . The steady-state creep compliance  $J_e$  of the blend is

$$J_e \approx \frac{\lambda_1^2 \eta_1^2 \phi_1 J_{e1} + \lambda_2^2 \eta_2^2 \phi_2 J_{e2}}{\eta_b^2} \quad (53)$$



The stress relaxation shear modulus of the blend,  $G_b(t)$  is

$$G_b(t) = \phi_1 G_1 \left( \frac{t}{\lambda_1} \right) + \phi_2 G_2 \left( \frac{t}{\lambda_2} \right) \quad (54)$$

Only the long-time (or high-temperature) response is affected (i.e., where  $\tau$  drops off from the rubbery plateau). The broader the distribution, the narrower the plateau and the more gradual the drop beyond it. Here the  $\lambda$  terms are shift factors on the time scale used in making master curves; the  $\lambda_i$  change the time scale from  $t$  to  $t/\lambda_i$ . These equations are semiempirical and must be used with caution. Schausberger et al. (161) and Tider et al. (162) have developed a more complete description for the effect of molecular weight distribution and multiraction blending based on the Doi-Edwards theory and assumed additivity of dynamic modulus components. The results can be applied to stress relaxation.

An example of experimental stress-relaxation data is shown in Figure 14 (160). Master stress-relaxation curves made from the experimental data on different molecular weight materials are shown in Figure 15. The temperature-shift factors used in making the master curves are shown in Figure 16. Note that the shift factors  $a_i$  are the same for all molecular weights

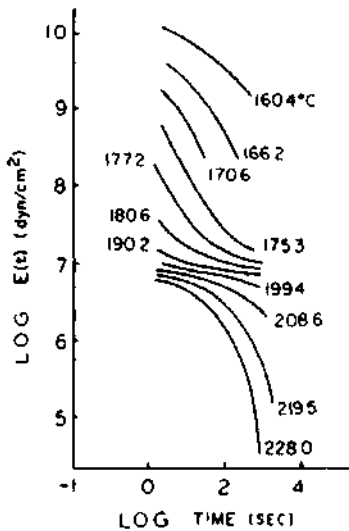


Figure 14 Stress-relaxation data on poly(a-methylstyrene) at various temperatures. Molecular weight is 460,000. (From Ref. 160.)

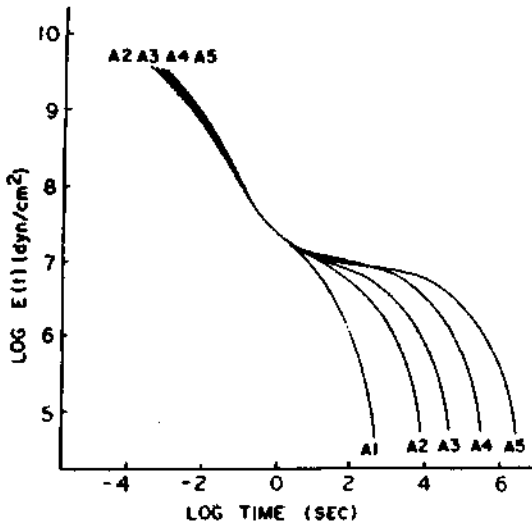


Figure 15 Stress-relaxation master curves for poly(a-methylstyrene) of various molecular weights. Reference temperature = 459 K. (From Ref. 160.)

and follow a WLF relation. The molecular weights covered the range shown in the following table:

| Sample | Molecular weight |
|--------|------------------|
| A1     | 39,000           |
| A2     | 91,000           |
| A3     | 135,000          |
| A4     | 280,000          |
| A5     | 460,000          |

The plateau in the stress-relaxation modulus  $E(t)$  near  $10^7$  dyn/cm<sup>2</sup> is due to the onset of reptational motion, or chain entanglements. The higher the molecular weight, the longer it takes for free chain diffusion to occur (i.e., for chain entanglements to disappear). Polymers behave as purely viscous liquids only at times beyond the plateau region where the stress-relaxation modulus decreases rapidly again. In the plateau region the materials have elasticity and behave very similar to vulcanized rubbers.

Chain branching affects the viscosity, the longest relaxation time, and the steady-state compliance and therefore influences creep and stress relaxation (19,163- 167). The effect is difficult to quantify because the length

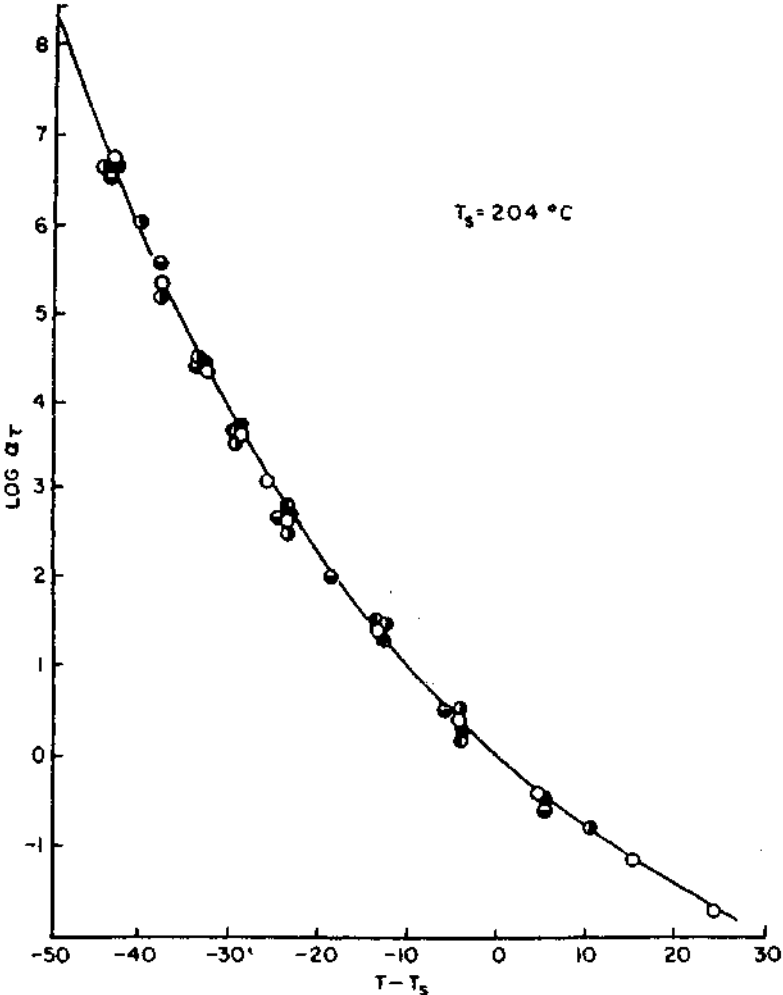


Figure 16 WLF shift factors for various molecular weight poly(a-methylstyrenes). Reference temperature, 2(14°C. (From Rcf. 160.)

and number of branches can vary, and the branches can all originate at one point (as in a cross or star), or they can be spaced along the chain (as in a comb). Molecules consisting of three or four long branches of equal length, which are long enough to form entanglements, have higher viscosity than that of linear polymers of the same molecular weight at very slow rates of deformation. At higher rates, however, the branched polymers have the smaller melt viscosity (165). If a branched polymer is to have a higher viscosity than a linear polymer of the same molecular weight, the branches must be so long that they can have entanglements (164) (i.e., move by reptation). Otherwise, branched polymers have lower viscosity than that of linear polymers (16K). Thus branching can either increase or decrease viscosity (167). Bueche (163) has attempted to explain theoretically the effect of branching on viscosity. The important factor is the ratio of the mean-square radius of the branched molecules to that of the linear polymer of the same molecular weight, since branching changes the volume occupied by a chain.

Star-shaped polymer molecules with long branches not only increase the viscosity in the molten state and the steady-state compliance, but the star polymers also decrease the rate of stress relaxation (and creep) compared to a linear polymer (169). The decrease in creep and relaxation rate of star-shaped molecules can be due to extra entanglements because of the many long branches, or the effect can be due to the suppression of reptation of the branches. Linear polymers can reptate, but the bulky center of the star and the different directions of the branch chains from the center make reptation difficult.

## IX. EFFECT OF PLASTICIZERS ON MELT VISCOSITY

Plasticizer or liquid diluents greatly reduce the melt viscosity of polymers (28.170-177). Small amounts of liquids at temperatures just above  $T_g$  produce an especially dramatic decrease in viscosity. Several factors are responsible for the decrease:

1. Liquids lower the glass transition temperature, and according to the WLF theory, the viscosity and relaxation times are decreased.
2. Diluents increase the molecular weight between entanglements according to the equation

$$M_e = \frac{M_e^0}{\Phi_1} \quad (55)$$

where  $M_e^0$  is the molecular weight between entanglements for the undiluted polymer, and  $\Phi_1$  is the volume fraction of polymer.

- Mixing a high-viscosity liquid with one of low viscosity reduces the viscosity just because of the dilution of the polymer.

At the high polymer concentration used in plasticized systems the viscosity of amorphous polymer is given by the modified Rouse theory at low molecular weight,  $M \leq 2M_c$  [from equation (47)] and by the modified Doi-Edwards equation at high molecular weight. In the first case

$$\frac{\eta}{\eta_0} = \frac{ca^2 \zeta_0}{c_0 a_0^2 \zeta_{00}} = \frac{c \langle r^2 \rangle \zeta_0}{c_0 \langle r_0^2 \rangle \zeta_{00}} \tag{56}$$

Here  $c$  is the polymer concentration by weight,  $c_0$  the density of the polymer,  $a$  an effective bond length or measure of the coil dimensions, and  $\zeta_0$  the monomeric friction factor. The subscript zero indicates the pure polymer. Since  $a^2 \propto \langle r^2 \rangle$ , the mean-square end-to-end chain separation, the viscosity will be directly proportional to the polymer concentration unless the plasticizer modifies the coil swelling. At high molecular weight the monomeric friction factor is increased by the factor  $(M/M_c)^n$  and  $M_c$  is increased relative to the undiluted polymer [equation (55)]. Thus

$$\zeta_0^H \rightarrow \zeta_0^L \left( \frac{M}{M_c} \right)^n = \zeta_0^L \left( \frac{\phi M}{M_c} \right)^n \tag{57}$$

where the superscripts  $H$  and  $L$  refer to high and low molecular weight polymer, respectively. Thus

$$\frac{\eta}{\eta_0} = \frac{ca^2 \phi^n \zeta_0^H}{c_0 a_0^2 \zeta_{00}} = \frac{c \langle r^2 \rangle \phi^n \zeta_0^H}{c_0 \langle r_0^2 \rangle \zeta_{00}} \tag{58}$$

Since  $\phi_1 = c/\rho_{\text{polymer}}$  and  $a = 2.3$  (modified Doi-Edwards) or 2.4 (by direct measurement), the viscosity should increase as  $c$  (or  $\phi_1$ ) to the 3.4 power at a fixed  $T - T_g$  where  $\zeta_0 = \zeta_{00}$ .

Bueche (16,172) proposed that the viscosity is proportional to the fourth power of the polymer concentration and a complex function of the free volume of the mixture. Kraus and Gruver (170) find that the 3.4 power fits experimental data better than does the fourth power. They used equation (58) with  $\langle r^2 \rangle$  replaced by the mean-square radius of gyration ( $s^2$ ). The term  $\langle r^2 \rangle / \langle r_0^2 \rangle$  indicates that poor solvents should lower the viscosity more than a good solvent. As the temperature increases, the factor  $\zeta(s^2) / \zeta_0(s_0^2)$  increases as a function of the ratio  $(T - T_{gD}) / (T - T_{gP})$ . The glass transition temperatures of the polymer and diluent are  $T_{gP}$  and  $T_{gD}$ , respectively.

Since experimental and theoretical results show variations in viscosity that range all the way from the first power to the fourteenth power of the solvent concentration, it is nearly impossible to predict accurately the viscosity of polymers containing a solvent or plasticizer. As a rough approx-

imation, the logarithmic mixture rule is useful:

$$\log \eta = \phi_1 \log \eta_1 + \phi_2 \log \eta_2 \quad (59)$$

In this equation  $\phi_1$  and  $\eta_1$  are the volume fraction and viscosity of the pure polymer at the temperature under consideration. The subscript 2 refers to the solvent or plasticizer.

## X. CROSS-LINKING

Well above the glass transition temperature  $T_g$ , the initial effect of adding cross-links is to increase the molecular weight and hence to widen the rubbery plateau in  $E(t)$ . This decreases the importance of viscous flow and increases the elasticity of the material as measured at long times or high temperature. Once a network or gel has formed, cross-linking gives stress relaxation curves that level off to a finite instead of a zero stress at long times and creep curves that tend to level off to a constant deformation at long times. In an ideal rubber the stress remains constant at all times during a stress-relaxation test. The creep curve of an ideal rubber shows a definite deformation on application of the load, and the strain remains at this constant value until the load is removed, at which time the rubber snaps back to its original length. Thus an ideal cross-linked rubber is a perfect spring at long times. However, in practice, cross-linked elastomers can have very imperfect network structures that contain dangling chain ends, loops in polymer chains, and branched molecules only partly incorporated into the network, as well as molecules entrapped in the network but not attached to it by chemical bonds (1,178-182).

As noted above, normal cross-linking does not appreciably modify the transition zone. Hence the stress-relaxation modulus is simply the sum of the time-dependent contributions of the Rouse-like segment motion of the cross-linked polymer chains  $E(t)_c$ , [equations (17) and (16) or (46)] and of the equilibrium modulus  $E_{eqm}$  representing the ideal rubber, modified at times longer than the longest segmental relaxation time by contributions from the dangling chain ends and entanglement slippage  $E(t)_{ent}$ :

$$E(t) = (E(t)_c + E_{eqm})E(t)_{ent} \quad (60)$$

Thus at a given temperature, the location of the transition zone of  $E(t)_c$  on the time scale is determined by the monomeric friction factor, the height of the entanglement plateau by  $M_e$ , and the width of the plateau by  $(M/M_e)^{3.4}$ . The time dependence of entanglement slippage,  $E(t)_{ent}$ , describes the rate at which the entanglement plateau will drop to the equilibrium

plateau. It was first given empirically by Plazek (183) for creep and subsequently derived for stress relaxation from reptation dynamics by Curro et al. (184,185). A useful expression for Plazek's tabulated  $E(t)_{cni}$  function is (185a):

$$\log E(t)_{cni} = -4.72 \times 10^{-4} - 2.98 \times 10^{-3} \log(t/a_x) - 4.32 \times 10^{-4} \log^2(t/a_x) - 6.23 \times 10^{-5} \log^3(t/a_x) \quad (59)$$

valid over the range  $-16 < \log(t/a_x) < 0$ , where  $a_x$  is a shift factor which depends on the degree of cross-linking and shifts  $\log E(t)_{cni}$  along the line  $\log E_{cqm}$  until it joins with the curve  $\log[E(t)_c + E(t)_{cqm}]$ .

Figure 17 shows the course of  $E(t)$  for live uncross-linked rubbers as calculated by Landel and Fedors (186) from the Marvin (187) extension of the Rouse theory to undiluted polymers, which gives the time dependence of  $E(t)$ . The Marvin theory employs the Rons\*, parameters  $a$ , the bond length, and  $\zeta_0$ , the monomeric friction factor, plus the ratio  $M/M_c$ . The addition of a term  $E_{cqm}$ , whose magnitude will be determined by the extent of cross-linking (i.e., the elastic chain concentration as determined by swelling) would give rise to the dashed-line response shown in Figure 18 for the silicone rubber. Finally, the solid line shows the expected response when the entanglement term is added. Using this approach, Landel

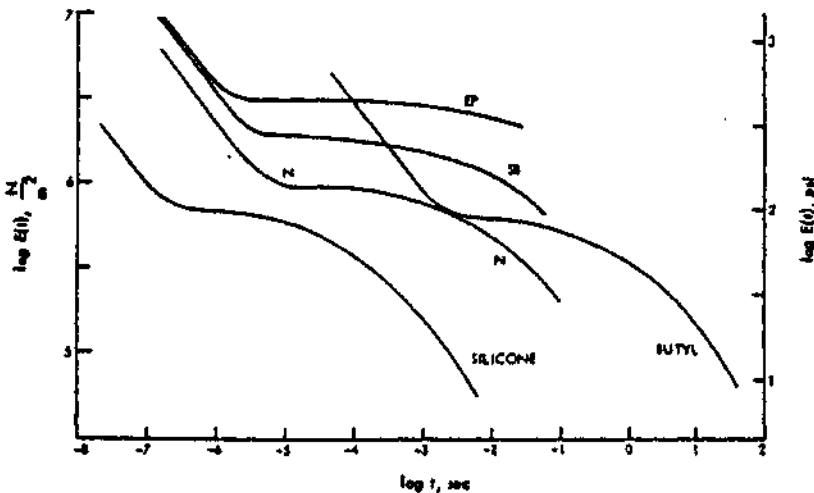
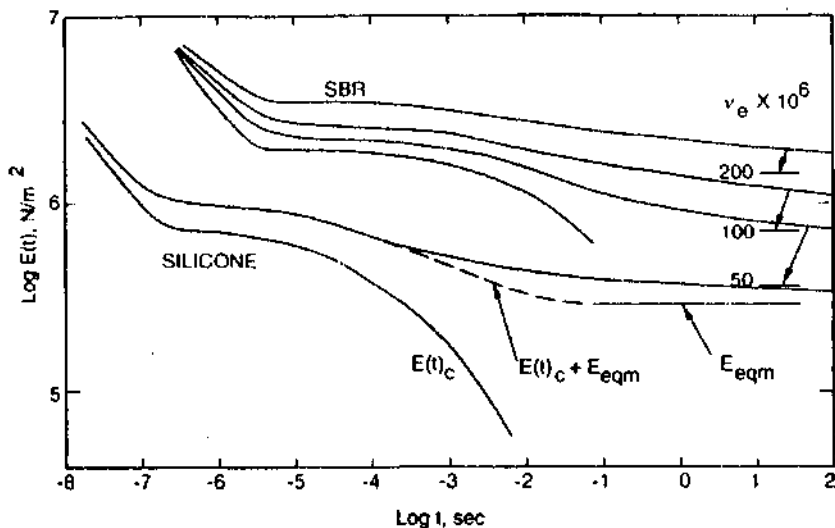


Figure 17 Calculated stress-relaxation behavior at 298 K for five uncross-linked elastomers of  $M = 200,000$ : EP, ethylene-propylene (56:44); styrene-butadiene (23.5:76.5), SB; natural rubber, N; butyl; and dimethyl siloxane.



**Figure 18** Calculated stress-relaxation curves for styrene-butadiene and silicone rubbers, both uncross-linked (from Figure 17) and cross-linked to  $\nu_e = 50 \times 10^{-6}$  mol/cm<sup>3</sup>, and for SBR additionally, cross-linked to  $\nu_e = 100$  and  $200 \times 10^{-6}$  mol/cm<sup>3</sup>. The horizontal bars show the location of the equilibrium modulus for SBR.  $M = 200,000$ ,  $T = 298$  K.

and Fedors calculated  $E(t)$  for four quite different types of elastomers. They showed that  $E(t)$  can be predicted with no adjustable parameters, using molecular constants evaluated a priori, over at least seven decades of reduced time (Figure 19). Table 4 gives the constants for these and some other typical polymers (186).

The earlier, semiphenomenological Marvin theory is identical to the detailed Doi-Edwards (DE) molecular theory in the transition zone and mimics the DE response in the plateau and flow region rather well, especially if the effects of the molecular weight distribution are included in the DE response. A more refined treatment of the effect of chemical cross-links in reducing the number of entanglements would remove the slight hump seen in the calculated curves of Figures 18 and 19. The chemical nature of the polymer chains is only of minor importance as long as labile groups are not introduced.

Highly cross-linked rubbers swell less in good solvents than do lightly cross-linked rubbers (188,189). For this reason, swelling in solvents is often used to determine quantitatively the degree of cross-linking. However, in



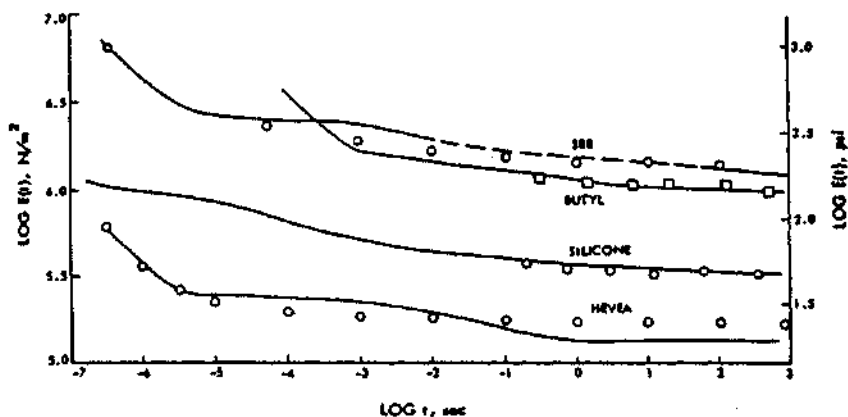


Figure 19 Comparison of calculated (curves) versus experimental (points) modulus results for the same elastomers shown in Figure 17.  $M$  assumed 200,000 in each case;  $T = 298$  K. The values of  $\nu_e \times 10^6$  are SBR, 100; butyl, 113; silicone, 38; and hevea, 168.

Table 4 Molecular Parameters for Various Polymers (from Ref. 186).

|  | $\rho$<br>g/cm <sup>3</sup> | $T_g$<br>°K | $\log \zeta_0$<br>dynes · cm/sec | $M_w$<br>g/mole     | $M_0$<br>g/mole |
|--|-----------------------------|-------------|----------------------------------|---------------------|-----------------|
| Styrene-butadiene <sup>a</sup>             | 0.93                        | 210         | -6.11                            | 3,000               | 65.5            |
| Hevea                                      | 0.91                        | 200         | -6.41                            | 5,750               | 68              |
| Butyl (PIB)                                | 0.937                       | 205         | -4.35                            | 8,900               | 56              |
| Butadiene <sup>b</sup>                     | —                           | 172         | -6.75                            | 2,950               | 54              |
| Ethylene-propylene <sup>c</sup><br>(56/44) | 0.87                        | 216         | -6.36                            | 1,660               | 34.3            |
| Dimethyl siloxane                          | 0.980                       | 150         | -8.05                            | 8,100               | 74              |
| Vinyl acetate                              | 1.18                        | 305         | 4.29 <sup>d</sup>                | 12,250 <sup>e</sup> | 86              |
| Methyl acrylate                            | —                           | 276         | 0.32                             | 12,000 <sup>f</sup> | 86              |
| Ethylene                                   | 0.85                        | (148)       | —                                | 1,900 <sup>e</sup>  | 28              |

<sup>a</sup>Random copolymer

<sup>b</sup>dis/trans/vinyl = 43/50/7, lightly vulcanized with dicumyl peroxide

<sup>c</sup>Ethylene/propylene = 56/44, by mole

<sup>d</sup>At  $T_g$

<sup>e</sup> $M_w/2$

<sup>f</sup>Estimated from plateau height of  $E(t)$

<sup>g</sup>At 100°C

many respects, mechanical tests such as elastic moduli are more suitable for estimating the degree of cross-linking, especially moduli determined on swollen specimens. This topic is discussed later when we cover the kinetic theory of rubber elasticity. The effect of cross-linking (as indicated by swelling tests) on creep is illustrated in Figure 20 (190). The degree of cross-linking is given in terms of the swelling ratio  $q$ , which is defined as the ratio of the volume of the swollen gel to the volume of the unswollen gel.

A crude estimate of the perfection of the network structure is given by the sol fraction, which is the fraction of the cross-linked polymer that can be extracted by a good solvent. The higher the sol fraction the less perfect is the network structure. As noted above, an especially important type of imperfection in networks appears to be entrapped entanglements (181,182). An entanglement is trapped when both ends of each of the two chain segments involved in an entanglement arc attached to the network structure. Otherwise the entanglement can eventually disappear by dragging the unattached branched segments through the network to relieve the applied stress. These entrapped entanglements can have extremely long relaxation or retardation times, as can be seen in Figures 18 and 19.

As might be expected, the creep response resembles an inverted image of the stress relaxation response. Figure 20 shows the creep response over a short region of the time scale where the uncross-linked polymer is in the flow regime. The deformation increases nearly linearly with log time and its rate shows no tendency to decrease even at long times. Small degrees of cross-linking greatly decrease the creep rate, but creep still continues, apparently forever (138,191 -194,183). Higher degrees of cross-linking cut down both the creep and the creep rate, so that after a time, the creep reaches essentially a limiting value even though the creep rate may never drop completely to zero in some cases. In very long time tests or in use conditions, the possibility of chemical degradation or cross-linking from oxygen and ultra-violet light must be kept in mind. The great decrease in compliance that occurs when cross-linking converts the polymer from a soluble material into a gel has also been found for other rubbers, such as polybutadiene (195) and plasticized methacrylate (196).

Farlie (197) has measured both the rate of creep and the rate of stress relaxation of natural rubber as a function of the degree of cross-linking. As expected from the results of Figure 18, both rates decrease with cross-linking. Farlie's results, and those of Berry and Watson (198), also illustrate the effect of either network morphology or the chemical nature of the cross-linking agent since the rates for sulfur vulcanizates at a given degree of cross-linking are two or three times as great as the rates found for peroxides as the vulcanizing agent; the sulfide linkages in sulfur vulcani-

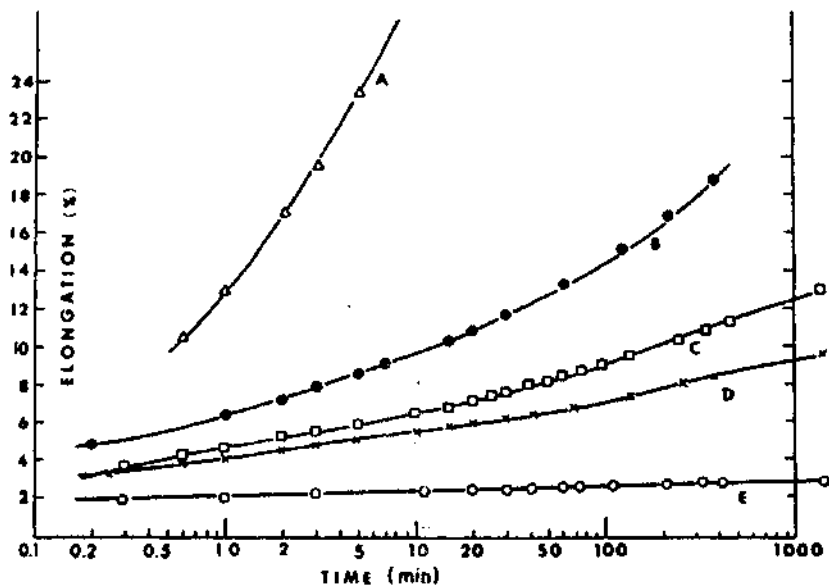


Figure 20 Creep of SBR rubbers at 24°C. (A) Uncross-linked,  $\bar{M}_w = 280,000$ . (B) Lightly cross-linked,  $M_c \approx 29,000$ ,  $q = 33.5$ , sol fraction = 34%. (C) Moderately cross-linked,  $M_c \approx 18,200$ ,  $q = 25.8$ , sol fraction = 24%. (D) Moderately cross-linked,  $M_c \approx 14,400$ ,  $q = 21$ , sol fraction = 20.4%. (E) Highly cross-linked,  $M_c \approx 5200$ ,  $q = 6.8$ , sol fraction = 9.5%. Swelling liquid was benzene. Load = 5 lb/in.<sup>2</sup>. (From Ref. 190.)

zates may be labile and undergo interchange reactions that relieve the stress.

Experiments have been made in which uncross-linkable polymer rubbers have been added to a similar rubber that is subsequently cross-linked (199). As an example, polyisobutylene was added to butyl rubber before it was cross-linked. The polyisobutylene molecules were not attached to the network structure, so they could be extracted by a solvent. As expected, the polyisobutylene greatly increased the creep compliance over that of the pure butyl rubber.

Plazek (183) carried out very accurate creep experiments on natural rubber as a function of cross-linking. He found that data at different temperatures could be superimposed by the usual WLF shift factors which were developed for non-cross-linked polymers (27). Temperature-superposed

civet curves for different degrees of cross-linking could be further superimposed to give a master creep curve by horizontal shifts and by vertical shifts determined by the degree of cross-linking. The vertical shift factor is given in  $\log\{E(M)/E(M_c^*)\}$ , where  $E(M_c)$  is the long-time equilibrium modulus of a rubber with a molecular weight between cross-links of  $M_c$ , while  $E(M_c^*)$  is the equilibrium modulus of a reference rubber with a molecular weight between cross-links of  $M_c^*$ . The horizontal shifts are a very strong function of the degree of cross-linking,  $(M_c/M_c^*)^{0.74}$ .

Creep measurements in the glassy state are complicated by the physical aging process, which can go on in imaged samples or as the measurement temperature is raised. Furthermore, the cure cycle itself can affect the magnitude of the compliance (modulus), the creep rate, and the apparent  $E_c$  (200,201). Although the effects are often small, their lack of control reduces the scientific interest in many creep studies, just as in earlier work the omission of cross-link density measurements prevented full interpretation of results. It appears that cross-linking has no major effect on the creep of polymers at temperatures well below their glass transition region. In rigid, brittle polymers, molecular motions are so frozen-in that the additional restrictions of cross-links are hardly noticeable. The creep of rigid polymers is strongly dependent on the elastic modulus, the mechanical damping, and the difference between  $E_c$  and the ambient temperature. Some thermoset materials, such as phenol-formaldehyde and melamine resins, have high moduli, low mechanical damping, and high glass transition temperatures; all of these factors tend to reduce creep and creep rate, so these types of polymers generally have low creep and very good dimensional stability. On the other hand, some epoxy and polyester resins have much greater creep. They may have shear moduli less than  $10^{10}$  dyn/cm<sup>2</sup> because of low-temperature secondary glass transitions (202-205) or because of free volume frozen-in during the cure process. Because of this effect, Plazek and Choy (200,201) have found that more highly cross-linked epoxies can actually have a lower modulus, and thus greater creep, than more lightly cross-linked ones. In addition, because of their chemical structure and low curing temperature, many epoxy and polyester resins have relatively low glass transition temperatures. For these reasons, such resins may have considerably greater creep than the more highly cross-linked phenol-formaldehyde resins.

An effect of network morphology is illustrated by the work of Shen and Tobolsky (ISO). They cross-linked rubbers in the presence of inert diluents; such polymerizations tend to promote intramolecular chain loops rather than interchain cross-links. Their polymers had very low stress-relaxation

moduli compared to normal vulcanized rubbers containing similar concentrations of cross-linking agent.

## XI. CRYSTALLINITY

Above  $T_g$ , Crystallinity decreases creep compliance, creep rate, and rate of stress relaxation while increasing the stress relaxation modulus. Several theories have been developed to explain these phenomena (206-212). These effects of Crystallinity come about from the apparent cross-linking as a result of the ends of many chain segments being immobilized in different crystallites and from the rigid crystallites acting as filler particles (206-208). Figures 21 and 22 illustrate schematically the effects of changing the degree of Crystallinity on creep and stress relaxation above  $T_g$ . (The shapes and absolute values of these curves are rough approximations to any real polymer, as the properties can vary considerably from polymer to polymer. The curves illustrate general trends as the degree of Crystallinity is changed.) Even small amounts of Crystallinity can dramatically decrease creep or stress relaxation without greatly increasing the modulus of the material (213-215). Plasticized poly(vinyl chloride) film is an example; this elastomer maintains reasonable dimensional stability for long periods of time

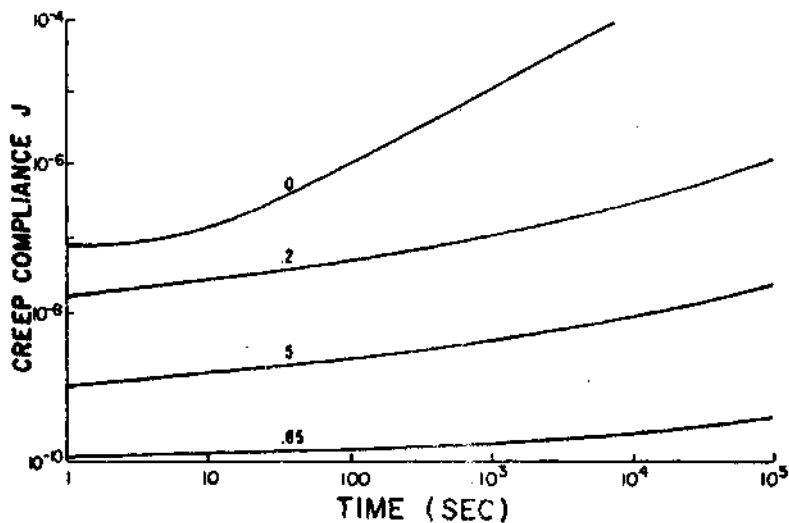


Figure 21 Creep compliance as a function of degree of crystallinity above  $T_g$ . Numbers on curves are rough values of the degree of crystallinity.

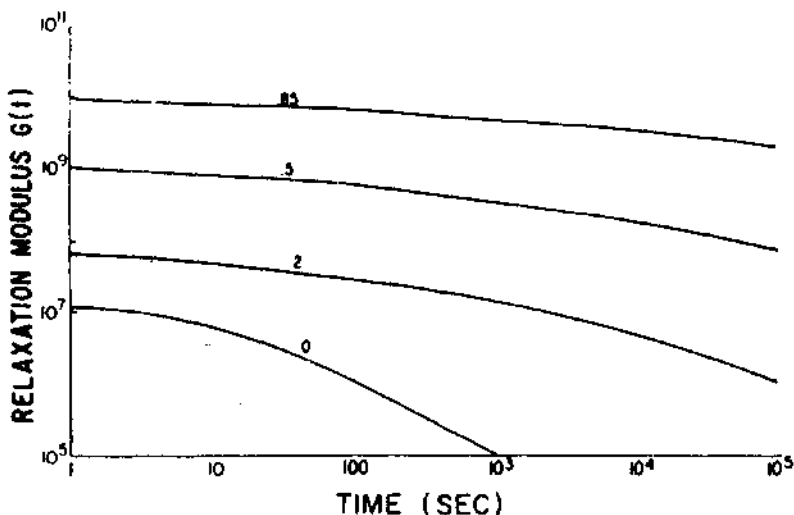


Figure 22 Stress-relaxation modulus as a function of Crystallinity at temperatures above  $T_g$ . Numbers on the curves are rough values of the degree of Crystallinity.

without excessive flow (213). The degree of Crystallinity is so low, or the crystallites are so imperfect, that in many cases Crystallinity cannot be detected by x-ray diffraction. Poly(vinyl alcohol) copolymers of low to moderate hydroxyl content are another example (214). Low- $T_g$ -value polymers containing less than about 15 to 20% Crystallinity behave essentially as cross-linked rubbers (52,216,217). At crystallinities greater than about 40 or 50%, the crystallites may become a continuous phase instead of just a dispersed phase in a rubbery matrix (212); in such materials the modulus is high, and it becomes only very slightly dependent on time.

The temperature dependence of the compliance and the stress relaxation modulus of crystalline polymers well above  $T_g$  is greater than that of cross-linked polymers, but in the glass-to-rubber transition region the temperature dependence is less than for an amorphous polymer. A factor in this large temperature dependence at  $T \gg T_g$  is the decrease in the degree of Crystallinity with temperature. Other factors are the recrystallization of strained crystallites into unstrained ones and the rotation of crystallites to relieve the applied stress (38). All of these effects occur more rapidly as the temperature is raised.

The distribution of relaxation or retardation times is much broader for crystalline than for amorphous polymers. The Boltzmann superposition

principle often does not hold for crystalline polymers at long times (H9). Recrystallization and other changes in the crystallites are the probable cause. The WLF time-temperature superposition principle (27) generally is not applicable to crystalline polymers except at low degrees of Crystallinity (52,89,214,215,218,219). This is again partly due to the change of Crystallinity and other factors with temperature. In many cases master curves cannot be made for crystalline polymers; in other cases master curves can be made by using vertical as well as horizontal shifts of the experimental curves (36-38,218,219). The horizontal shifts may not correspond to the usual WLF shifts, however. Figures 23 to 25 illustrate the typical differences in the stress-relaxation behavior of amorphous and crystalline materials (52). (It is believed that the values of Crystallinity given on these curves are low by a factor of at least 2.) These figures show how Crystallinity flattens out the stress-relaxation curves (i.e., broadens the distribution of relaxation times). In this case of polycarbonate, the  $T_K$  value appears to increase slightly with the degree of Crystallinity.

Annealing and also aging can change the degree of Crystallinity to some extent, but thermal treatments often change the morphology more by increasing the length between folds in the crystallites or by making spherulitic structure more pronounced (220). Thus annealing and aging above  $T_K$  increase the modulus and decrease the creep and stress-relaxation rates (89,92). If the polymer is aged below the  $T_K$  value of the amorphous region, the modulus increases because of physical aging as discussed above.

Only a few representative cases of the hundreds of articles on the creep and stress relaxation of crystalline polymers can be referred to here. The creep of polyethylene has been discussed by Carey (95), Findley (98), Turner (84), Nielsen (89) and Nakayasu et al. (221). In the latter case the response was clarified by extending the time scale through combined creep and dynamic compliance measurements. The contributions of different mechanisms (and their temperature dependence) could then be resolved by analyzing the dynamic data. The stress relaxation of polyethylene has been studied by Becker (72), Catsiff et al. (221), Nagamatsu et al. (218), and Faucher (33). Results on polypropylene are given by Faucher (33) and Turner (92). The stress relaxation of polycarbonate over a range of Crystallinity is reported by Mercier and Groeninckx (217), that of nylon 6 by Yoshitomi et al. (223) and Onogi et al. (224), that of poly(vinyl acetals) by Fujino et al. (214), and that of fluorinated polymers by Nagamatsu and co-workers (225,226). The creep of poly(vinyl alcohol) as affected by water was studied by Yamamura and Kuramoto (227), while the creep of a fluorinated polymer was investigated by Findley and Khosla (228). The stress relaxation of polyoxymethylene was measured by Gohn and Fox (229).

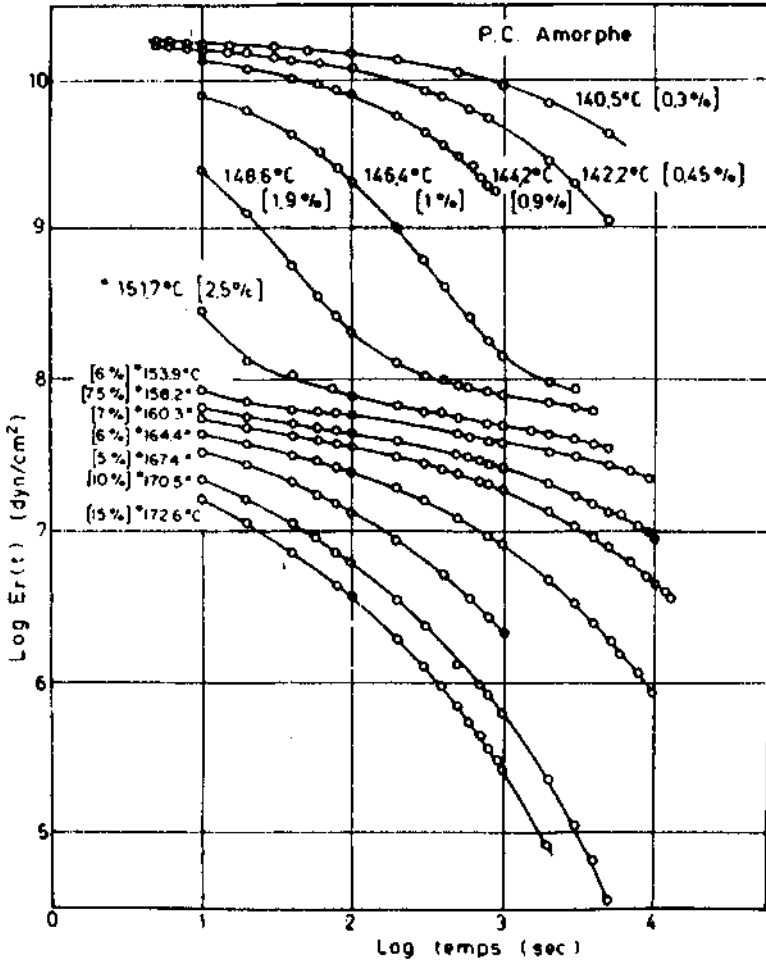


Figure 23. Stress-relaxation curves of amorphous bisphenol A polycarbonate at the different temperatures shown by the curves. The numbers in brackets are the maximum deformations used in the tests. (From Ref. 217.)

The stretching of amorphous but crystallizable materials can greatly increase the rate of crystallization in some cases. Natural rubber and polyethylene terephthalate are examples. The stretching of the polymer initially causes the crystallites to grow so that the chains in the crystallites are oriented parallel to the applied stress. Thus the growth of the crystallites



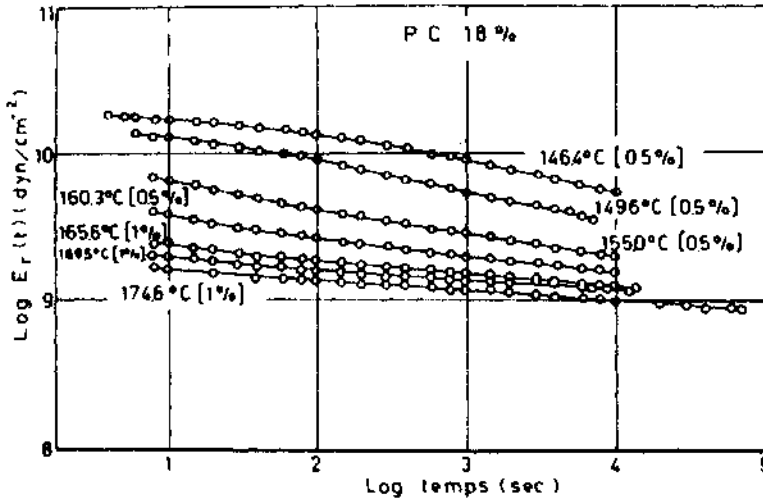


Figure 24. Stress-relaxation curves of crystalline bisphenol A polycarbonate at the temperatures shown by the curves. The degree of Crystallinity was IX%. (From Ret. 217.)

straightens out the curled-up chain segments and causes the stress to relax rapidly or causes the specimen to elongate rapidly in the case of a creep test (230,231).

## XII. COPOLYMERS AND PLASTICIZATION

The primary effect of Copolymerization and plasticizer<sup>^</sup> is to shift the glass transition temperature, so the creep, and stress-relaxation curves are also shifted on the temperature scale the same amount as  $T_g$ . Time-temperature superposition still holds for such materials. A second major effect that can occur is a change in the plateau modulus. Plasticizers decrease it; copolymers either increase or decrease it depending on their own plateau modulus and the concentration. However, two secondary effects are often observed with both copolymers and plasticized polymers that modify the creep and stress-relaxation behavior somewhat. Occasionally, Copolymerization and some Plasticizers broaden the glass transition region compared to the pure homopolymers (232-234). This broadening can cause some decrease in  $da_T/dT$ . A second effect is sometimes found in the glassy state when Plasticizers are added to polymers with secondary glass transitions. The plasticizer (or comonomer) may increase the modulus in the temper-

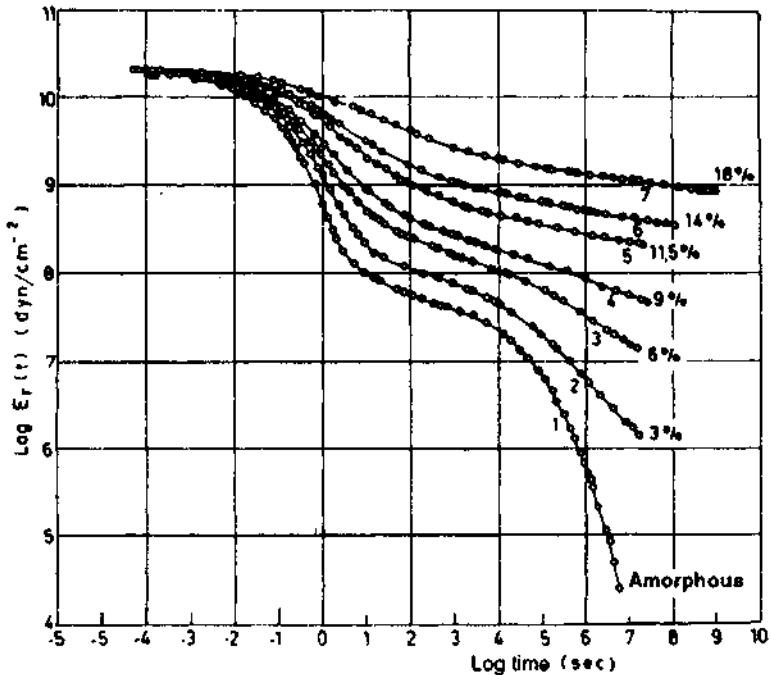


Figure 25 Master stress-relaxation curves of bisphenol A polycarbonate of different degrees of Crystallinity. Degrees of Crystallinity are shown by curves. Reference temperature is 155°C. (From Ref. 217.)

ature region between the secondary and main glass transitions; this effect has been called the antiplasticizer effect (235-237).

Water is a natural plasticizer for many polar polymers such as the nylons (23K), polyester resins (239), and cellulosic polymers (240). It strongly shifts  $T_g$  in epoxics (241,242). Thus the creep and stress-relaxation behavior of such polymers can be strongly dependent on the relative humidity of the atmosphere.

Poly(vinyl chloride) and its copolymers are probably the most important polymers that are often used in the plasticized state. Even though enough plasticizer is used to shift  $T_g$  well below room temperature, the material does not show excessive creep (and has no contribution of viscous flow to the compliance) even after long times under load. This behavior is very similar to that of a cross-linked rubber. However, in this case there are no chemical cross-links; the material is held together by a small amount of

Crystallinity—about 1 to 15% (213,232). The creep of plasticized poly(vinyl chloride) polymers as a function of temperature, concentration, and kind of plasticizer has been studied by many workers, including Aiken et al. (232), Neilsen et al. (234), and Sabia and Eirich (243). These last workers also studied stress relaxation (244). In the case of crystalline polymers, plasticizers and Copolymerization reduce the melting point and the degree of Crystallinity. These factors tend to increase the creep and stress relaxation, especially at temperatures approaching the melting point.

Block polymers can have complex creep and stress-relaxation behavior and are not thermorheologically simple. Although apparent time-temperature superposition can be found if data are obtained over moderate time scales, it usually will not work for data obtained over wide time scales. For diblocks the complexity depends on the  $T_g$  value of the two polymers, the blockiness of the chain, the compatibility of the two components, and the morphology of the resulting two-phase system. Thus for di- or triblocks of the AB or ABA type with well-separated  $T_g$  values and B the high- $T_g$ -value segment, the response will have a two-step appearance with the modulus dropping at the respective  $T_g$  values (in a plot versus  $T$ ) or transition times (in a plot versus log time). As the concentration of B increases, the morphology changes from glassy polymer B spheres embedded in rubber, to B cylinders, to lamellae, to rubbery A cylinders in a rigid matrix, to rubbery A spheres- in a glassy matrix. With this progression in morphology, the first step is large when B is small and small when A is large, and conversely at the second step. As the two  $T_g$  values approach each other or the polymers are more compatible or a diblock AB polymer is added to enhance miscibility, the steps became less pronounced and a long, broad transition from glass to the flow region can be produced. Blends of polymers show similar complex responses. When viewed on the time scale, however, each blend component can influence the other's  $\zeta_0$  value and apparent  $M_r$  value, so that the transitions and plateau heights tend to shift in a rather regular fashion as the composition changes. The description of these shifts is complex (1,159,161,162).

### XIII. EFFECT OF ORIENTATION

Orientation effects are strongly coupled to nonlinear behavior, discussed in Section V, and the stress-strain response discussed in Chapter 5, Orientation makes an initially isotropic polymer anisotropic so that five or nine modulus/compliance values are required to describe the linear response instead of two, as discussed in Chapter 2. For an initially anisotropic polymer the various modulus/compliance components can be altered by the orientation. It may not be necessary to know all components for an

engineering application (e.g., the through-the-thickness modulus may be unimportant for a film or plate application). Ward has reviewed the theoretical and experimental aspects of orientation effects, especially in crystalline polymers (245).

Creep and stress relaxation are generally much less in the direction parallel to the uniaxial orientation than they are perpendicular to the orientation for rigid polymers (245-253). At least part of this decreased creep must be due to the increased modulus in the direction parallel to the oriented chains. For example, many highly oriented fibers have Young's moduli about an order of magnitude greater than that of unoriented polymers. The increase in modulus parallel to the direction of orientation arises because the applied stress largely acts on strong covalent bonds. Perpendicular to the orientation, the force is applied mostly to van der Waals forces between molecules. Uniaxially oriented polyethylene made by cold-drawing has a lower creep compliance (higher modulus) parallel to the stretching direction than in the transverse direction (3,245). However, at 45° to the stretching direction, the modulus as determined by a creep test is even less than the modulus of unoriented polyethylene.

Analogous results have been found for stress relaxation. In fibers, orientation increases the stress relaxation modulus compared to the unoriented polymer (69,247,248,250). Orientation also appears in some cases to decrease the rate, as well as the absolute value, at which the stress relaxes, especially at long times. However, in other cases, the stress relaxes more rapidly in the direction parallel to the chain orientation despite the increase in modulus (247,248,250). It appears that orientation can in some cases increase the ease with which one chain can slip by another. This could result from elimination of some chain entanglements or from more than normal free volume due to the quench-cooling of oriented polymers.

Biaxially oriented films, made by stretching in two mutually perpendicular directions, have reduced creep and stress relaxation compared to unoriented materials. Part of the effect is due to the increased modulus, but for brittle polymers, the improved behavior can be due to reduced crazing. Biaxial orientation generally makes crazing much more difficult in all directions parallel to the plane of the film.

Another effect of orientation shows up as changes in Poisson's ratio, which can be determined as a function of time by combining the results of tension and torsion creep tests. Poisson's ratio of rigid unoriented polymers remains nearly constant or slowly increases with time. Orientation can drastically change Poisson's ratio (254). Such anisotropic materials actually have more than one Poisson's ratio. The Poisson's ratio as determined when a load is applied parallel to the orientation direction is expected to

be greater than that of the unoriented polymer, but this is not always the case, especially for crystalline polymers such as polyethylene (248).

Although nearly all creep and stress-relaxation tests are made in uniaxial tension, it is possible to make biaxial tests in which two stresses are applied at  $90^\circ$  to one another, as discussed in Section VI. In a uniaxial test there is a contraction in the transverse direction, but in a biaxial test the transverse contraction is reduced or even prevented. As a result, biaxial creep is less than uniaxial creep—in equibiaxial loading it is roughly half as much for equivalent loading conditions. In the linear region the biaxial strain  $\epsilon_2$  in each direction is (255.256)

$$\epsilon_2 = \frac{\sigma_0}{E} (1 - \nu) = \frac{\epsilon_1}{2} + \frac{\sigma_0}{6K} \quad (61)$$

where  $\epsilon_1$  is the uniaxial strain that would result from a stress  $\sigma_0$ ,  $\epsilon_2$  is the biaxial strain in each of the mutually perpendicular directions produced by the same stress  $\sigma_0$  in each direction,  $\nu$  is Poisson's ratio, and  $K$  is the bulk modulus. For most polymers, Poisson's ratio is between 0.35 and 0.50, so biaxial creep is generally between 50 and 65% as great as uniaxial creep. Conversely, the stress-relaxation modulus is higher.

#### XIV. BLOCK POLYMERS AND POLYBLENDS

The mechanical properties of two-phase polymeric systems, such as block and graft polymers and polyblends, are discussed in detail in Chapter 7. However, the creep and stress-relaxation behavior of these materials will be examined at this point. Most of the systems of practical interest consist of a combination of a rubbery phase and a rigid phase. In many cases the rigid phase is polystyrene since such materials are tough, yet low in price.

Even in cases where the rigid polymer forms the continuous phase, the elastic modulus is less than that of the pure matrix material. Thus two-phase systems have a greater creep compliance than does the pure rigid phase. Many of these materials craze badly near their yield points. When crazing occurs, the creep rate becomes much greater, and stress relaxes rapidly if the deformation is held constant.

One type of block polymer is known as thermoplastic elastomers. They consist of a number of rubber blocks tied together by hard crystalline or glassy blocks. These materials can be processed in injection molding and extrusion equipment since the crystalline blocks melt or the glassy ones soften at high temperatures. However, at lower temperatures, such as at room temperature, the hard blocks behave very much as cross-links to reduce creep and stress relaxation. Thermoplastic elastomers have creep behavior between that of very lightly cross-linked rubbers and highly cross-

linked rubbers (114,257). These block polymers have mechanical properties that can be changed quite dramatically by molding conditions, thermal history, and annealing. Annealing can reduce the creep very much, especially if the specimen was quenched during its preparation.

Several attempts have been made to superimpose creep and stress-relaxation data obtained at different temperatures on styrene-butadiene-styrene block polymers. Shen and Kaelble (258) found that Williams-Landel-Ferry (WLF) (27) shift factors held around each of the glass transition temperatures of the polystyrene and the polybutadiene, but at intermediate temperatures a different type of shift factor had to be used to make a master curve. However, on very similar block polymers, Lim et al. (25\*) found that a WLF shift factor held only below 15°C in the region between the glass transitions, and at higher temperatures an Arrhenius type of shift factor held. The reason for this difference in the shift factors is not known. Master curves have been made from creep and stress-relaxation data on partially miscible graft polymers of poly(ethyl acrylate) and poly(methyl methacrylate) (260). WLF shift factors held approximately, but the master curves covered 20 to 25 decades of time rather than the 10 to 15 decades for normal one-phase polymers.

The properties of two-phase systems can be changed dramatically by casting the materials from different solvents. The effects are due to changes in morphology and phase inversion which switch one polymer from the continuous to the dispersed phase. Good solvents for a polymer tend to make that polymer the continuous phase, while poor solvents coil the polymer chains up tightly and tend to force the polymer into being a dispersed phase. Examples of the change in stress relaxation of styrene-rubber block polymers as a result of casting films from different kinds of solvents have been reported by Beecher et al. (261) and by Wilkes and Stein (262).

## SUMMARY

Time is the major factor in determining the mechanical properties of a polymer. This is seen directly in creep and stress-relaxation experiments. These tests cover long periods of time, so that they are sensitive to the types of molecular motions that require long times. They give little direct information on the types of molecular motion that take place at short times. However, by using the time-temperature superposition principle and the WLF equations, access to these short times can be achieved even though they may not easily be attainable by direct experimentation.

Above  $T_K$  the time-dependent mechanical properties of a polymer are determined fundamentally by the distribution of relaxation or retardation

times, which in turn are determined by numerous structural and molecular factors as well as by environmental factors. The most important structural factors are the monomeric friction factor and the molecular weight between entanglements. The former locales the distribution and hence the response curve on the time scale at a given reference temperature such as  $T_R$  or some fixed number of degrees above  $T_R$ . The molecular weight between entanglements controls the magnitude and breadth of the entanglement plateau in creep or stress relaxation and the strain recovery in creep recovery. The distribution functions and the time-dependent property curves or functions are qualitatively similar in shape/form for different polymers, but significant differences exist between polymers.

Temperature affects the response because the spectra and the properties are shifted bodily along the logarithmic time scale (i.e., with no change in shape). This happens because the monomeric friction factor is changed. The temperature dependence of the friction factor and hence the shift factor  $a_T$  is given by the WLF equation. The temperature dependence of  $a_T$  is very nearly the same for different pure polymers. The various structural and environmental factors that can affect the shift factor do so primarily through their influence on the free volume and thus on  $T_R$ . Because of the strong temperature dependence of  $a_T$  near  $T_R$ , the response curves shift dramatically in this temperature region. As a result, the modulus or compliance can change by a factor of  $10^3$  over a relatively short temperature range.

At temperatures below  $T_R$ , the free volume is a major factor in determining the creep and stress-relaxation behavior. Molecular motions cannot occur unless enough space is available, so that fewer types of molecular motions can occur as the free volume decreases. Free volume can be reduced by lowering the temperature, increasing the pressure, or annealing at a temperature near  $T_R$ . All of these factors tend to reduce the rate of creep or stress relaxation. The free volume, and hence the rates, can be increased by adding solvent or plasticizer. In glassy polymers below  $T_K$  the free volume may be so low that very little creep or stress relaxation due to molecular motion is possible. In such materials much of the stress relaxation and creep can really be due to crazing phenomena.

Molecular weight of the polymer is the most easily varied and important structural variable for amorphous polymers at temperatures above  $T_R$  because the melt viscosity (i.e., friction factor or longest relaxation time) is strongly dependent on molecular weight. Above a critical value of molecular weight, materials contain entanglements, which not only increase the viscosity but also introduce rubberlike elasticity to the melts. These entanglements impose restrictions on the motion of long-chain segments, so that additional long-time relaxation and retardation times are given to the

polymer. Entanglements eventually relax, but chemical cross-links impose restrictions on chain motions of a much more permanent nature. Thus there is little, if any, long-term creep or stress relaxation for well cross-linked rubbers.

Crystallization ties polymer chains together and immobilizes parts of the chains in the crystallites. The restrictions to motion resulting from crystallization are very similar to those due to cross-linking as far as reducing creep and stress relaxation are concerned at temperatures between  $T_g$  and the melting point. There is an additional effect in that the crystallites act as any other hard filler and raise the modulus. The mechanical properties thus depend on the degree of Crystallinity and the crystallite morphology; therefore, thermal history and annealing can have unusually large effects on the behavior of crystalline polymers.

Block polymers and similar two-phase systems are somewhat analogous to crystalline materials at temperatures between the lower  $T_g$  value and the  $T_g$  or melting point of the other phase. The glassy (or crystalline) phase both imposes restrictions on the long-range motions of the polymer chains with the lower  $T_g$  and raises the overall modulus. Thus the creep or stress relaxation of two-phase systems is quite small unless the temperature is above the softening temperature of the higher softening component.

## PROBLEMS

1. A creep test is made on a polyethylene specimen that has a length of 4 in., a width of 0.50 in., and a thickness of 0.125 in. A load of 62.5 lb is applied to the specimen, and its length as a function of time is given by

| Time (min) | Length (in.) |
|------------|--------------|
| 0.1        | 4.033        |
| 1          | 4.049        |
| 10         | 4.076        |
| 100        | 4.110        |
| 1000       | 4.139        |
| 10,000     | 4.185        |

Plot the creep compliance ( $\text{cm}^2/\text{dyn}$ ) as a function of time using a logarithmic time scale. Would the curve show the upward curvature on a linear time scale?

2. Assuming that the Boltzmann superposition principle holds for the polymer in Problem 1, what would the creep elongation be from 100 to 10,000 min if the load were doubled after 100 min?



3. Assuming that the Boltzmann superposition principle holds and that all of the creep is recoverable, what would the creep recovery curve be for the polymer in Problem 1 if the load were removed after 10,000 min?
4. Derive equation (6) for the elongation  $\epsilon$  of a four-element model.
5. A material has two relaxation times—10 and 100 s. Plot its relaxation curve from 1 to 1000 s.
6. The creep of a polymer obeys the following equation:  $\epsilon(t) = Kr^n \sinh(\alpha/\sigma_c)$  with  $n = 0.10$ ,  $K = 10^{-5}$ , and  $\alpha_c = 1000$  psi. Plot the creep curve for loads  $\sigma$  of 500, 1000, and 2000 psi from 1 to  $10^4$  s. Why is it undesirable to apply loads greater than 1000 psi to this polymer for long periods of time?
7. A material has a viscosity of  $10^4$  P at  $0^\circ\text{C}$ . If it obeys the WLF equation, what is its viscosity at  $25^\circ\text{C}$ ? Assume that the viscosity is  $10^{13}$  P at  $T_g$ .
8. A polymer degrades during processing from a weight-average molecular weight of 1 million to  $8 \times 10^5$ . What is the ratio of the melt viscosity after processing to the melt viscosity before processing?
9. What will radiation during a test do to the stress relaxation of an elastomeric material if the radiation brings about chain scission? Compare a cross-linked polymer with a high-molecular-weight un-cross-linked one.
10. A horizontal cantilever beam is made of an idealized material that has only two retardation times: 10 and 1000 s. The beam is bent downward for 100 s. Then it is bent upward for 1 s and released without any vibrations taking place. Describe the motion of the beam for the next 10,000 s.
11. A polymer above its  $T_g$  value shows only a very slow creep rate. How would you distinguish between cross-linking and crystallinity as the cause of the small creep rate? Suggest at least two types of mechanical experiments or combinations of mechanical and other kinds of tests.
12. Use Figures 14 and 16 to construct the master curve for stress relaxation of the polymer at a reference temperature  $T_r$  of  $204^\circ\text{C}$ .
13. In cross-linked rubbers in which there is a chemical reaction that involves breaking of network chains, the rate of reaction in many cases is given by

$$\frac{dN}{dt} = -KN$$

where  $N$  is the number of network chains carrying stress at any time  $t$ . Show that the stress relaxation is

$$\frac{\sigma(t)}{\sigma_0} = \exp(-Kt)$$

14. The distribution of relaxation times  $H(\ln \tau)$  is a constant over several decades of time. What is the shape of the stress-relaxation curve over this time interval?
15. The  $T_g$  value of poly(methyl methacrylate) is 105°C. How much faster is its rate of stress relaxation at 155°C than at 125°C?
16. (a) The accompanying table (from Ref. 263) gives  $E(t)$  for polyisobutylene at 25°C over a wide range in  $t$ . (The original data form a continuous curve over the indicated time scale.) Use equation (13) to determine a first approximation to  $H$ .

| $\log t$ (h) | $\log E(t)$ | $\log t$ (h) | $\log E(t)$ | $\log t$ (h) | $\log E(t)$ |
|--------------|-------------|--------------|-------------|--------------|-------------|
| -12          | 10.20       | -6           | 7.00        | -1           | 6.62        |
| -10          | 9.12        | -5           | 6.91        | 0            | 6.40        |
| -9           | 8.46        | -4           | 6.99        | 1            | 5.86        |
| -7           | 7.30        | -3           | 6.84        | 2            | 5.18        |

(b) Using the data from  $t = 10^{-9}$  to  $10^{-4}$  as Prony series parameters for a hypothetical polymer, calculate  $E(t)$  at  $t = \tau$ . Are the original data reproduced? Are the Prony series  $E_i$  coefficients simply the values of  $E(t)$  at  $t = \tau$ ?

(c) Is the resulting curve smooth, or does it oscillate slightly? Recalculate with  $\log t$  spaced every 0.1 log unit. What happens to the oscillations? Repeat these calculations using only every other  $\tau_i$ ,  $E_i$  data pair. What is the effect on the oscillation if the  $\tau_i$  values are far apart?

(d) Extend the data at long and short times such that  $E(t)$  drops more or less rapidly but smoothly (e.g., sketch an extension to the curve or curve fit the last few points with a power series and then choose coefficients that fit the real data well but cause the extrapolated curve to tail off in varying ways). Determine the slopes and recalculate  $H$  using equation (13). Do drastic changes in the extrapolated regions affect the calculated values of  $H$  near the ends of the experimentally observed time scale (i.e., at  $\log \tau = 10^{-9}$  and  $10^{-8}$  or  $10^{-3}$  and  $10^{-4}$ )?

## REFERENCES

1. J. D. Ferry, *Viscoelastic Properties of Polymers*, 3rd ed., Wiley, New York, 1980.
2. L. E. Nielsen, *Mechanical Properties of Polymers*, Van Nostrand Reinhold, New York, 1962.
3. G. R. Smoluk, *Mod. Plastics*, 41(12), 119 (1964).
4. I. M. Ward and M. A. Wildung, *J. Polymer Sci. (Phys.)*, 22, 561 (1984).
5. H. Leaderman, in *Rheology*, Vol. 1, F. R. Eirich, Ed., Academic Press, New York, 1958, p. 1.
6. A. V. Tobolsky, *Properties and Structures of Polymers*, Wiley, New York, 1960.
7. N. W. Tschoegl, *The Phenomenological Theory of Linear Viscoelastic Behavior*, Springer-Verlag, New York, 1989.
8. D. J. Plazek, *J. Colloid Sci.*, 15, 50 (1960).
9. G. Link and F. R. Schwarzl, *Rheol. Acta*, 26, 375 (1987).
10. B. E. Read and G. E. Dean, *Polymer*, 25, 1679 (1984).
11. F. R. Schwarzl, *Polymer-mechanik*, Springer-Verlag, New York, 1990 (in German); *Rheol. Acta*, 8, 6 (1969); 9, 382 (1970); 10, 166 (1971); 14, 581 (1975).
12. R. A. Schapery, *Proc. 5th U.S. Natl. Congr. Appl. Mech.*, ASME, New York, 1966, p. 511; *J. Polymer Eng. Sci.*, 9, 295 (1969).
13. P. E. Rouse, Jr., *J. Chem. Phys.*, 21, 1272 (1953).
14. B. H. Zimm, *J. Chem. Phys.*, 24, 269 (1956).
15. F. Bueche, *J. Chem. Phys.*, 22, 603, 1570 (1954).
16. F. Bueche, *Physical Properties of Polymers*, Interscience New York, 1962.
17. M. Doi and S. F. Edwards, *J. Chem. Soc. Faraday Trans. 2*, 74, 1789, 1802, 1818 (1975).
18. D. S. Pearson, *Rubber Chem. Technol.*, 60, 439 (1987).
19. W. W. Graessley, *Adv. Polymer Sci.*, 16, 1 (1974).
20. R. B. Bird, O. Hassager, R. C. Armstrong, and C. F. Curtiss, *Dynamics of Polymeric Liquids*, Vol. 2, *Kinetic Theory*, 2nd ed., Wiley, New York, 1987.
21. J. D. Ferry, R. F. Landel, and M. L. Williams, *J. Appl. Phys.*, 26, 359 (1955).
22. H. Leaderman, *Elastic and Creep Properties of Filamentous Materials and Other High Polymers*, Textile Foundation, Washington, D.C., 1943.
23. P. Nutting, *Proc., ASTM*, 21, 1162 (1921).
24. R. Buchdahl and L. E. Nielsen, *J. Appl. Phys.*, 22, 1344 (1951).
25. J. D. Ferry, *J. Am. Chem. Soc.*, 72, 3746 (1950).
26. E. Catsiff and A. V. Tobolsky, *J. Colloid Sci.*, 10, 375 (1955).
27. M. L. Williams, R. F. Landel, and J. D. Ferry, *J. Am. Chem. Soc.*, 77, 3701 (1955).
28. G. C. Berry and T. G. Fox, *Adv. Polymer Sci.*, 5, 261 (1968).
29. N. G. McCrum and E. L. Morris, *Proc. Roy. Soc.*, A281, 258 (1964).

30. N. G. McCrum, B. E. Read, and G. Williams, *Anelastic and Dielectric Effects in Polymeric Solids*, Wiley, New York, 1967.
31. K. C. Rusch, *J. Macromol. Sci.*, **B2**, 179 (1968).
32. N. Nemoto, M. Moriwaki, H. Odani, and M. Kurata, *Macromolecules*, **4**, 215 (1971).
33. J. A. Faucher, *Trans. Soc. Rheol.*, **3**, 81 (1959).
34. K. Fujino, T. Horino, K. Miyamoto, and H. Kawai, *J. Colloid Sci.*, **16**, 411 (1961).
35. S. Onogi, T. Asada, Y. Fukui, and T. Fujisawa, *J. Polymer Sci.*, **A2**, **5**, 1067 (1967).
36. K. Nagamatsu, *Kolloid Z.*, **172**, 141 (1960).
37. R. W. Penn, *J. Polymer Sci.*, **A2**, **4**, 545 (1966).
38. Y. Fukui, T. Sato, M. Ushirokawa, T. Asada, and S. Onogi, *J. Polymer Sci.*, **A2**, **8**, 1195 (1970).
39. M. Takahashi, M. C. Shen, R. B. Taylor, and A. V. Tobolsky, *J. Appl. Polymer Sci.*, **8**, 1549 (1964).
40. N. Nemoto, *Polymer J.*, **1**, 485 (1970).
41. J. Bischoff, E. Catsiff, and A. V. Tobolsky, *J. Am. Chem. Soc.*, **74**, 3378 (1952).
42. T. Murayama, J. H. Dumbleton, and M. C. Williams, *J. Macromol. Sci.*, **B1**, 1 (1967).
43. E. Catsiff, T. Alfrey, Jr., and M. T. O'Shaughnessy, *Textile Res. J.*, **23**, 808 (1953).
44. J. R. McLoughlin and A. V. Tobolsky, *J. Colloid Sci.*, **7**, 555 (1952).
45. K. Fujino, K. Senshu, and H. Kawai, *J. Colloid Sci.*, **16**, 262 (1961).
46. E. Catsiff and A. V. Tobolsky, *J. Appl. Phys.*, **25**, 1092 (1954).
47. A. V. Tobolsky and J. R. McLoughlin, *J. Polymer Sci.*, **8**, 543 (1952).
48. R. L. Bergen, Jr., and W. E. Wolstenholme, *SPE J.*, **16**, 1235 (1960).
49. P. S. Theocoris, *Kolloid Z.*, **236**, 59 (1970).
50. K. Arisawa, H. Hirose, M. Ishikawa, T. Harada, and Y. Wada, *Japan. J. Appl. Phys.*, **2**, 695 (1963).
51. Y. Fukui, T. Sato, M. Ushirokawa, T. Asada, and S. Onogi, *J. Polymer Sci.*, **A2**, **8**, 1211 (1970).
52. J. P. Mercier and G. Groeninckx, *Rheol. Acta*, **8**, 510 (1969).
53. J. Bares, *J. Polymer Sci.*, **A2**, **9**, 1271 (1971).
54. D. I. G. Jones, *Shock Vibrat. Bull.*, **48**, 13 (1978).
55. P. Thirion and R. Chasset, *Chim. Ind. (Paris)*, **97**, 617 (1967).
56. E. Guth, P. E. Wack, and R. L. Anthony, *J. Appl. Phys.*, **17**, 347 (1946).
57. G. M. Martin, F. L. Roth, and R. D. Stiehler, *Trans. Inst. Rubber Ind.*, **32**, 189 (1956).
58. J. C. Halpin, *J. Appl. Phys.*, **36**, 2975 (1965).
59. R. F. Landel and P. J. Stedry, *J. Appl. Phys.*, **31**, 1885 (1960).
60. M. Ilavsky and W. Prins, *Macromolecules*, **3**, 415, 425 (1970).
61. J. Glucklich and R. F. Landel, *J. Polymer Sci. (Phys.)*, **15**, 2185 (1977).

62. K. Tsuge, R. J. Arenz, and R. F. Landel, in *Mechanical Behavior of Materials*, Vol. III, Society of Materials Science, Kyoto, Japan, 1972, p. 443; reprinted in *Rubber Chem. Technol.*, **51**, 848 (1978).
63. J. Gluecklich and R. F. Landel, unpublished.
64. G. W. Becker and H. J. Rademacher, *J. Polymer Sci.*, **58**, 621 (1962).
65. Y. Obata, S. Kawabata, and H. Kawai, *J. Polymer Sci.*, **A2**, **8**, 903 (1970).
66. T. L. Smith, *Trans. Soc. Rheol.*, **6**, 61, (1962).
67. M. H. Wagner, *Rheol. Acta*, **15**, 136 (1976); **18**, 68 (1979).
68. R. G. Larson, *Rheol. Acta*, **24**, 327 (1985).
69. E. Passaglia and H. P. Koppchele, *J. Polymer Sci.*, **33**, 281 (1958).
70. R. Meredith and B. Hsu, *J. Polymer Sci.*, **61**, 253 (1962).
71. O. Nakada, T. Hirai, and Y. Maeda, *J. Japan. Soc. Test. Mater.*, **8**, 284 (1959).
72. G. W. Becker, *Kolloid Z.*, **175**, 99 (1961).
73. J. A. Sauer and W. J. Oliphant, *Proc. ASTM*, **49**, 1119 (1949).
74. J. Marin and G. Cuff, *Proc. ASTM*, **49**, 1158 (1949).
75. R. R. Dixon, *SPE J.*, **14**(4), 23 (1958).
76. M. G. Sharma and P. R. Wen, *Trans. SPE*, **4**, 282 (1964).
77. W. Kauzmann and H. Eyring, *J. Am. Chem. Soc.*, **62**, 3113 (1940).
78. A. V. Tobolsky and H. Eyring, *J. Chem. Phys.*, **11**, 125 (1943).
79. K. Van Holde, *J. Polymer Sci.*, **24**, 417 (1957).
80. D. R. Reid, *Brit. Plastics*, **32**, 460 (1959).
81. D. R. Reid, *Rheol. Acta*, **1**, 603 (1961).
82. W. N. Findley, *SPE J.*, **16**(1), 57 (1960).
83. D. O'Connor and W. N. Findley, *Trans. SPE*, **2**, 273 (1962).
84. S. Turner, *Brit. Plastics*, **37**, 501, 567 (1964).
85. M. Goldstein, *J. Polymer Sci.*, **B4**, 87 (1966).
86. O. Ishai, *J. Appl. Polymer Sci.*, **11**, 1863 (1967).
87. R. S. Moore and C. Gieniewski, *Macromolecules*, **1**, 540 (1968).
88. L. E. Nielsen, *J. Appl. Polymer Sci.*, **13**, 1800 (1969).
89. L. E. Nielsen, *Trans. Soc. Rheol.*, **13**, 141 (1969).
90. F. Schwarzl, *Kolloid Z.*, **165**, 88 (1959).
91. F. H. Mueller and C. Engelter, *Kolloid Z.*, **186**, 36 (1962).
92. S. Turner, *Trans. Plastics Inst.*, **31**, 60 (1963).
93. R. L. Bergen, Jr., *SPE J.*, **23**(10), 57 (1967).
94. E. A. W. Hoff, P. L. Clegg, and K. Sherrard-Smith, *Brit. Plastics*, **31**, 384 (1958).
95. R. H. Carey, *Ind. Eng. Chem.*, **50**, 1045 (1958).
96. G. R. Gohn and J. D. Cummings, *ASTM Bull.*, **247**, 64 (1960).
97. S. Turner, *Brit. Plastics*, **37**, 682 (1964).
98. W. Findley, *Trans. Plastics Inst.*, **30**, 138 (1962).
99. H. Leaderman, *Trans. Soc. Rheol.*, **7**, 111 (1963).
100. J. A. Sauer, J. Marin, and C. C. Hsiao, *J. Appl. Phys.*, **20**, 507 (1949).
101. R. S. Moore and C. Gieniewski, *Polymer Eng. Sci.*, **9**, 190 (1960).
102. S. Turner, *Brit. Plastics*, **37**, 440 (1964).

103. I. M. Ward and J. M. Wolfe, *J. Mech. Phys. Solids*, **14**, 131 (1966).
104. M. G. Sharma and L. Gesinski, *Mod. Plastics*, **40**(5), 164 (1963).
105. S. Matsuoka, C. Aloisio, and H. E. Bair, *J. Appl. Phys.*, **44**, 4625 (1973).
106. R. Fillers and N. W. Tschoegl, *Trans. Soc. Rheol.*, **21**, 51 (1977).
107. K. I. DeVries and D. K. Backman, *J. Polymer Sci.*, **B9**, 717 (1971).
108. L. C. E. Struik, *Ann. N.Y. Acad. Sci.*, **279**, 78 (1976).
109. J. R. McLoughlin and A. V. Tobolsky, *J. Polymer Sci.*, **7**, 658 (1951).
110. D. H. Enders, *J. Macromol. Sci.*, **B4**, 635 (1970).
111. F. A. Myers, F. C. Cama, and S. S. Sternstein, *Ann. N.Y. Acad. Sci.*, **279**, 94 (1976).
112. C. M. R. Dunn and S. Turner, *Polymer*, **15**, 451 (1974).
113. C. J. Su, *Polymer Plastics Technol. Eng.*, **4**, 221 (1975).
114. L. E. Nielsen, in *Copolymers, Polyblends, and Composites*, N. Platzer, Ed., Adv. Chem. Ser. 142, American Chemical Society, Washington, D. C., 1975, p. 257.
115. J. M. Augl, *J. Rheol.*, **31**, 1 (1987).
116. J. G. Curro, R. R. Lagasse, and R. Simha, *J. Appl. Phys.*, **52**, 5892 (1981).
117. M. Cizmecioglu, R. F. Fedors, S. D. Hong, and J. Moacanin, *Polymer Prepr. Am. Chem. Soc. Div. Polymer Chem.*, **21**(2), 31 (1980).
118. S. S. Sternstein and T. C. Ho, *J. Appl. Phys.*, **43**, 4370 (1972).
119. T. L. Smith, *Proc. 28th IUPAC Macromol. Symp.*, 1982, p. 863.
120. A. F. Yee, *Polymer Prepr. Am. Chem. Soc. Div. Polymer Chem.*, **21**(2), 29 (1980).
121. S. Matsuoka, *Polymer Eng. Sci.*, **9**, 105 (1969).
122. C. B. Bucknall and D. Clayton, *J. Mater. Sci.*, **7**, 202 (1972).
123. W. Lortsch and H. Vogel, *Kunststoffe*, **61**, 933 (1971).
124. M. Kitagawa and M. Kawagoe, *J. Polymer Sci. (Phys.)*, **17**, 663 (1979).
125. N. Brown, B. D. Metzger, and Y. Imai, *J. Polymer Sci. (Phys.)*, **16**, 1085 (1978).
126. J. B. C. Wu and N. Brown, *J. Rheol.*, **23**, 231 (1979).
127. D. McCammond and C. A. Ward, *Polymer Eng. Sci.*, **14**, 831 (1974).
128. L. A. Wood, G. W. Bullman, and F. L. Roth, *J. Res. Natl. Bur. Std.*, **A78**, 632 (1974).
129. E. H. Merz, L. El Nielsen, and R. Buchdahl, *Ind. Eng. Chem.*, **43**, 1396 (1951).
130. R. F. Rudd, *J. Polymer Sci.*, **B1**, 1 (1963).
131. L. Z. Rogovina and G. L. Slonimskii, *Polymer Sci. (USSR)*, **8**, 236 (1966).
132. G. Menges and H. Schmidt, *Kunststoffe*, **57**, 885 (1967).
133. D. A. Thomas, *Plastics Polymers*, **37**, 485 (1969).
134. L. H. Drexler, *J. Appl. Polymer Sci.*, **14**, 1857 (1970).
135. T. G. Fox and P. J. Flory, *J. Phys. Chem.*, **55**, 221 (1951).
136. T. G. Fox and S. Loshaek, *J. Appl. Phys.*, **26**, 1080 (1955).
137. F. Bueche, *J. Chem. Phys.*, **25**, 599 (1956).
138. F. Bueche, *J. Polymer Sci.*, **25**, 305 (1957).
139. L. E. Nielsen and R. Buchdahl, *J. Chem. Phys.*, **17**, 839 (1949).

140. L. E. Nielsen and R. Buchdahl, *J. Colloid Sci.*, **5**, 282 (1950).
141. H. Markovitz, T. G. Fox, and J. D. Ferry, *J. Phys. Chem.*, **66**, 1567 (1962).
142. M. L. Williams, *J. Appl. Phys.*, **29**, 1395 (1958).
143. A. V. Tobolsky and D. B. DuPre, *Adv. Polymer Sci.*, **6**, 103 (1969).
144. K. L. Ngai, R. W. Rendell, A. K. Rajagopal, and S. Teitler, *Ann. N.Y. Acad. Sci.*, **484**, 150 (1986); K. L. Ngai, A. K. Rajagopal, and S. Teitler, *J. Chem. Phys.*, **88**, 5086 (1988).
145. G. Williams and D. C. Watts, *Trans. Faraday Soc.*, **66**, 80 (1970).
146. W. F. Busse, *J. Phys. Chem.*, **36**, 2862 (1932).
147. P.-G. DeGennes, *J. Chem. Phys.*, **55**, 572 (1971); *Scaling Concepts in Polymer Physics*, Cornell University Press, Ithaca, N.Y., 1979.
148. J. Roovers, *Polymer J.*, **18**, 153, (1986).
149. J. Klein, *Macromolecules*, **11**, 852 (1978).
150. W. W. Graessley, *Adv. Polymer Sci.*, **47**, 67 (1982).
151. M. Doi, *J. Polymer Sci. Polymer Lett.*, **19**, 265 (1981); *J. Polymer Sci., Polymer Phys.*, **21**, 667 (1983).
152. F. Bueche, *J. Chem. Phys.*, **20**, 1959 (1952).
153. T. G. Fox and V. R. Allen, *J. Chem. Phys.*, **41**, 337, 344 (1964).
154. J. Brandrup and E. H. Immergut, Eds., *Polymer Handbook*, Wiley, New York, 1989.
155. R. L. Ballman and R. H. M. Simon, *J. Polymer Sci.*, **A2**, 3557 (1964).
156. R. Longworth and W. F. Busse, *Trans. Soc. Rheol.*, **6**, 179 (1962).
157. K. Ninomiya, *J. Colloid Sci.*, **14**, 49 (1959).
158. K. Ninomiya, *J. Colloid Sci.*, **17**, 759 (1962).
159. N. Ninomiya and J. D. Ferry, *J. Colloid Sci.*, **18**, 421 (1963).
160. T. Fujimoto, M. Ozaki, and M. Nagasawa, *J. Polymer Sci.*, **A2**, **6**, 129 (1968).
161. A. Schausberger, H. Knoglinger, and H. Janeschitz-Kriegl, *Rheol. Acta*, **26**, 468 (1987).
162. G. Eder, H. Janeschitz-Kriegl, and A. Schausberger, *J. Rheol.*, **33**, 805 (1989).
163. F. Bueche, *J. Chem. Phys.*, **40**, 484 (1964).
164. V. C. Long, G. C. Berry, and L. M. Hobbs, *Polymer*, **5**, 517 (1964).
165. G. Kraus and J. T. Gruber, *J. Polymer Sci.*, **A3**, 105 (1965).
166. J. E. Guillet, R. L. Combs, D. F. Slonaker, D. A. Weems, and H. W. Coover, Jr., *J. Appl. Polymer Sci.*, **9**, 757, 767 (1965).
167. R. P. Chartoff and B. Maxwell, *J. Polymer Sci.*, **A2**, **8**, 455 (1970).
168. J. S. Ham, *J. Chem. Phys.*, **26**, 625 (1957).
169. C. A. Berglund, C. J. Carriere, and J. D. Ferry, *J. Rheol.*, **25**, 251 (1981).
170. G. Kraus and J. T. Gruber, *Trans. Soc. Rheol.*, **9**(2), 17 (1965).
171. L. J. Garfield and S. E. Petric, *J. Phys. Chem.*, **68**, 1750 (1964).
172. F. N. Kelley and F. Bueche, *J. Polymer Sci.*, **50**, 549 (1961).
173. R. N. Haward, *Chem. Ind.*, **33**, 1442 (Aug. 1964).
174. H. Fujita and E. Maekawa, *J. Phys. Chem.*, **66**, 1053 (1962).
175. G. Pezzin, *J. Appl. Polymer Sci.*, **10**, 21 (1966).

176. L. Utracki and R. Simha, *J. Polymer Sci.*, **A1**, 1089 (1963).
177. P. F. Lyons and A. V. Tobolsky, *Polymer Eng. Sci.*, **10**, 1 (1970).
178. L. E. Nielsen, *J. Macromol. Chem.*, **C3**, 69 (1969).
179. A. R. H. Tawn, *J. Oil Colour Chem. Assoc.*, **52**, 814 (1969).
180. M. C. Shen and A. V. Tobolsky, *J. Polymer Sci.*, **A2**, 2513 (1964).
181. N. R. Langley, *Macromolecules*, **1**, 348 (1968).
182. N. R. Langley and J. D. Ferry, *Macromolecules*, **1**, 353 (1968).
183. D. J. Plazek, *J. Polymer Sci.*, **A2**, **4**, 745 (1966).
184. J. G. Curro and P. Pincus, *Macromolecules*, **16**, 559 (1983).
185. J. G. Curro, D. S. Pearson, and E. Helfand, *Macromolecules*, **18**, 1157 (1985).
- 185a. R. F. Landel, previously unpublished.
186. R. F. Landel and R. F. Fedors, in *Mechanical Behavior of Materials*, Vol. III, Materials Science, Kyoto, Japan, 1972, p. 496. See also J. O. Ferry, *Viscoelastic Properties of Polymers*, 1st ed., Wiley, New York, 1961, p. 463 for tabulated values of the Marvin function.
187. R. S. Marvin, in *Viscoelasticity: Phenomenological Effects*, J. T. Bergen, Ed., Academic Press, New York, 1960, p. 27.
188. P. J. Flory, *Chem. Rev.*, **39**, 137 (1946).
189. P. J. Flory, *Principles of Polymer Chemistry*, Cornell University Press, Ithaca, N.Y., 1953.
190. L. E. Nielsen, *J. Appl. Polymer Sci.*, **8**, 511 (1964).
191. F. Bueche, *J. Appl. Polymer Sci.*, **1**, 240 (1959).
192. L. A. Wood, *U.S. Natl. Bur. Std., Rept. 5796* (May 12, 1958).
193. L. A. Wood, *J. Rubber Res. Inst. Malaya*, **22**, 309 (1969); *Rubber Chem. Technol.*, **43**, 1482 (1970).
194. L. A. Wood and G. W. Bullman, *J. Polymer Sci.*, **A2**, **10**, 43 (1972).
195. R. H. Valentine, J. D. Ferry, T. Homma, and K. Ninomiya, *J. Polymer Sci.*, **A2**, **6**, 479 (1968).
196. J. Janáček and J. D. Ferry, *Rheol. Acta*, **9**, 208 (1970).
197. E. D. Farlie, *J. Appl. Polymer Sci.*, **14**, 1127 (1970).
198. J. P. Berry and W. F. Watson, *J. Polymer Sci.*, **18**, 201 (1955).
199. O. Kramer, R. Greco, R. A. Neira, and J. D. Ferry, *J. Polymer Sci. (Phys.)*, **12**, 2361 (1974).<sup>1</sup>
200. D. J. Plazek and I.-C. Choy, *J. Polymer Sci. Polymer Phys. Ed.*, **27**, 307 (1988).
201. D. J. Plazek and I.-C. Choy, *J. Polymer Sci. Polymer Phys.*, **29**, 17 (1991).
202. A. S. Kenyon and L. E. Nielsen, *J. Macromol. Sci.*, **A3**, 275 (1969).
203. C. A. May and F. E. Weir, *SPE Trans.*, **2**, 207 (1962).
204. F. R. Dammont and T. K. Kwei, *J. Polymer Sci.*, **A2**, 761 (1967).
205. K. Shibayama and Y. Suzerki, *J. Polymer Sci.*, **A3**, 2637 (1965).
206. A. V. Tobolsky, *J. Chem. Phys.*, **37**, 1139 (1962).
207. A. V. Tobolsky and V. D. Gupta, *Textile Res. J.*, **33**, 761 (1963).
208. L. E. Nielsen and F. D. Stockton, *J. Polymer Sci.*, **A1**, 1995 (1963).
209. F. Bueche, *J. Polymer Sci.*, **22**, 113 (1956).



210. P. J. Flory, *Trans. Faraday Soc.*, **51**, 848 (1955).
211. W. R. Krigbaum, R. J. Roe, and K. J. Smith, Jr., *Polymer*, **5**, 533 (1964).
212. A. Bondi, *J. Polymer Sci.*, **A2**, **5**, 83 (1967).
213. T. Alfrey, Jr., N. Wiederhorn, R. S. Stein, and A. V. Tobolsky, *J. Colloid Sci.*, **4**, 211 (1949).
214. K. Fujino, K. Senshu, T. Horino, and H. Kwai, *J. Colloid Sci.*, **17**, 726 (1962).
215. A. Crugnola, M. Pegoraro, and F. Danusso, *J. Polymer Sci.*, **A2**, **6**, 1705 (1968).
216. L. E. Nielsen, *J. Appl. Polymer Sci.*, **2**, 351 (1959).
217. J. P. Mercier and G. Groeninckx, *Rheol. Acta*, **8**, 504 (1969).
218. K. Nagamatsu, T. Takemura, T. Yoshitomi, and T. Takemoto, *J. Polymer Sci.*, **33**, 515 (1958).
219. T. Takemura, *J. Polymer Sci.*, **38**, 471 (1959).
220. P. H. Geil, *Polymer Single Crystals*, Interscience, New York, 1963.
221. H. Nakayasu, H. Markovitz, and D. J. Plazek, *Trans. Soc. Rheol.*, **5**, 261 (1961).
222. E. Catsiff, J. O. Offenbach, and A. V. Tobolsky, *J. Colloid Sci.*, **11**, 48 (1956).
223. T. Yoshitomi, K. Nagamatsu, and K. Kosiyama, *J. Polymer Sci.*, **27**, 335 (1958).
224. S. Onogi, K. Sasaguri, T. Adachi, and S. Ogihara, *J. Polymer Sci.*, **58**, 1 (1962).
225. K. Nagamatsu, T. Yoshitomi, and T. Takemoto, *J. Colloid Sci.*, **13**, 257 (1958).
226. K. Nagamatsu and T. Yoshitomi, *J. Colloid Sci.*, **14**, 377 (1959).
227. H. Yamamura and N. Kuramoto, *J. Appl. Polymer Sci.*, **2**, 71 (1959).
228. W. N. Findley and G. Khosla, *SPE J.*, **12**(12), 20 (1956).
229. G. R. Gohn and A. Fox, *Mater. Res. Std.*, **1**, 957 (1961).
230. A. Gent, *Trans. Faraday Soc.*, **50**, 521 (1954).
231. A. V. Tobolsky and G. M. Brown, *J. Polymer Sci.*, **17**, 547 (1955).
232. W. Aiken, T. Alfrey, Jr., and H. Mark, *J. Polymer Sci.*, **2**, 178 (1947).
233. L. E. Nielsen, *J. Am. Chem. Soc.*, **75**, 1435 (1953).
234. L. E. Nielsen, R. Buchdahl, and R. Levreault, *J. Appl. Phys.*, **21**, 607 (1950).
235. W. J. Jackson, Jr., and J. R. Caldwell, *Adv. Chem. Ser.*, **48**, 185 (1965).
236. W. J. Jackson, Jr., and J. R. Caldwell, *J. Appl. Polymer Sci.*, **11**, 211, 227 (1967).
237. L. M. Robeson and J. A. Faucher, *J. Polymer Sci.*, **B7**, 35 (1969).
238. S. Turner, *Brit. Plastics*, **38**, 44 (1965).
239. N. A. Brunt, *Kolloid Z.*, **185**, 119 (1962).
240. M. T. O'Shaughnessy, *Textile Res. J.*, **18**, 263 (1948).
241. P. Peyser and W. D. Bascom, *J. Mater. Sci.*, **16**, 75 (1981).
242. O. J. Boll, W. D. Bascom, and B. Mottee, *Composite Sci. Technol.*, **24**, 253 (1985).

243. R. Sabia and F. R. Eirich, *J. Polymer Sci.*, **A1**, 2511 (1963).
244. R. Sabia and F. R. Eirich, *J. Polymer Sci.*, **A1**, 2497 (1963).
245. J. M. Ward, *Mechanical Properties of Solid Polymers*, 2nd ed., Wiley, New York, 1983.
246. G. B. Jackson and J. L. McMillan, *SPE J.*, **19**, 203 (1963).
247. R. G. Cheatham and A. G. H. Dietz, *Trans. ASME*, **74**, 31 (1952).
248. R. G. Cheatham and A. G. H. Dietz, *Mod. Plastics*, **29**, 113 (Sept. 1951).
249. M. W. Darlington and D. W. Saunders, *J. Macromol. Sci.*, **B5**, 207 (1971).
250. C. D. Pomeroy, *Brit. J. Appl. Phys.*, **12**, 3 (1961).
251. M. W. Darlington, B. H. McConkey, and D. W. Saunders, *J. Mater. Sci.*, **6**, 1447 (1971).
252. M. W. Darlington and D. W. Saunders, *Polymer Eng. Sci.*, **14**, 616 (1974).
253. A. J. DeVries, C. Bonnebat, and J. Beautemps, *J. Polymer Sci. (Phys.)*, **58**, 109 (1977).
254. M. J. Bonnin, C. M. R. Dunn, and S. Turner, *Plastic Polymers*, **37**, 517 (1969).
255. S. Timoshenko and J. N. Goodier, *Theory of Elasticity*, 2nd ed., McGraw-Hill, New York, 1951, p. 7.
256. F. L. McCrackin and C. F. Bersch, *SPE J.*, **15**, 791 (1959).
257. W. H. Buck, R. J. Cella, E. K. Gladding, and J. R. Wolfe, *J. Polymer Sci. (Symp.)*, **48**, 47 (1974).
258. M. Shen and D. H. Kaelble, *J. Polymer Sci.*, **B8**, 149 (1970).
259. C. K. Lim, R. E. Cohen, and N. W. Tschoegl, *Adv. Chem. Ser.*, **99**, 397 (1971).
260. L. H. Sperling, H. F. George, V. Huelck, and D. A. Thomas, *J. Appl. Polymer Sci.*, **14**, 2815 (1970).
261. J. F. Beecher, L. Marker, R. D. Bradford, and S. L. Aggarwal, *J. Polymer Sci.*, **C26**, 117 (1969).
262. G. L. Wilkes and R. S. Stein, *J. Polymer Sci.*, **A2**, **7**, 1525 (1969).
263. A. V. Tobolsky and E. Catsiff, *J. Polymer Sci.*, **19**, 111 (1956).